T.C.
REPUBLIC OF TURKEY
HACETTEPE UNIVERSITY
GRADUATE SCHOOL OF HEALTH SCIENCES

INVESTIGATION OF THE IN VITRO AND IN VIVO EFFECTS OF TELOMERE-TARGETED NEW DRUG CANDIDATE COMPOUNDS ON DIFFERENT CANCER CELL LINES

Merve YILMAZ

Program of Biochemistry

DOCTOR OF PHILOSOPHY THESIS

ANKARA

2023

T.C.
REPUBLIC OF TURKEY
HACETTEPE UNIVERSITY
GRADUATE SCHOOL OF HEALTH SCIENCES

INVESTIGATION OF THE IN VITRO AND IN VIVO EFFECTS OF TELOMERE-TARGETED NEW DRUG CANDIDATE COMPOUNDS ON DIFFERENT CANCER CELL LINES

Merve YILMAZ

Program of Biochemistry

DOCTOR OF PHILOSOPHY THESIS

SUPERVISOR
Prof. Dr. Z. Günnur DİKMEN

Co-SUPERVISOR
Ph.D. Sergei M. GRYAZNOV

ANKARA

2023

INVESTIGATION OF THE IN VITRO AND IN VIVO EFFECTS OF TELOMERE-TARGETED NEW DRUG CANDIDATE COMPOUNDS ON DIFFERENT CANCER CELL LINES

Student: Merve YILMAZ

Supervisor: Prof. Dr. Z. Gunnur DİKMEN

Co-supervisor: Ph.D. Sergei M. GRYAZNOV

This thesis study has been approved and accepted as a PhD dissertation in "Biochemistry Program" by the assessment committee, whose members are listed below, on 08.12.2023

Chairman of the Committee:	Prof. Dr. Kamil Can AKÇALI (Ankara University)
Member:	Associate Prof. Kevser BİBEROĞLU (Hacettepe University)
Member:	Associate Prof. Gamze TUNA (Dokuz Eylül University)
Member:	Associate Prof. Oytun PORTAKAL (Hacettepe University)
Member:	Assistant Prof. Başak ÇELTİKÇİ (Hacettepe University)

This dissertation has been approved by the above committee in conformity to the related issues of Hacettepe University Graduate Education and Examination Regulation.

Prof. Müge YEMİŞCİ ÖZKAN, MD, PhD

Director

YAYIMLAMA VE FİKRİ MÜLKİYET HAKLARI BEYANI

Enstitü tarafından onaylanan lisansüstü tezimin/raporumun tamamını veya herhangi bir kısmını, basılı (kağıt) ve elektronik formatta arşivleme ve aşağıda verilen koşullarla kullanıma açma iznini Hacettepe Üniversitesine verdiğimi bildiririm. Bu izinle Üniversiteye verilen kullanım hakları dışındaki tüm fikri mülkiyet haklarım bende kalacak, tezimin tamamının ya da bir bölümünün gelecekteki çalışmalarda (makale, kitap, lisans ve patent vb.) kullanım hakları bana ait olacaktır.

Tezin kendi orijinal çalışmam olduğunu, başkalarının haklarını ihlal etmediğimi ve tezimin tek yetkili sahibi olduğumu beyan ve taahhüt ederim. Tezimde yer alan telif hakkı bulunan ve sahiplerinden yazılı izin alınarak kullanılması zorunlu metinlerin yazılı izin alınarak kullandığımı ve istenildiğinde suretlerini Üniversiteye teslim etmeyi taahhüt ederim.

Yükseköğretim Kurulu tarafından yayınlanan ***"Lisansüstü Tezlerin Elektronik Ortamda Toplanması, Düzenlenmesi ve Erişime Açılmasına İlişkin Yönerge"*** kapsamında tezim aşağıda belirtilen koşullar haricince YÖK Ulusal Tez Merkezi / H.Ü. Kütüphaneleri Açık Erişim Sisteminde erişime açılır.

o Enstitü / Fakülte yönetim kurulu kararı ile tezimin erişime açılması mezuniyet tarihimden itibaren 2 yıl ertelenmiştir.(1)
o Enstitü / Fakülte yönetim kurulunun gerekçeli kararı ile tezimin erişime açılması mezuniyet tarihimden itibaren ... ay ertelenmiştir.(2)
o Tezimle ilgili gizlilik kararı verilmişti

…… /……/……

Merve YILMAZ

1"Lisansüstü Tezlerin Elektronik Ortamda Toplanması, Düzenlenmesi ve Erişime Açılmasına İlişkin Yönerge"

(1) Madde 6. 1. Lisansüstü tezle ilgili patent başvurusu yapılması veya patent alma sürecinin devam etmesi durumunda, tez **danışmanının** önerisi ve **enstitü anabilim dalının** uygun görüşü üzerine **enstitü veya fakülte yönetim kurulu** iki yıl süre ile tezin erişime açılmasının ertelenmesine karar verebilir.

(2) Madde 6. 2. Yeni teknik, materyal ve metotların kullanıldığı, henüz makaleye dönüşmemiş veya patent gibi yöntemlerle korunmamış ve internetten paylaşılması durumunda 3. şahıslara veya kurumlara haksız kazanç imkanı oluşturabilecek bilgi ve bulguları içeren tezler hakkında tez **danışmanının** önerisi ve **enstitü anabilim dalının** uygun görüşü üzerine **enstitü** veya **fakülte yönetim kurulunun** gerekçeli kararı ile altı ayı aşmamak üzere tezin erişime açılması engellenebilir.

(3) Madde 7. 1. Ulusal çıkarları veya güvenliği ilgilendiren, emniyet, istihbarat, savunma ve güvenlik, sağlık vb. konulara ilişkin lisansüstü tezlerle ilgili gizlilik kararı, **tezin yapıldığı kurum** tarafından verilir*. Kurum ve kuruluşlarla yapılan işbirliği protokolü çerçevesinde hazırlanan lisansüstü tezlere ilişkin gizlilik kararı ise, **ilgili kurum ve kuruluşun** önerisi ile **enstitü** veya **fakültenin** uygun görüşü üzerine **üniversite yönetim kurulu** tarafından verilir. Gizlilik kararı verilen tezler Yükseköğretim Kuruluna bildirilir. Madde 7.2. Gizlilik kararı verilen tezler gizlilik süresince enstitü veya fakülte tarafından gizlilik kuralları çerçevesinde muhafaza edilir, gizlilik kararının kaldırılması halinde Tez Otomasyon Sistemine yüklenir.

***** Tez **danışmanının** önerisi ve **enstitü anabilim dalının** uygun görüşü üzerine **enstitü** veya **fakülte yönetim kurulu tarafından karar verilir.**

ETHICAL DECLARATION

In this thesis study, I declare that all the information and documents have been obtained in the base of the academic rules and all audio-visual and written information and results have been presented according to the rules of scientific ethics. I did not do any distortion in data set. In case of using other works, related studies have been fully cited in accordance with the scientific standards. I also declare that my thesis study is original except cited references. It was produced by myself in consultation with Prof. Dr. Z. Günnur DİKMEN (Investigation of the *in vitro* and *in vivo* effects of the telomere-targeted new drug candidate compounds on different cancer cell lines, Merve YILMAZ and written according to the rules of thesis writing of Hacettepe University Institute of Health Sciences.

Merve YILMAZ

ACKNOWLEDGEMENT

I am grateful for the invaluable support and guidance provided by all the faculty members at Hacettepe University Faculty of Medicine, Department of Biochemistry, Hacettepe University Faculty of Medicine, Oncology Department, Hacettepe University Faculty of Medicine, Neurological and Psychiatric Research and Application Center, Dokuz Eylül University, Institute of Health Sciences Department of Molecular Medicine during my doctoral education.

In particular, I would like to express my deep gratitude to my dear supervisor, Prof. Dr. Z. Gunnur Dikmen for giving me a number of amazing opportunities to both initiate and expand my research career. Throughout my graduate education, she consistently provided me with invaluable insights and guidance, going beyond mere encouragement of my ideas. Thanks to Prof. Dr.Dikmen's unwavering support, I have not only been guided in my instrumental planning but also in shaping my future prospects. Her dedication and mentorship played fundamental role in my academic and personal growth. Furthermore, I want to extend my thanks to my Co-supervisor, Ph.D. Sergei M. Gryaznov, whose unwavering guidance and patience throughout the entire process. His consistence financial and moral support have played a pivotal role in my successful completion of my doctoral thesis.

I would like to express my gratitude to PhD. Ilgen Mender for her invaluable guidance and assistance throughout my experiments, drawing her extensive expertise. Furthermore, I am thankful to Prof. Dr. Gunes Esendaglı and Sibel Goksen for their invaluable support during the in vivo experiments and the evaluation of results. Additionally, I am grateful to Assoc. Prof. Sefik Evren Erdener for his guidance in the quantification of the in vitro studies. A special thanks to Assoc. Prof. Gamze Tuna and her amazing team, who provided assistance during the in vitro studies and the quantification of results. Thanks to these exceptional teams, the entire process was both convenient and meaningful.

Lastly and especially, I would like to express my heartfelt thanks to my architect and mother, Prof. Dr. Meryem YILMAZ. She has consistently stood by my side, providing unwavering support and guidance. Her patience and unwavering belief in me go beyond what words can convey.

Thank you endlessly.

ABSTRACT

Yılmaz M., Investigation of The *In Vitro* and *In Vivo* Effects of The Telomere-Targeted New Drug Candidate Compounds On Different Cancer Cell Lines, Hacettepe University Graduate School of Health Sciences, Department of Medical Biochemistry, Doctor of Philosophy Thesis, Ankara, 2023.

Cancer, characterized by its heterogeneity, metastatic character, and limited treatability, stands as a leading global cause of mortality. Cancer cells elongate their telomeres through the activity of the telomerase enzyme, thereby gaining immortality by evading control checkpoints in the cell cycle. The expression of telomerase is present in approximately 95% of cancer cells, while its activity is absent in somatic cells. Consequently, in recent years telomerase/telomere-targeted therapies have shown significant promise. Due to the heterogeneity of cancer cells and their varying telomere lengths, long-term anti-telomerase therapies can lead to adverse effects. Therefore, there is a need for novel molecules that can target telomeres, regardless of their telomeric lengths, and exhibit rapid efficacy. Within the scope of this doctoral thesis research, the objective was to investigate molecules added to telomeric structures by telomerase, which may induce genomic instability and cell death through telomeric DNA damage, both *in vitro* and *in vivo*. These molecules were synthesized by the MAIA biotechnology company (Chicago, USA) and delivered to the Department of Medical Biochemistry. The candidate drug molecules were tested on different cancer cell lines [breast cancer (MCF-7), non-small cell lung cancer (A549), cervical cancer (HeLa), and colon cancer (HT29)] at nine different concentrations for 96 hours, and cytotoxicity was assessed using the MTT (3-(4,5-Dimethylthiazol-2-yl)-2,5-Diphenyltetrazolium Bromide) assay. The obtained EC_{50} results were compared with 6-thio-dG in each cell line, and a molecule named "L6" was identified as a new potential drug candidate with a lower EC_{50} value compared to 6-thio-dG. The EC_{50} values of different cell lines to the L6 molecule were evaluated, and HT29 colon cancer cells, which exhibited the highest sensitivity to the L6 molecule, were selected as the target cell line. The DNA damage induced by these molecules at telomeric ends was assessed using the Telomere Induced Foci (TIF) method with confocal microscopy. In this method, co-localization of telomeric probes and staining with the γH2AX antibody specific to DNA damage was used to demonstrate TIF. The results obtained from the

TIF method indicate that the telomeric DNA damage caused by the L6 molecule is statistically significant compared to the control group and 6-thio-dG. Additionally, an assessment of global genomic damage reveals that the L6 molecule and 6-thio-dG induce DNA damage to an equal extent. Furthermore, the effects of the candidate molecules on the base excision repair (BER) pathway proteins Apurinic/Apyrimidinic Endonuclease-1 (APE1) and Poly(ADP-ribose) polymerase-1 (PARP1), as well as the quantities of DNA damage product 8-Hydroxy-2'-deoxyguanosine (8-OH-dG) was investigated liquid chromatography-high resolution mass spectrometry (LC-HR/MS) and liquid chromatography-tandem mass spectrometry (LC-MS/MS) techniques. L6 promotes a significant downregulation in the expression levels of both PARP1 and APE1 in HT29 cells. The *in vivo* efficacy of L6 was evaluated both in CD1 nude mice and BALB/c mice. In the xenograft model established with the HT29 cell line, the optimal dosage of L6 was determined to be 3 mg/kg, administered in a total of 4 doses, with a treatment frequency of twice per week. A syngeneic animal model was generated using the CT26 cell line, followed by the administration of sequential therapy with the L6 molecule and anti-PD-L1. After the euthanize the animals, immunophenotyping was performed by flow-cytometry on excised tumor tissues. The results obtained indicate that the L6 molecule led to a reduction in tumor size, decrease in Treg cell count, and an increase in the activated $CD8^+$ cells.

Key words: Cancer, telomere, telomerase, TIF (telomeric induced foci), xenograft, syngeneic, LC-MS/MS, APE1, PARP1, 8-OH-dG

ÖZET

Yilmaz M., Telomer Hedefli Yeni İlaç Adayı Bileşiklerinin Farklı Kanser Hücre Hatlarında İn Vitro ve İn Vivo Etkilerinin İncelenmesi Hacettepe Üniversitesi Sağlık Bilimleri Enstitüsü, Tıbbi Biyokimya Anabilim Dalı, Doktora Tezi, Ankara, 2023. Kanser, heterojenitesi ve metastatik özelliklerinin yanı sıra tedavi edilebilirliğinin sınırlı oluşu ile küresel olarak önde gelen ölüm nedenlerinden biridir. Kanser hücreleri telomeraz enzimi aktivitesi ile telomerlerini uzatmakta ve hücre siklusundaki kontrol noktalarından kaçarak immortal özellik kazanmaktadır. Kanser hücrelerinin %95'inde telomeraz ekspresyonu varken normal somatik hücrelerde baskılanmış olması nedeniyle, son yıllarda telomeraz/telomer hedefli tedaviler umut vaat etmektedir. Kanser hücrelerinin heterojenitesi ve farklı telomer uzunluklarına sahip olması nedeniyle, uzun süreli anti-telomeraz tedavilere bağlı yan etkiler görülebilmektedir. Bu nedenle telomerik uzunluklardan bağımsız olarak kısa sürede etki edebilecek telomerleri hedef alan yeni moleküllere ihtiyaç vardır. Bu doktora tezi çalışması kapsamında, telomerik yapılara telomeraz tarafından eklenen ve telomerik DNA hasarına neden olarak genomik kararsızlığa ve hücre ölümüne yol açabilecek moleküllerin *in vitro* ve *in vivo* olarak test edilmesi amaçlanmıştır. Bu moleküller, MAIA (Chicago, USA) biyoteknoloji firması tarafından sentezlenmiş ve Tıbbi Biyokimya Anabilim Dalı'na gönderilmiştir. Bu ilaç adayı moleküller, farklı kanser hücre hatlarına [meme kanseri (MCF-7), küçük hücre dışı akciğer kanseri (A549), rahim ağzı kanseri (HeLa) ve kolon kanseri (HT29)] 9 farklı konsantrasyonda 96 saat süre ile uygulanmış, sitotoksisite MTT (3-(4,5-Dimethylthiazol-2-yl)-2,5-Diphenyltetrazolium Bromide) ile değerlendirilmiştir. Elde edilen EC_{50} sonuçları her bir hücre hattında 6-thio-dG ile karşılaştırılmış ve L6 olarak adlandırılan molekül 6-thio-dG'ye oranla daha düşük EC_{50} değeriyle yeni potansiyel ilaç adayı olarak belirlenmiştir. Farklı hücre hatlarının L6 molekülüne karşı verdikleri yanıtlar değerlendirilmiş ve L6 molekülüne en duyarlı hücre hattı olan HT29 kolon kanser hücreleri hedef hücre hattı olarak seçilmiştir. Telomeraz enzimi ile telomerik uçlara eklenen bu moleküllerin, telomerik uçlarda yarattığı DNA hasarı, TIF (Telomer induced foci) yöntemi ile konfokal mikroskop kullanılarak incelenmiştir. Bu yöntemde telomerik prob ve DNA hasarına özgü γH2AX Ab ile yapılan boyamaların kolokalizasyonu ile TIF odakları gösterilmiştir. TIF yöntemi sonuçları, L6

molekülünün oluşturduğu telomerik DNA hasarının kontrol grubu ve 6-thio-dG'ye göre istatistiksel olarak daha yüksek olduğunu göstermiştir. Global genomik hasar incelendiğinde 6-thio-dG ile L6 molekülünün eşit ölçüde global DNA hasarı oluşturduğu gözlemlenmiştir. Ek olarak, kullanılan adayı moleküllerin baz eksizyon onarımı (BER) yolu proteinlerinden Apürinik/Apirimidinik endonükleaz 1 (APE1) ve Poli(ADP-riboz) polimeraz 1 (PARP1) üzerindeki etkileri ve DNA hasar ürünleri olan 8-hidroksi- 2'-deoksiguanozin (8-OH-dG), miktarları da sıvı kromatografi-yüksek rezolüsyonlu kütle spektrometre (LC-HR/MS) ve sıvı kromatografi-sıralı kütle spektrometre (LC-MS/MS) kullanılarak incelenmiştir. Buradan elde edilen sonuçlara göre L6 molekülü, HT29 hücrelerinde PARP1 ekspresyonunda artışa ve APE1 ekspresyonunda ise azalmaya neden olmaktadır. *İn vitroda* etkinliği gösterilen moleküllerin *in vivo* etkinliği CD1 nude fareler ve BALB/c üzerinde test edilmiştir. HT29 hücre hattı ile oluşturulan ksenograft modelde L6'nın optimal dozu 3 mg/kg ve tedavi süresi haftada 2 kere olmak üzere toplam 4 doz uygulama olarak belirlenmiştir. CT26 hücre hattı kullanılarak singeneik hayvan modeli oluşturulmuş, takiben L6 molekülü ile anti-PD-L1 kombinasyonel tedavisi uygulanmıştır. Hayvanlar sakrifiye edildikten sonra çıkarılan tümör dokularında flow-sitometre ile immünfenotipleme yapılmıştır. L6 molekülünün tümör boyutunda küçülmeye, Treg hücre miktarında azalmaya ve aktive $CD8^+$ hücrelerinde artışa yol açtığı tespit edilmiştir.

Anahtar kelimeler: Kanser, telomer, telomeraz, TIF (telomeric induced foci), DNA, ksenograft, singeneik, LC-MS/MS, APE1, PARP1, 8-OH-dG

TABLE OF CONTENTS

SYMBOLS AND ABBREVIATIONS

µl : Microliter

5-FU : Fluoropyrimidine

6-thio-dG : 6-thio-2'-deoxyguanosine

8-OHdG : 8-Hydroxy-2'-deoxyguanosine

A549 : Human lung carcinoma epithelial cells

AP : Apurinic/apyrimidinic site

APCs : Antigen-presenting cells

APE1 : Apurinic/Apyrimidinic Endonuclease 1

ATCC : American Type Culture Collection

ATM : Ataxia telangiectasia–mutated gene

ATP : Adenosine triphosphate

ATR : Ataxia telangiectasia and Rad3-related

BER : Base excision repair

BSA : Bovine serum albümin

CAFs : Cancer-associated fibroblasts

CAP : Capecitabine

CAPIRI : Capecitabine + irinotecan

CD8 : Cytotoxic T lymphocytes

CD4 : T lymphocytes or helper T cells

cGAMP : 2',5'-cyclic GMP-AMP

cGAS : Cyclic GMP-AMP synthase

CHK1 : Checkpoint kinase 1

CHK2 : Checkpoint kinase 2

CIN : Chromosomal instability

CNS : Central nervous system

CRC : Colorectal cancer

CT26 : Murine colorectal carcinoma cells

CTLs : $CD8^+$ cytotoxic T lymphocytes

CTLA-4 : Cytotoxic T-lymphocyte-associated protein 4

DAMPs : Danger-associated molecular patterns

DAPI : 4',6-diamidino-2-fenilindol

DCs : Dendritic cells
DDR : DNA damage response
DiAna : Distance Analysis
DMEM : Dulbecco Modified Eagle Medium
dMMR : DNA mismatch repair deficiency
DNA : Deoxyribonucleic acid
dNMP : Deoxyribonucleoside monophosphate
DSBs : Double-strand breaks
EC_{50} : Half maximal effective concentration
ELISA : The enzyme-linked immunosorbent assay
ER : Endoplasmic reticulum
FBS : Fetal bovine serum
FDA : Food and Drug Administration
FOLFOX : 5-fluorouracil + oxaliplatin
FOXFIRI : 5-fluorouracil + irinotecan
GRN163L : Imetelstat
GTP : Guanosine triphosphate
HCl : Hydrochloric Acid
HDFa : Human dermal fibroblast cells
HeLa : Human cervix adenocarcinoma epithelial cells
HR : Homologous recombination
HT29 : Human colorectal adenocarcinoma cells
hTERT : Human telomerase reverse transcriptase
ICB : Immune checkpoint blockade
IFN : Type I interferon
IFN-I : Interferon type I
IFN-γ : Cytokine interferon-γ
IRI : Irinotecan
IS : Internal standards
LC-HR/MS : Liquid chromatography-high resolution mass spectrometry
LC–MS/MS : Liquid chromatography with tandem mass spectrometry
M2 cells : Type 2 macrophages

mAbs : Monoclonal antibodies
MCF7 : Human breast adenocarcinoma cells
$MgCl_2$: Magnesium chloride
MHC : Major histocompatibility complex
MTT : 3-(4,5-Dimethylthiazol-2-yl)-2,5-Diphenyltetrazolium Bromide
MSI : Microsatellite instability
MSI-H : MSI-High
NaCl : Sodium chloride
NAD : Nicotinamide adenine dinucleotide
NHEJ : Non-Homologous End Joining
NK cells : Natural killer cells
NIR : Nucleotide incision repair
OGG1 : 8-Oxoguanine DNA glycosylase 1
OX : Oxaliplatin
PARP1 : Poly (ADP-ribose) polymerase 1
PBS : Phosphate-buffered saline
PBST : Phosphate-buffered saline with Tween 20 or Triton X-100
PD-1 : Programmed death-1
PD-L1 : PD-1 ligand
PI3K : Phosphatidylinositol 3-kinase
pMMR : Proficient in mismatch repair
PNA : Peptide nucleic acid
POT1 : Protection of telomeres
RAP1 : Ras-related protein
RAF : RAS/rapidly accelerated fibrosarcoma
RNA : Ribonucleic acid
RcdA : *(5′R)* 5′,8-cyclo-2′-deoxyadenosine
ROS : Reactive oxygen species
RPM : Revolutions Per Minute
RPMI : Roswell Park Memorial Institute Medium
ScdA : *(5′S)* 5′,8-cyclo-2′-deoxyadenosine

SDS : Sodium dodecyl sulfate
SSB : Single-strand break
SSC : Saline-sodium citrate
SSBR : Single-strand break repair
STING : Stimulator of IFN Gene
TBPs : Telomere-binding proteins
TFs : Transcription factors
TIF : Telomere Dysfunction Induced Foci
TIN2 : Interacting nuclear factor-2
TLR : Toll-like receptor
TME : Tumor microenvironment
TNR : Trinucleotide repeat
TRAP : Telomerase Repeated Amplification Protocol
Tregs : Regulatory T cells
TRF1 : Telomeric repeat binding factor 1
TRF2 : Telomeric repeat binding factor 2
TPP1 : Tripeptidyl peptidase 1
U87 : Human glioblastoma cells
WHO : World Health Organization
XELOX : Capecitabine + oxaliplatin
ZnCl : Zinc chloride

FIGURES

TABLES

1. INTRODUCTION

1.1 Aim

Comprehending the significance of telomeric DNA in carcinogenesis holds promise for the development of novel screening and diagnostic methodologies, as well as innovative strategies for cancer treatment.

Telomerase is an appealing target for cancer therapy due to its fundamental role in mediating immortalization in cancer cells through telomere elongation. Telomerase serves as a remarkably precise objective for transformed cells since the reverse transcriptase activity being suppressed in the majority of normal adult somatic cells. However, there are exceptions such as certain stem-like cells and T cells, which exhibit transient activation of telomerase during proliferation [1]. Hence, therapeutic approaches focused on telomerase hold the extensive potential for wide-ranging medical treatments. Furthermore, oncogenic signaling pathways often demonstrate significant duplicity which mostly contributes to the therapeutic resistance. Based on current understanding, tumor cells are therefore will have a restricted ability to develop resistance against telomerase therapies. Consequently, considerable effort has been directed towards developing novel drugs that target specifically telomerase. Although the inhibition of telomerase activity may initially appear promising, it is important to note that upon completion of treatment, the reactivation of telomerase activity can occur, subsequently leading to tumor relapse. Therefore, the implementation of efficient approaches focused on telomeres rather than telomerase activity could revolutionize cancer therapy. In summarize, strategies focused on targeting telomeres present a remarkable potential for the development of impactful and efficient therapeutic approaches. Herein, we investigated in vitro and in vivo effects of the telomere-targeted new drug candidate compounds on different cancer cell lines.

2. GENERAL INFORMATION

2.1. The Structure and Significance of Telomeres

Telomeres at the ends of chromosomes are vital for maintaining chromosome stability by preventing DNA damage, unnecessary repair, and fusion with other chromosomes. Telomeres in mammals are structured from repetitive nucleotide sequences, consisting precisely of tandem repeats of the TTAGGG sequence [2, 3]. In a diploid human cell, the two ends of each of the 46 chromosomes are capped with telomeres, resulting in a total of 92 telomeres. Human telomeric DNA consists of tandem repeats of double-stranded DNA nucleotide sequence 5′-TTAGGG-3′, with each repeat spanning 10-15 kilobases (kb) at birth. Additionally, there is a 3′ G-rich single-stranded overhang that is 150-200 nucleotides long. These telomeric structures are stabilized and regulated by telomere-binding proteins (TBPs) [2]. The formation of the telomere spatial structure involves the invasion of the 3′G-rich overhang into the homologous double-stranded TTAGGG region, leading to the establishment of a smaller D-loop. Subsequently, the assembly of the larger T-loop is facilitated by the shelterin protein complex, which provides protective functions [3]. In order to facilitate shelterin binding and inhibition of a DNA damage response (DDR) at chromosome ends, telomere protection necessitates the presence of a minimum length of TTAGGG repeats [4]. Chromosome stability necessitates a dynamically regulated equilibrium between DNA attrition and acquisition within each terminal tract of telomeric repeats. Eukaryotic chromosomal DNAs, necessitate supplementary mechanisms beyond conventional DNA polymerases to achieve the replication of their terminal regions. The maintenance of this balance is significantly influenced by telomeric repeat integration facilitated by a specialized reverse transcriptase enzyme known as telomerase.

Telomerase, primarily facilitates the synthesis of telomere sequences by appending telomeric DNA onto the ends of chromosomes [5, 6]. One of the inherent risks associated with the linear configuration of chromosomal DNA involves the need to protect telomeres against end-to-end fusion, a typical mechanism utilized for repairing DNA breaks within chromosomes. Telomere fusion can lead to

chromosomal instability, necessitating its prevention to maintain genomic integrity [5].

Telomeres also play a crucial role in protecting the integrity of chromosomes by shielding their ends from degradation and preserving vital genetic information. With each cell division, telomeres undergo a shortening process, losing genetic content that is essential for the cell's function. This phenomenon arises from the combination of end replication and DNA processing at the chromosomal termini. During the semiconservative replication of DNA, the delayed strand (formed by the merging of Okazaki fragments) possesses an incomplete 5′ end after the RNA primer is removed. As a consequence, this resulting gap remains unfilled due to the inherent 5′ to 3′ directionality of DNA polymerases responsible for synthesizing the polynucleotide chain [3].

Therefore, the regulation of telomere function significantly influences crucial aspects of human cancer biology. Primarily, active maintenance of telomeres is nearly always essential for complete oncogenic transformation of human cells, enabling cellular immortalization by conferring them with infinite replicative potential. Secondly, the gradual shortening of telomeres during replication leads to the finite replicative lifespan of cells in culture, resulting in a process known as senescence. This process plays a paramount role in tumor suppression in vivo.

2.2. The Association of Telomere Organization and Function with Cancer

Cancer is predominantly a genetic disorder associated with aging, characterized by the progressive accumulation of genomic instability in otherwise healthy cells, leading to the development of immortality. The process involves successive cell divisions that induce chromosomal instability due to telomere attrition, consequently contributing significantly to genomic rearrangements that facilitate tumorigenesis. Telomere dysfunction has been observed to play a pivotal role in the process of carcinogenesis, predominantly due to its association with chromosomal instability and cellular immortalization [7].

The maintenance of chromosome stability primarily depends on the dynamics of telomeres, with alterations in telomere length potentially contributing to the premature onset of cancer [8]. Cellular division represents a potentially hazardous process, prompting organisms with renewable tissues to develop sophisticated mechanisms aimed at constraining the maximum number of allowable divisions. During the process of cellular division in normal cells, telomeres gradually shorten with each cell replication, caused by the depletion of repetitive TTAGGG sequence. This continues until a critical threshold known as the Hayflick limit is reached, at which point the cells enter a state of senescence [9]. The progressive shortening in telomere length observed during cellular aging is hypothesized to serve as a protective mechanism, inhibiting unregulated cell proliferation and thereby preventing the risk of cancer formation in both humans and other mammals [2, 10].

The maintenance of telomere length and the protecting of telomere integrity are both orchestrated by shelterin complex. Shelterin, also known as telosome, has the capacity to engage or temporarily recruit distinct functionalities that play a crucial role in the maintenance of telomere integrity [11]. The shelterin complex is composed of six polypeptides and assembles through the binding of the double stranded TTAGGG. Telomeric repeat binding factor 1 (TRF1), telomeric repeat binding factor 2 (TRF2) the protection of telomeres 1 (POT1), ras-related protein (RAP1), tripeptidyl peptidase 1 (TPP1) and interacting nuclear factor-2 (TIN2) proteins form shelterin complex. TRF1 and TRF2 are two sequence-specific DNA binding proteins that directly bind to the double-stranded telomere sequences and recruit RAP1, TIN2, TPP1 and POT1 (Figure 2.2). Both TRF1 and TRF2 have the regulatory effect over telomerase, thereby inhibiting telomere elongation. TIN2 functions as a stabilizing protein that facilitates the interaction between TRF1, TRF2, and the TPP1-POT1 complex, thereby serving as a molecular bridge between components associated with double-stranded DNA and those associated with single-stranded DNA [12]. RAP1 is a stabilizing protein that is intricately linked with TRF2 and plays a pivotal role in the inhibition of DNA repair processes [13]. TPP1 engages in protein-protein interactions with TIN2 via its C-terminal domain and with POT1 through its central domain. Furthermore, TPP1 functions as a recruiter, facilitating the localization of POT1 to telomeric regions [14].

TPP1 enhances telomerase processivity in the presence of POT1 [15]. POT1, with its N-terminal domain, crucially defines cis-inhibition of telomerase by specifically binding to the single-stranded telomeric DNA sequence 5'-TAGGGTTAG-3', which includes the G-strand overhang and likely the displaced G-strand at the D-loop (Figure 2.3). The abundance of POT1 molecules at telomeric regions was diminished when the amount of single-stranded DNA content was decreased. Additionally, the interaction between POT1 and telomeric DNA was found to be modulated by the TRF1 complex in response to telomere length [16]. Shelterin, facilitated by G-rich nucleotide repeats in telomeres, suppresses DNA damage signaling, inhibits DNA repair processes, and protects telomeres from being identified as double-strand breaks (DSBs), preventing incorrect repair via non-homologous end joining (NHEJ) and homologous recombination (HR) pathways [4, 17, 18]. The unpaired overhang strand has the ability to undergo a folding process, resulting in the formation of a lariat structure known as the t-loop. This unique configuration allows the chromosome terminus to be securely protected [4, 19, 20].

Telomere maintenance-associated proteins have been observed to be recruited to telomeres alongside DDR early response proteins, indicating their participation in DDR mechanisms. In normal circumstances, there appears to be a paradoxical relationship between DDR factors and the restoration and preservation of telomeres, as they seem to interfere the process. Depletion or dysfunction of shelterin components induces the activation of the ATM (ataxia telangiectasia–mutated gene) or ATR (ataxia telangiectasia and Rad3-related) DNA damage responses, leading to the arrest of the cell cycle and the emergence of chromosomal instability [11].

The protein TRF2 exhibits the ability to interact with and downregulate ATM, whereas POT1, when specifically bound to the G-tail via TPP1 acts as an inhibitor of ATR. The inhibition of TRF2 function triggers the activation of p53 and ATM, resulting in the formation of telomere dysfunction-induced foci (TIFs). TIFs, are formed through the NHEJ mechanism, leading to the fusion of telomeres throughout the entire DNA strand. The presence of TIFs is closely associated with the initiation of cellular senescence **[21]**. In addition, TRF2 plays a fundamental protection role in

the ends of telomeres promoting the establishment of the t-loop structure. In TRF2-knockout mouse embryo fibroblasts, the disruption of the TRF2 structure has been demonstrated to result in the loss of the protective capped structure. This loss is characterized by the processing of the 3′ overhang and the ligation of chromosome ends **[22]**. Additionally, the removal of POT1 leads to the occurrence of chromosomal end-to-end fusions. The two POT1 proteins found in mice, POT1a and POT1b, exhibit distinct roles. Disrupting the POT1a gene triggers DDR at telomeres, resulting in increased chromosomal fusions and anomalous HR at telomeres **[23, 24]**. TRF1 also plays a dual role in regulating telomere length and promoting DNA replication at telomere repeats, which are known as fragile DNA loci **[25, 26]**.

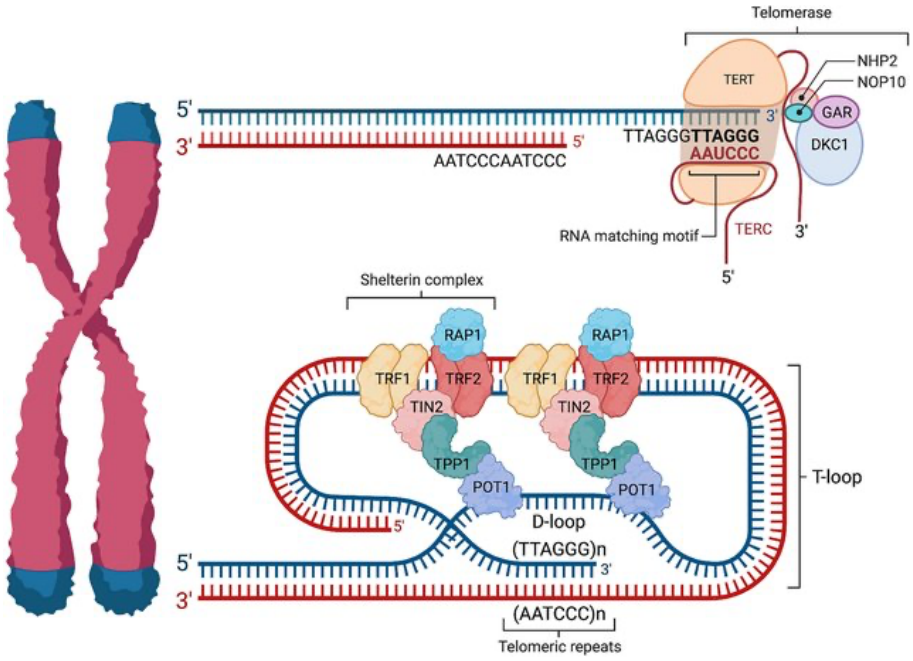

Figure 2.2. Telomere structure, shelterin complex and telomerase [27].

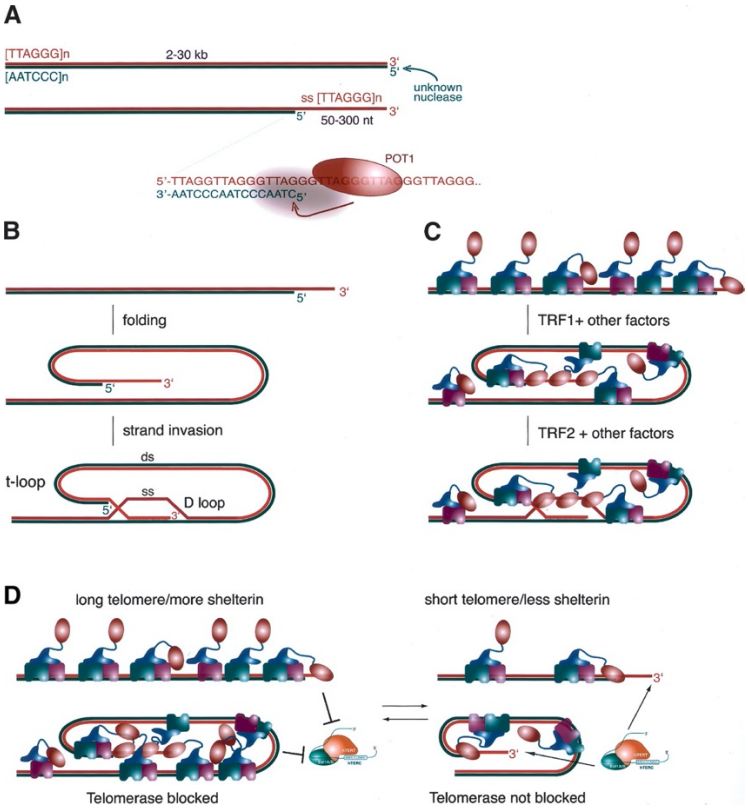

Figure 2.3. How shelterin shape telomeres. (A) Telomere terminus generation involves post-replication processing of chromosome ends to acquire a lengthy 3′ overhang, with the responsible nuclease remaining unidentified. The resulting 5′ end consistently exhibits the ATC-5′ sequence, a precision disrupted when POT1 is inhibited. The mechanism by which POT1 determines the 5′ end sequence is unknown, yet the resultant terminal structure becomes a favored binding site for POT1 in vitro. (B) The t-loop structure emerges as the 3′ overhang invades the adjacent duplex telomeric repeat array, forming a variable-sized D-loop. (C) TRF1, within shelterin, can potentially fold the telomere, while TRF2 is capable of mediating t-loop formation in vitro. (D) Regarding telomere length regulation, longer telomeres with increased shelterin are proposed to enhance POT1 loading on the overhang, inhibiting telomerase. Conversely, shorter telomeres with reduced shelterin decrease the likelihood of POT1 binding, allowing telomerase to elongate the telomere [28]

Genomic instability, a prevalent feature observed in many cancer types, have a fundamental contribution in the process of tumorigenesis by facilitating the rapid accumulation of genetic alterations, thereby driving the evolutionary progression of

cancer cells. In certain cancer subtypes, specifically in hereditary non-polyposis colon cancer, there is evidence of genomic instability occurring at the nucleotide level. This instability arises from mutations within the mismatch repair pathway, resulting in nucleotide insertions, deletions, and substitutions [29]. Excessive proliferation of preneoplastic cells may result in a significant source of genomic instability due to the occurrence of critical telomere shortening [30].

2.3. The Relationship Between the Replication End Problem and Senescence

Telomeres are composed of repetitive DNA sequences and associated proteins that serve as protective structures located at the ends of chromosomes. These structures prevent the identification of telomeres as DNA double-strand breaks, thereby avoiding their degradation or fusion by DNA repair mechanisms [31]. The 'end replication problem' occurs when DNA polymerase is unable to successfully replicate the terminal region of the chromosome during lagging strand synthesis. This, combined with potential processing events in both the leading and lagging daughter strands, leads to the progressive loss of telomeric repeats with each cell division resulting in a state of irreversible growth arrest known as cellular senescence. Therefore, telomeres function as a "chronometer" that regulates cellular lifespan [32, 33]. The capacity to overcome replicative senescence is believed to represent a crucial rate-limiting event in the progression of the significant proportion of malignancies.

Cellular senescence is initiated through the engagement of two interconnected pathways, encompassing irreversible cessation of the cell cycle, concomitant with a critical reduction in telomere length. The first mechanism induces an irreversible cell cycle exit, wherein the tumor suppressor genes, p53 and pRb, are activated at a specific temporal checkpoint. This activation is triggered by a critical shortening of chromosomal ends, a consequence of the end-replication problem encountered during DNA synthesis. The second mechanism takes place when telomeres reach a critically short length, leading to extensive end-fusion events that hinder further replication. The occurrence of telomere loss or shortening within telomerase-deficient somatic cells has demonstrated significant associations with genomic instability and the onset of carcinogenesis [34].

The expression of telomerase allows the majority of tumor cells, specifically more than 80%, to re-activate mechanisms responsible for preserving their telomeres. Telomerase-positive cells uphold telomeres at a consistent length, leading to the evasion of senescence and acquisition of cellular immortality. Genetic mutations that inactivate crucial regulators involved in G1 phase progression within mammalian cells are prevalent in the majority of human cancers. When only a few telomeres became short, they induce DNA damage signal resulting in growth arrest, also named as Mortality Stage 1 (M1). M1 is under the control of cell-cycle checkpoint pathways such as p53 / p16 / Rb. Due to the loss of cell-cycle checkpoint proteins, the cells continue to replicate and telomeres shorten critically resulting in Mortality Stage 2 (M2), also called as crisis [35]. Some of the cells may exhibit reactivation or up-regulation of telomerase activity to evade M2-induced consequences [36]. Notably, certain cancer types may experience up-regulation of telomerase at earlier stages of development [31].

2.4. Role of Telomerase in Cancer

The vast majority of human tumor types exhibit evasion of cellular senescence and DNA damage-induced inhibitory signaling pathways through the upregulation of telomerase enzyme activity. Telomerase has fundamental roles in bypassing cellular senescence and promoting oncogenic processes through its regulation of telomere homeostasis and preservation. The enzymatic activity of telomerase exhibits a direct correlation with the proliferation of cancer cells and their stem-like properties. Additionally, reactivation mechanisms encompass gene locus amplification and rearrangements [37, 38]. In the initial phases of oncogenesis in adult somatic cells, the upregulation of telomerase activity synchronizes with concurrent alterations in pro-oncogenic factors [39]. Typically, malignant neoplasms exhibit telomerase expression, correlating with the potential for unrestricted cellular proliferation, while the majority of benign and pre-malignant tumors are distinguished by the absence of telomerase. Somatic mutations within the proximal promoter region of the human telomerase reverse transcriptase (hTERT) are presently regarded as the prevailing noncoding mutations in cancer. For instance, a significant proportion of primary melanomas

(67%–85%), glioblastomas (28%–84%), liposarcomas (74%–79%), and urothelial cancers (47%) contain TERT promoter mutations [40-43].

Telomerase is responsible for adding telomeric repeats onto the 3′ ends of chromosomes. The telomerase complex comprises two major components namely the catalytic subunit of hTERT, an enzymatic entity, and the RNA component (hTR or hTERC) [44]. Telomerase uses its integral concise template RNA, which encompasses an 11-base pair sequence that complements the telomeric single-stranded overhang, as a template to catalyze the synthesis of telomeric DNA with the repeating sequence (TTAGGG)n directly at the chromosome 3′-end. Following the addition of six bases, the enzyme undergoes a temporary pause to translocate the template RNA, facilitating the subsequent synthesis of the next 6-base pair repeat. This processive nature of telomerase allows for the extension of the 3' DNA template, eventually enabling further replication of the C-rich strand, thereby resolving the end-replication problem. During embryonic development, the enzyme is actively expressed; however, the hTERT gene undergoes silencing in most human somatic cells mainly due to the various tumor suppressor pathways [45] that leads to inhibition of the TERT gene expression [46], leading to the repression of telomerase activity. Betts and King examined telomerase activity across various developmental stages, from immature oocytes to blastocysts, using the Telomerase Repeated Amplification Protocol (TRAP) assay. They found decreasing telomerase activity during oocyte maturation and a subsequent reduction at the 8-cell stage, followed by a significant increase during the morula and blastocyst stages [47]. Xu and Yang also demonstrated a progressive decline in telomerase activity from the zygote stage to the 8-cell stage, with the highest level observed at the blastocyst stage, coinciding with the maternal-zygotic transition [48]. The analysis reveals that telomerase enzymatic activity exhibits an elevated presence during the initial and middle trimesters of gestation in comparison to the latter trimester. Particularly noteworthy is the substantial increase in activity detected within the early chorion at 5 to 9 weeks gestation. Nevertheless, a progressive decline in activity was noted over the temporal continuum, ultimately culminating in the absence of discernible activity within term placentas. Consequently, telomerase activity within the chorion is thus lasted over the course of gestation. The retention of telomerase

activity within the chorionic tissue may, therefore, be attributed to a stem cell subpopulation of trophoblast cells [49, 50]. However, stem cells, germ line cells and some normal somatic cells, such as hematopoietic cells, epidermal, endometrial and cervical cells with high regenerative potential exhibit telomerase activity [51].

Furthermore, TERT expression is influenced by the WNT signaling pathway, which plays a crucial role in maintaining stem cell identity. Specifically, in embryonic and adult stem cells and cancer cells, β-catenin, a pivotal component of the WNT signaling pathway, directly facilitates the activation of TERT transcription [52]. Additionally, the c-Myc oncogene exerts a positive regulatory effect on TERT transcription [53]. The pro-oncogenic potential of telomerase extends beyond its role in telomere elongation, contributing intricate interactions between the hTERT subunit and the signaling pathways regulating cellular survival and transformation [54].

In the absence of telomerase activity, the cycle of alternating lengthening and shortening of telomeres during cellular division has become disrupted. Consequently, the length of telomeres undergoes a reduction of 50–200 base pairs during each round of replication. Once telomeres reach a critically short state, leading to a loss of their protective function, the majority of cells exit the cell cycle until the cell population senesces [31]. This progressive shortening of telomeres ultimately results in an enduring cessation of cellular replication termed replicative senescence. However, this growth arrest is circumvented in immortal cell lines and the majority of tumors through the activation of a telomere maintenance mechanism.

Conclusive evidence has been presented supporting the involvement of telomerase in the regulation of apoptosis through a telomere maintenance-independent mechanism. TERT contains a mitochondrial localization signal peptide at its N-terminal region, which directs the translocation of TERT to mitochondria, where its activity has been demonstrated using the TRAP [55].

On the other hand, the dysregulation of telomeres, resulting from either telomeric repeat attrition or the breakdown of the telomere sheltering complex, induces

genomic instability, consequently influencing tumorigenesis. Specifically, the investigation of telomerase-deficient cells and mice exhibiting deficiencies in certain shelterin proteins supports the model. Artandi et al. [56] demonstrated that the intersection of telomerase-knockout mice with p53+/− mice led to a discernible alteration in the tumor profile typically observed in the p53-deficient context. Especially, the prevalent occurrence of lymphomas and sarcomas was dominated by carcinomas, which exhibited characteristic karyotypic anomalies such as nonreciprocal translocations frequently observed in human epithelial cancers [30, 56-58].

2.5. Role of DNA Repair Systems in Protecting Telomeres

Genomic instability represents a pivotal hallmark in the majority of cancer types, exhibiting a spectrum of consequences encompassing extensive point mutations, alterations in the length of repetitive sequences, and substantial chromosomal rearrangements. The genetic alterations play a fundamental role in the pathogenesis of cancer, primarily by activating oncogenes or inactivating tumor-suppressor genes. Additionally, numerous tumors exhibit persistent high-frequency mutagenesis, attributed to compromised checkpoint mechanisms, impaired DNA repair processes, and immortalization culminating in uncontrolled cellular replication [59, 60].

Certain elements of the DNA damage response pathways, initially characterized by their involvement in chromosomal DNA break repair, have been identified within telomeres and are essential for the regular maintenance and functionality of telomeres. Chromosomal DSBs can be repaired by two distinct mechanisms: nonhomologous end-joining (NHEJ) or homologous recombination (HR) [32].

Telomeres demonstrate heightened sensitivity to DNA damage elicited by oxidative stress [61]. Cells within tissues and organs experience continuous exposure to endogenous and exogenous stimuli, leading to the generation of reactive oxygen

species (ROS). Endogenous ROS largely originate from mitochondrial respiration, inflammatory cascades, and by-products of cellular signaling pathways. On the contrary, prominent exogenous origins of ROS encompass environmental contaminants, ionizing radiation, exposure to ultraviolet (UV) light, cigarette smoking, particular dietary selections, and specific pharmaceutical agents [62]. Nucleobase damages are typically investigated more extensively in relation to chemical carcinogenesis, given their direct association. These damages include oxidation, deamination, alkylation, and cross-linking, occurring at various nucleobase sites. Examples include N-7, O-6, C-8, and N-2 of guanine; N-1, N-3, and N-7 of adenine; O-2 and O-4 of thymine; and O-2 and N-4 of cytosine (Figure 2.4). Physiologically, maintaining low levels of ROS plays a crucial role in cellular signaling [63]. However, the occurrence of oxidative stress results from an imbalance between heightened ROS production and deficiencies in the antioxidant mechanisms responsible for the regulation and detoxification of ROS species. ROS-mediated oxidative DNA damage has been shown to significantly enhance mutagenesis and carcinogenesis, concomitant with senescence and the pathogenesis of degenerative ailments associated with the aging phenomenon [64]. In vitro studies reveal that telomeric DNA exhibits heightened susceptibility to cleavage by ROS in comparison to non-telomeric sequences [65].

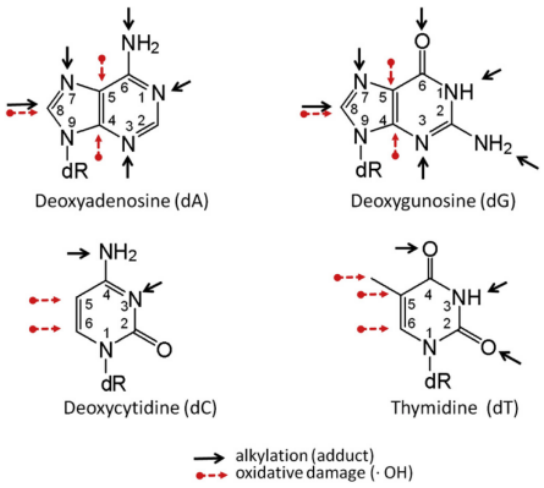

Figure 2.4. Nucleobases (nucleotides) possess reactive sites where damage is more likely to occur preferentially [66].

One of the prevailing oxidative DNA base alterations is 8-Oxo-7,8-dihydroguanine (8-oxoG) (Figure 2.5), which occurs within the genome at approximately 2,800 lesions per cell per day in unstressed cellular conditions (Figure 2.7) [67]. Extensive research has been devoted to 8-OxoG, revealing its profound biological impact and establishing it as a universal indicator of DNA damage resulting from oxidative processes [68-70].

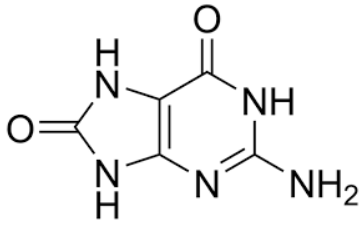

Figure 2.5. The structure of 7,8-dihydro-8-oxoguanine (8-oxoG)

Telomeric TTAGGG repeats have been identified as highly favored loci for the formation of 8-oxoG [71, 72]. The relatively elevated occurrence of this phenomenon can be attributed, in part, to the diminished redox potential exhibited by guanine, making it exceedingly prone to oxidation (Figure 2.6) [70]. Prior studies have demonstrated that the presence of 8-oxoG lesions and abasic repair intermediates in telomeric DNA interferes with the in vitro binding of TRF1 and TRF2 [73]. The base excision repair (BER) mechanism facilitates the elimination of 8-oxoG modification. Repair is initiated through the activity of the bi-functional glycosylase OGG1, which facilitates the excision of 8-oxoG located opposite C in duplex DNA and also exhibits the ability to cleave the DNA backbone. Apurinic/apyrimidinic endonuclease 1 (APE1) catalyzes the excision of the terminal 3′ sugar residue, leading to the formation of a single-nucleotide gap or the incision of the DNA backbone at an abasic site [74]. Poly [ADP-ribose] polymerase 1 (PARP1)'s interaction with the repair intermediate triggers the activation of poly(ADP-ribose) (PAR) biosynthesis, consequently expediting the prompt recruitment of the downstream proteins [75]. Nevertheless, the proficiency of this repair pathway necessitates the presence of a complementary DNA strand. Consequently, telomeres, characterized by a single-stranded 3′ overhang comprising approximately 50-100 nucleotides, may be subjected to persistent damage [76].

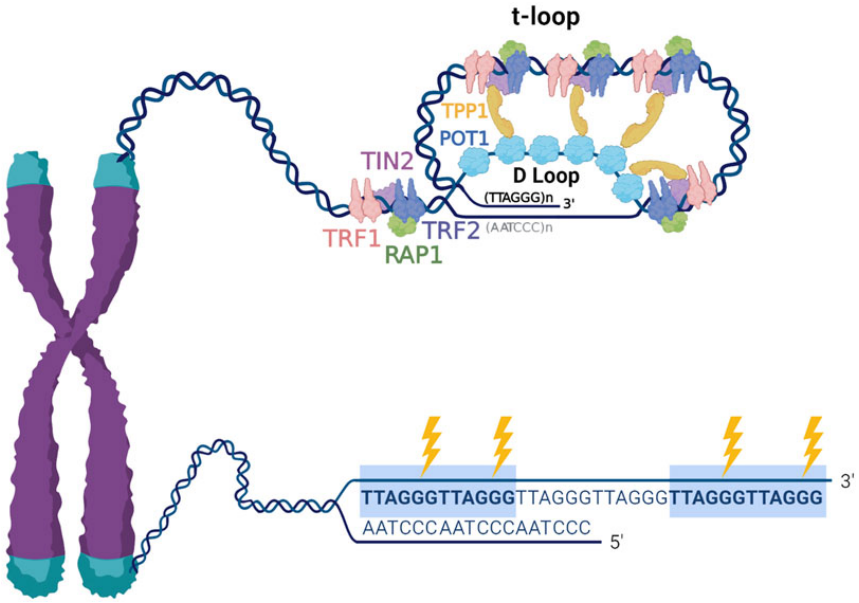

Figure 2.6. The structural composition of telomeres and their susceptibility to oxidative damage [72].

2.5.1. Base Excision Repair (BER)

Typically, the restoration of minor DNA base lesions, frequently those that do not distort the helical structure, such as 8-oxoG, is accomplished through the one of the major mechanisms for DNA repair; BER pathway. This pathway employs a set of remarkably conserved proteins responsible for crucial stages of lesion identification and DNA repair processes, such as the induction of DNA glycosylases, to impede the progression of additional DNA lesions. 8-Oxoguanine DNA glycosylase 1 (OGG1), an enzyme involved in the initial stages of the BER pathway, exhibits specialized activity in the excision of 8-oxoG lesions.

The process of BER comprises several key steps: initial recognition of DNA damage, removal of the damaged base, cleavage of the sugar-phosphate backbone, processing of the resulting gap (including the insertion of deoxyribonucleoside monophosphate, dNMP), and ultimately, DNA ligation. During the initiation phase, a lesion-specific DNA glycosylase identifies a damaged heterocycle and catalyzes the hydrolysis of the N-glycosidic bond, resulting in the creation of an

apurinic/apyrimidinic (AP) site within the DNA duplex. Furthermore, the appearance of an AP site within DNA may arise as a consequence of the spontaneous hydrolysis of the N-glycosidic bond. AP sites are predominantly subjected to cleavage by APE1 through hydrolytic mechanisms, leading to the formation of a single-strand gap harboring 5′-deoxyribose phosphate and 3′-hydroxyl groups during the synthetic phase of the BER process [77].

APE1 endonuclease catalyzes the incision of the phosphodiester bond at the 5' position of the AP, resulting in the formation of a single-strand break (SSB) harboring a 3' hydroxyl group and a 5' sugar phosphate. Subsequently, DNA polymerase (Pol) β excises the 5' sugar phosphate utilizing its lyase activity, and subsequently repairs the gap via templated DNA synthesis. Furthermore, PARP1 plays pivotal roles in orchestrating and recruiting proteins implicated in single-strand break repair (SSBR) and BER processes [61].

2.5.2. Apurinic/Apyrimidinic Endonuclease 1 (APE1)

Engaging in DNA repair mechanisms and orchestrating cellular responses to oxidative stresses, APE1 emerges as a multifunctional enzyme crucial for safeguarding genome integrity. APE1 exerts its enzymatic function in DNA repair by its nuclease domain, possesses with both endonuclease and 3′–5′ exonuclease activities [78].

In the BER pathway, APE1 functions as an AP site-specific endonuclease, catalyzing the initiation of repair processes for prevalent DNA lesions, such as uracil, alkylated and oxidized bases, and abasic sites. This enzymatic activity involves cleaving the phosphodiester backbone at the site of damage to facilitate subsequent repair steps [79]. The nuclease domain of APE1 exhibits 3′–5′ exonuclease activity, which plays a crucial role in various cellular processes, including DNA mismatch repair [80], nucleotide incision repair (NIR), trinucleotide repeat (TNR) expansion-associated BER [81], DNA SSB repair, removal of 3′-blocking groups in a nucleotide excision repair (NER)-independent pathway [82], and facilitation of apoptosis [83]. Moreover, The AP endonuclease activity and gene regulatory domains of APE1 play

a vital role in the stabilization of telomeric DNA. Consequently, this unanticipated function of APE1 at telomeres establishes a direct association between BER and telomere metabolism [84]. Indeed, APE1's localization at telomeres plays a crucial role in facilitating the proper interaction with the protective protein TRF2 [84]. Conversely, the absence of APE1 results in an augmented association of POT1 with telomeres, thereby instigating a notable enhancement in APE1's AP-endonuclease activity in an in vitro [85, 86]. Furthermore, in cells expressing telomerase, the telomeres exhibit a rapid reduction in length following APE1 depletion, undergo frequent aberrations and fusions [87].

Recent findings have demonstrated that the DNA repair functionality of APE1 exerts an influential role in the modulation of transcriptional regulation. Amongst the diverse array of DNA lesions provoked by oxidative stress, 8-oxoG emerges as the most prevalent form [88]. The occurrence of 8-oxoG can delay the progression of RNA polymerase, eliciting a state of transcriptional arrest and instigating the process of DNA repair. Consequently, 8-oxoG acts as a transcriptional repressor in the regulatory mechanism of genes [89]. Moreover, APE1 exerts regulatory control over the transcription factors (TFs) involved in target gene expression and upholds genomic integrity by facilitating DNA damage repair.

DNA repair mechanisms are linked to the acquisition of resistance to anticancer drugs, counteraction of the effects of radiotherapy, promotion of tumor aggressiveness, and poor prognosis. Consequently, targeting and inhibiting APE1 represents a highly promising approach for the development of novel antitumor drugs [90, 91].

2.5.3. Poly(ADP-ribose)polymerase 1 (PARP1)

Poly(ADP-ribose) polymerase 1 (PARP1) has been firmly established as a pivotal regulator of the cellular DNA damage response and apoptosis. Moreover, PARP1 plays a crucial role in the comprehensive control of DNA repair, transcription, telomere maintenance, and inflammation response through its modulation of diverse

DNA-protein and protein-protein interactions on a global scale. In terms of abundance, PARP1 stands as the preeminent chromatin-associated protein, surpassing histones. Remarkably, PARP1 plays a pivotal role in diverse cellular pathways, encompassing DNA damage response, apoptosis, transcriptional regulation, and chromatin organization, primarily facilitated by its catalysis of Poly(ADP-ribosyl)ation (PARylation) with utilizing nicotinamide adenine dinucleotide (NAD^+) as its biochemical substrate [92]. The expeditious and robust synthesis of Poly(ADP-ribose) (PAR) molecules, occurring locally at sites of damage, induces alterations in protein-protein and protein-DNA interactions. It concurrently acts as a molecular scaffold, facilitating the subsequent recruitment of chromatin modulators and DNA repair proteins (Figure 2.7) [93]. Consistently, PARP1 plays a pivotal role in initiating diverse DNA repair pathways, and targeted suppression of PARP1 induces synthetic lethality in DNA repair gene mutations, such as BRCA1/2 and PALB [94].

PARP1, operating as a DNA nick-sensor, engages with BER DNA intermediates harboring single-strand breaks. Upon binding to DNA lesions, PARP1 facilitates the catalysis of PAR synthesis, forming covalent attachments to itself and certain nuclear proteins. ADP-ribosylation of PARP1 is known to promote its detachment from DNA lesions, and it serves as a crucial regulatory factor in DNA repair processes. The autopoly(ADP-ribosyl)ation event induces a reduction in the DNA-binding affinity of PARP1, leading to enhanced dissociation from DNA substrates [95]. PARylation of PARP1 appears to play a pivotal role in modulating DNA repair processes. Substantial evidence supports the notion that PARP1 establishes a direct association with the incised AP site [96] and forms physical interactions with key constituents of the multiprotein short-patch BER (SP BER) machinery.

At telomeric regions, the involvement of PARP1 in the facilitation of DNA damage repair is evident by its activation of the alternative Non-Homologous End Joining (alt-NHEJ) and HR pathways [97]. Furthermore, it has been observed that PARP1 engages in interactions with TRF2 and induces covalent modifications on this protein [98]. Additionally, specific PARPs that are localized to telomeres, namely

Tankyrase 1 and Tankyrase 2, have been identified to perform modifications on TRF1, thereby governing telomere elongation and facilitating the separation of sister chromatids during the mitotic process. Moreover, PARP1 exhibits a higher concentration at telomeric chromatin during G-quadruplex stabilization, which plays a critical role in resolving replication-dependent damage [99, 100].

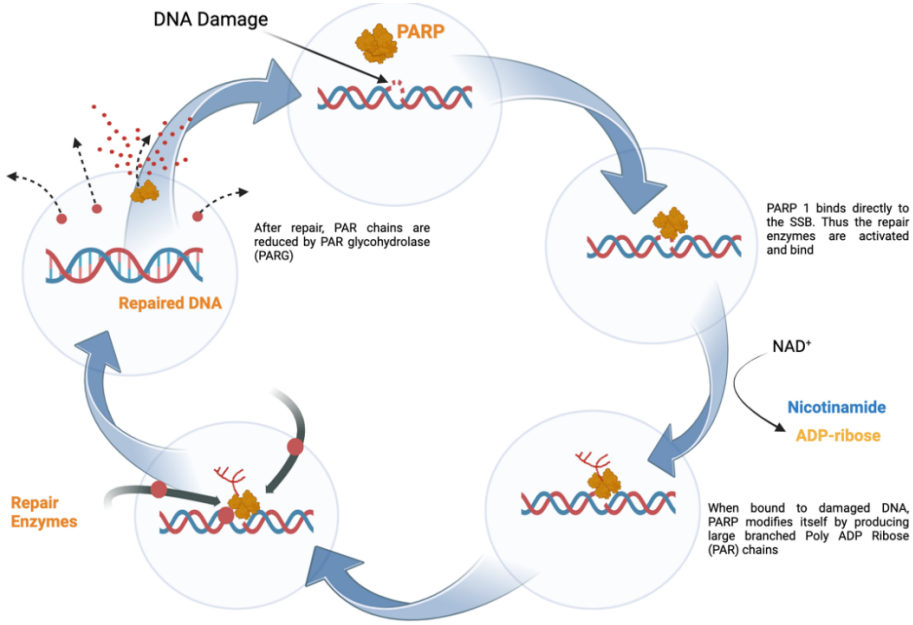

Figure 2.7. PARP1 is a key enzyme involved in the repair of single-stranded DNA breaks

2.5.4. Dysfunctional Telomeres Induce a DDR via ATM-ATR, Suppressing Tumor Formation

Despite the shelterin complex's primary function in safeguarding telomeres against detection as a DDR, numerous DDR proteins are found to localize to telomeres. Rather than identifying telomeres as damaged DNA, these proteins seem to be intricately involved in facilitating the accurate replication of telomeric DNA [101, 102]. At the core of the DDR two pivotal protein kinases hold significant importance, ATM and ATR. ATM primarily participates in the detection and activation of signaling pathways in response to DSBs [103], whereas ATR primarily engages in the response to DNA lesions subsequent to their conversion into single-stranded DNA intermediates [104]. Upon activation, ATM and ATR kinases initiate phosphorylation

of a multitude of factors, including CHK1 (Checkpoint kinase 1) and CHK2 (Checkpoint kinase 2). Subsequently, these kinases direct their attention towards diverse effector proteins, such as p53, thereby exerting regulatory influence over processes like DNA repair, transcription, and cell-cycle progression [105].

POT1 exerts inhibitory effects on ATR-mediated cellular responses, while TRF2 acts to inhibit ATM, thereby protecting against the occurrence of an extensive DNA damage response at telomeres, which could lead to catastrophic chromosomal rearrangements [22]. In the preliminary stages, the dysfunctional telomeres are marked by the aggregation of DNA damage-associated constituents, such as p53BP1 or γH2AX, at telomeric regions, like their presence at double-stranded breaks triggered by agents that cause DNA damage. Upon the depletion of the shelterin protein TRF2, telomeres undergo functional disruption, leading to the DNA damage signals that detectable through immunofluorescence imaging methodologies. These certain signals of telomeres are referred as telomere-dysfunction induced foci or TIFs [106]. Visualization of TIFs can be achieved through the co-localization of telomeres with factors responsible for DNA damage response. Dysfunctional telomere protective proteins within the shelterin complex, coupled with critically shortened telomeres, may result in the formation of 'uncapped' telomere structures. Consequently, these aberrant telomere configurations can trigger accelerated senescence, apoptosis, and/or chromosomal end-to-end fusions [106, 107].

The potential stimulation of ATM and ATR kinases through 8-oxoG processing in normal cells with functional DNA damage response pathways could potentially modulate telomere length due to the compelling evidence suggesting that these kinases play a regulatory role in telomerase recruitment [108, 109].

2.6. Targeting Telomerase and Telomeres: An Avenue for Anticancer Therapeutics

The preservation of telomeres facilitated by telomerase serves as a critical determinant allowing stem and cancer cells to evade senescence, consequently endowing them with

immortality [110]. Telomeres and telomerase are currently being investigated as potential targets for anticancer therapy. Targeting telomerase and telomere maintenance pathways holds significant potential as a promising therapeutic strategy for diverse malignancies. Telomerase, an exceptional reverse transcriptase enzyme, is recognized as a crucial element in the majority of cancer cells, primarily responsible for the regulation of telomere length. Additionally, telomerase presents a promising candidate for cancer therapy owing to the limited or absent telomerase activities observed in the majority of somatic cells. Numerous methodologies exist for the implementation of telomerase-based gene therapy as a prospective strategy for cancer treatment. Notably, cancer cells exhibit elevated telomerase activity compared to most other cells. The inhibition of hTERT presents a promising therapeutic option, owing to the observed upregulation of telomerase complex components in the majority of tumor cells. The targeted suppression of telomerase activity through the inhibition of hTR or hTERT to induce apoptosis has been extensively explored and is regarded as a promising therapeutic approach in the realm of cancer treatment [111]. The causative relationship between the inhibition of telomerase activity and the induction of apoptosis has been systematically examined in consideration of the pivotal role of telomerase in protecting telomere integrity. Therefore, the suppression of telomerase activity culminates in a gradual reduction of telomere length or the incapacitation of the telomere capping function within the shelterin complex, ultimately triggering apoptosis. Indeed, comprehending the significance of telomerase inhibition necessitates acknowledging that the inhibitory outcomes become solely subsequent to a substantial reduction in telomere length within cancer cells, achieved through continuous proliferation, ultimately leading to their entry into a state of crisis and subsequent death. Consequently, the duration required to achieve an effective cessation of tumor growth is theoretically relies on the original length of telomeres in the cancer cells. Due to the cancer cell's ability to undergo continued proliferation until the reception of a signal triggering growth arrest or apoptosis, their efficacy in first-line therapy is diminished.

2.6.1. Telomerase Targeted Therapies

The observed disparities in telomerase activity between normal versus tumor derived cells led to the hypothesis that telomerase could potentially serve as an appropriate target for precise anti-cancer therapies. Concisely, employing a specific telomerase inhibitor as a therapeutic approach is expected to engender progressive telomere attrition within cancer cells, ultimately inducing their senescence and death.

Antisense oligonucleotides and chemically-modified nucleic acids have demonstrated the capability to inhibit telomerase activity and elicit telomere attrition, leading to the subsequent induction of cellular senescence and/or apoptosis in in vitro cell cultures [112, 113]. These inhibitors exert their effects either through direct molecular interactions or indirectly by initiate apoptosis. Inhibition of telomerase can be achieved through targeting essential components, including the RNA template, hTERT protein, and associated proteins.

Imetelstat (GRN163L), a lipidated 13-mer thio-phosphoramidate oligonucleotide inhibitor, (5′-TAGGGTTAGACAA-3′), exhibits specificity and high binding affinity towards the RNA template region of the hTR. This inhibition is achieved by effectively targeting the catalytic site of the telomerase enzyme. When subjecting cancer cells to GRN163L in vitro, a consequential manifestation of either cellular senescence or apoptosis was observed, presenting a consistent correlation with the initial telomere length. This correlation necessitated the attainment of a critical threshold of telomere shortening. For instance, Burchett et al. exhibit the potential for reversing the immortal state of pancreatic cancer cells by consistently administering GRN163L. Continuous GRN163L exposure eventually resulted crisis and complete loss of viability. They demonstrated that crisis in cells accompanied with the initiation of a DNA damage response (γ-H2AX), along with indications of senescence (SA-β-galactosidase activity) and apoptosis (sub-G1 DNA content and PARP cleavage) [114]. Furthermore, GRN163L demonstrated significant suppression of tumor growth in various mouse xenograft models, primarily reliant on the telomere length as a determining factor [113, 115].

Despite being an attractive candidate for cancer therapy, telomerase inhibition by GRN163L has exhibited significant toxicities in recent investigations [116-118], notably thrombocytopenia, characterized by diminished platelet counts, due to the regulated telomerase activity in certain hematopoietic proliferative cells. As a consequence of these toxicities, patients necessitate discontinuation of the telomerase inhibitor, leading to rapid telomere length restoration [39]. In a Phase II clinical investigation, the therapeutic application of GRN163L was employed to treat pediatric patients afflicted with recurrent central nervous system (CNS) malignancies, namely recurrent medulloblastoma, high-grade glioma, or ependymoma. This study sought to explore the impact of GRN163L treatment on telomerase inhibition and the resulting treatment responses. A cohort comprising 42 patients was recruited for the study. Despite a notable 95% reduction in telomerase activity among the patients considered evaluable there were no instances of observable positive tumor responses. It is worth mentioning that the investigation also revealed a number of severe (grade 3 and 4) toxic reactions. The investigation necessitated premature conclusion due to the mortality of two patients resulting from intratumoral hemorrhage secondary to thrombocytopenia [119]. An additional Phase II clinical investigation investigated the effectiveness of GRN163L as a "modulatory" intervention in individuals diagnosed with progressive non-small cell lung cancer. Prevailing severe grade 3 and 4 adverse effects encompassed neutropenia and thrombocytopenia. Nevertheless, this investigation did not reveal any enhancements in progression-free survival among these patients subsequent to their treatment with GRN163L [116].

The thrombocytopenic properties of Imetelstat have undergone repurposing to address patients afflicted with essential thrombocythemia [117] and myelofibrosis [118]. Encouraging preliminary outcomes have been observed, though they come with significant side effects. Imetelstat treatment induces progressive telomere shortening through the inhibition of telomerase [120, 121], unfortunately substantial reductions in tumor size with therapeutic significance typically necessitate extended treatment durations [120]. Throughout the treatment period, a substantial portion of tumor cells will exhibit persistent proliferation until critically shortened telomeres undergo further shortening, ultimately leading to cellular apoptosis or growth arrest. Hence, the

therapeutic application of Imetelstat without adjuvant therapy could potentially present limitations in its capacity as a comprehensive anti-tumor agent against tumors, owing to the prolonged lag period required to elicit discernible outcomes [122].

Significantly, the remarkable rates of response observed may possess non-specific attributes, as evidenced by the absence of alterations in telomere lengths during the treatment regimen, and the lack of correlation between initial telomere lengths and clinical responses. In an alternative scenario, imetelstat potentially exhibits the ability to impede terminal maturation in megakaryocyte precursors by acting as an inhibitor of telomerase. A novel strategy for directing therapeutic efforts towards telomerase-expressing cancer cells involves the synthesis of telomerase-mediated, telomere uncapping compounds [122]. This approach presents the potential benefit of inducing rapid tumor regression while predominantly preserving telomerase-silent normal cells. This strategy circumvents the prolonged latency period typically observed between the initiation of therapy and the onset of tumor reduction. In a recent study, Imetelstat effectively reduced acute myeloid leukemia (AML) burden, particularly targeting subgroups with specific genetic mutations and oxidative stress-related gene expressions. Bruedigam C. et al. discovered that ferroptosis regulators play a key role in Imetelstat's effectiveness, and the drug induces excessive lipid peroxidation and oxidative stress. Combining Imetelstat with oxidative stress-inducing chemotherapy in a preclinical trial resulted in substantial disease control in AML [123]. In another phase III trial, Imetelstat showed significant benefits, including long-lasting transfusion independence, reduced transfusion burden, and increased hemoglobin concentrations in patients with anemia and lower-risk myelodysplastic syndromes (LR-MDS) who had relapsed or were refractory to standard treatments. Notably, Imetelstat exhibited robust activity across patient groups, including those with high transfusion needs, setting it apart from existing therapies [124]. It's important to highlight that while Imetelstat has shown promise in treating hematological disorders such as LR-MDS and AML, its efficacy in solid tumors is limited.

2.6.2. Telomere Targeted Therapies

2.6.2.1. 6-thio-dG (6-thio-2'-deoxyguanosine) (THIO)

6-thio-2′-deoxyguanosine (6-thio-dG) is an altered nucleoside, exhibiting a base modification, and serves as an analogue to the approved pharmaceutical agent, 6-thioguanine (Figure 2.8). Upon administration, 6-thio-dG undergoes prompt conversion into its active form, namely, 6-thio-2′-deoxyguanosine-5′-triphosphate (6-thio-dGTP), which acts as a substrate for telomerase. Subsequently, the compound relies on telomerase-mediated incorporation into telomeres.

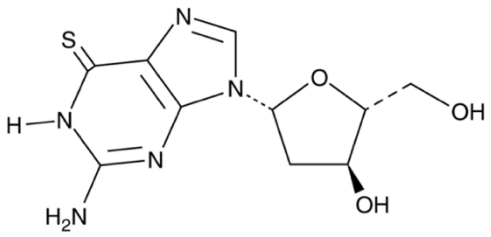

Figure 2.8. 6-thio-dG molecular structure

The compound exhibits the potential for integration within both genomic DNA (via DNA polymerases) and telomeric DNA (via telomerase) due to the swift conversion of 6-thio-dG into 6-thio-dGTP. After the integration of 6-thio-dG into telomeres, the guanine bases within the telomere sequence TTAGGG undergo modifications, leading to the decapping of telomeric DNA. This process is likely to cause the disassociation and reduced recognition of shelterin proteins from the newly formed, modified telomeres. This phenomenon induces the TIF and elicits prompt growth cessation or apoptotic death of telomerase-positive cells. The expeditious anti-cancer efficacy displayed by 6-thio-dG confers a significant advantage over alternative methodologies employing direct telomerase inhibition. The primary advantageous attribute of this telomere-targeted therapy, in comparison to direct telomerase inhibitors, lies in the absence of a prolonged latency period for tumor eradication, owing to the utilization of 6-thio-dG (Figure 2.9) [125].

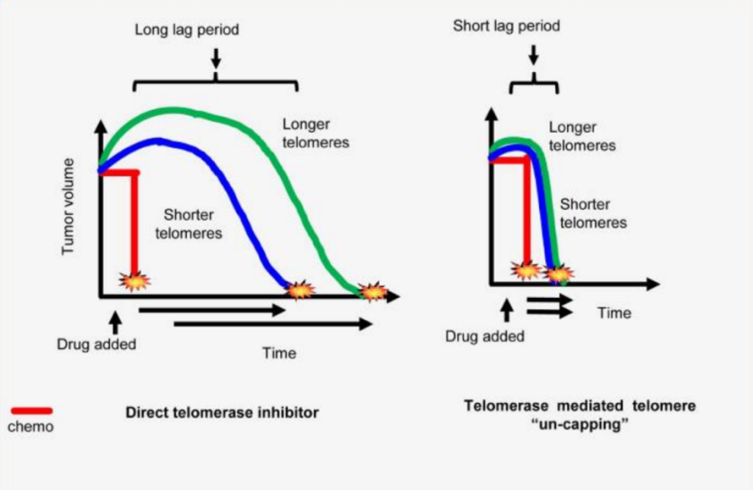

Figure 2.9. A comparative analysis of divergent methodologies in telomerase-targeted therapeutics [125]

THIO exploits the preferential integration into telomeres facilitated by telomerase, leading to the induction of telomere uncapping. It has minimal impacts on normal human telomerase-silent somatic cells. THIO induces cGAS/STING pathway, thereby eliciting antitumor immune responses [126]. Prior studies have demonstrated that mice that subjected to therapeutic dosages of THIO for a duration of up to one month exhibit no significant alterations in body mass and maintain normal hematological, hepatic, and renal functionalities [125]. In numerous studies, various tumor-derived xenograft models have rapid tumor shrinkage or growth cessation alongside minimal adverse effects [111-113]. Consistent outcomes were observed in vivo upon the administration of THIO to medulloblastoma xenograft models, it has been shown that THIO can cross the blood-brain barrier and selectively target telomerase-positive neoplastic cells [127]. Moreover, THIO has demonstrated remarkable anti-cancer efficacy against diverse solid malignancies in preclinical models [127, 128].

These findings demonstrate a compelling chemotherapeutic strategy for selectively targeting telomerase-expressing cancer cells while preserving normal cellular populations.

2.6.2.2. Second Generation Telomere Targeted Agents

The nucleoside prodrug analogue THIO represents a first-in-class telomerase-directed, telomere-targeted compound, exhibiting remarkable efficacy in diverse tumor models encompassing colorectal, lung, melanoma, and brain cancers. Second generation telomere-targeted agents are novel discovered compounds that are capable of engaging analogous mechanisms of action to THIO.

These molecules obtained by incorporation of unique lipid moieties into the 6-thio-dG molecules. The underlying hypothesis posits that the incorporation of diverse lipid moieties will significantly increase the cellular uptake and absorption of 6-thio-dG, leading to improved efficacy. These agents have improved specificity towards cancer cells relative to normal cells and potentially increased anticancer activity by selectively targeting and modifying telomeric structures of cancer cells.

2.7. Colorectal Cancer

Colorectal cancer (CRC) represents a highly lethal condition, demonstrating a 5-year survival rate of only 13% in the metastatic setting. Globally, it stands as the third most prevalent malignancy based on incidence and, concerning cancer-related mortality, holds the second position. The year 2020 witnessed a considerable burden of colorectal cancer, with 1,931,590 newly diagnosed cases worldwide, resulting in a distressing 935,173 fatalities. These statistics correspond to 10.0% and 9.4% of the total cancer incidence and mortality rates, respectively [129]. CRC is a condition that specifically arises in the colon or rectum due to the abnormal growth of glandular epithelial cells in the colon. CRC can be categorized into three main types: sporadic, hereditary, and colitis-associated. The susceptibility to CRC development is influenced by a combination of environmental and genetic factors. Furthermore, the incidence of CRC in individuals diagnosed with longstanding ulcerative colitis and Crohn's disease demonstrates an age-associated elevation [130].

CRC exhibits significant genetic diversity; nevertheless, it can undergo development through various mechanisms. Consequently, CRC is hypothesized to possess one of the most remarkable mutational burdens among all malignancies. CRC arises through a sequence of genetic or epigenetic modifications within epithelial cells, enable them to be hyperproliferative [131]. These hyperproliferative cells give rise to a benign adenoma, which has the potential to progress into cancer and initiate metastasis through various discrete mechanisms, encompassing microsatellite instability (MSI), chromosomal instability (CIN), and serrated neoplasia [132]. Cancer initiation begins with a small adenoma that evolves into giant adenoma and then eventually to cancer. This cascade highly correlates with the emergence of the CIN-positive subtype. According to the National Cancer Institute, this model accounts for 10-15% of cases within the sporadic colorectal cancer spectrum [133]. When an adenocarcinoma transitions into an invasive state, it can metastases via blood and lymphatic arteries. The process of colorectal carcinogenesis comprises four discernible phases: initiation, promotion, progression, and metastasis. Among these phases, the liver predominates as the principal metastatic locus, succeeded by the lung and bone in frequency of occurrence.

Hyperproliferation instigates the development of a (benign) polyp or adenoma to initiate (stage 0). Subsequently, ten percent of adenomatous polyps have the potential to undergo malignant transformation, giving rise to an adenocarcinoma that infiltrates the muscularis propria (stage I). The neoplasm exhibits progressive volumetric expansion and extends deeper into the tissue involving the serosa (stage II) and visceral peritoneum (stage III). This progression is followed by the potential manifestation of lymphatic or hematogenous metastases (stage IV). The disease's stage determines the severity of the disease and accessible therapeutic options [133].

Surgical intervention represents the established therapeutic protocol for CRC particularly for stage 0 to stage II [134]. In addition to surgical intervention, adjuvant therapy, chemotherapy, and targeted therapy are necessary for managing the other stages. Current chemotherapy protocols comprise single-agent therapy, predominantly fluoropyrimidine (5-FU), as well as polytherapy regimens incorporating agents such

as oxaliplatin (OX), irinotecan (IRI), and capecitabine (CAP or XELODA or XEL). The combined therapeutic regimens FOLFOX (5-fluorouracil + oxaliplatin), FOXFIRI (5-fluorouracil + irinotecan), XELOX, or CAPOX (capecitabine + oxaliplatin), along with CAPIRI (capecitabine + irinotecan), continue to serve as the predominant approaches in first-line treatment [135]. Numerous agents have been formulated and introduced into both preclinical and clinical investigations with the aim of targeting CRC. In 2004, the Food and Drug Administration (FDA) granted approval to cetuximab as the initial targeted therapeutic agent for CRC, succeeded within the same year by bevacizumab. Subsequently, further FDA-endorsed targeted pharmaceuticals designed for CRC treatment have emerged. CRC involves intricate downstream signaling pathways that regulate the initiation, progression, and migration. These pathways encompass significant mediators including Wnt/β-catenin, Notch, Hedgehog, and TGF-β/SMAD, alongside activators of signaling cascades like phosphatidylinositol 3-kinase (PI3K)/AKT or RAS/rapidly accelerated fibrosarcoma (RAF). These pathways also present favorable target for specific therapeutic interventions. Considering the intricate cascade of downstream signaling and the challenges associated with achieving complete inhibition of precise biological interactions, it is important to note that not all CRC-associated pathways currently identified can be effectively intervened [135].

The emergence of drug resistance to chemotherapeutic regimens presents an additional challenge in managing the growing population of CRC patients. Over the past few decades, the general prognosis for individuals dealing with advanced colon cancer has shown improvement owing to novel chemotherapy protocols. Despite response rates to contemporary systemic chemotherapies reaching noteworthy levels of up to 50%, the emergence of drug resistance appears to be nearly all among CRC patients. This phenomenon limiting the therapeutic potency of anticancer drugs and ultimately leading to chemotherapy failure [136].

2.8. Immunotherapeutic Approaches

While chemotherapy, targeted therapy, radiation therapy, immunotherapy, and surgery are the available treatment options, the dynamic nature of a patient's response to therapy and the progression of the disease necessitate an adaptable treatment plan [137, 138]. Notably, current clinical practice includes the use of three FDA-approved immune checkpoint inhibitors (ICIs)—Pembrolizumab, Nivolumab, and Ipilimumab—targeting programmed cell death 1 (PD-1) and cytotoxic T lymphocyte antigen 4 (CTLA-4) for colorectal cancer [139]. Despite their clinical utilization, ICIs demonstrate a limited impact on patient survival in research studies [140-142]. Therefore, it is crucial to have new advances in expanding the efficacy of immunotherapy. Immunotherapy has exhibited encouraging efficacies and favorable tolerability in gastrointestinal (GI)-related malignancies, including gastro-esophageal cancer and hepatocellular carcinoma [143].

Cancer immunotherapy represents the fourth cornerstone of cancer therapeutics, succeeding surgical intervention, chemotherapy, and radiation therapy. It encompasses the administration of cytokines, antibodies, checkpoint inhibitors, as well as immunocompetent cells like dendritic cells (DCs) and Cytotoxic T lymphocytes (T cells) [144]. Tumors consist of a heterogeneous cellular population, encompassing the cell of origin harboring genetic modifications, alongside a multitude of other cellular components, including fibroblasts, endothelial cells, and potentially various types of immune cells. In the early stages, the immune infiltrates exhibit limited presence, however, as the process evolves, they may consist of natural killer (NK) cells and lytic-capable macrophages, with a particularly crucial addition of T cells (Figure 2.10). T cells selectively target neoplastic cells presenting tumor-specific antigens as complexes of tumor-derived peptides bound to major histocompatibility complex (MHC) molecules on their cell membrane. Due to the notable efficacy exhibited by cancer immunotherapy approaches within the clinical settings, investigations in oncology and immunology have reaffirmed the pivotal significance of T cells in the recognition of tumor antigens and the subsequent eradication of cancer cells [145, 146]. Immune checkpoint therapy, by modulating regulatory pathways in

T cells to potentiate antitumor immune responses, has yielded significant clinical breakthroughs, presenting a novel weapon against cancer [147].

Immunotherapies have revolutionized the therapeutic landscape for numerous malignancies, representing a paradigm shift in the field of immuno-oncology [147-150]. Prominent therapeutic strategies in cancer treatment focus on inhibitory signaling molecules expressed on tumor and immune cells. These key molecules, including programmed death-1 (PD-1), its ligand PD-1 ligand (PD-L1), and cytotoxic T-lymphocyte-associated protein 4 (CTLA-4), play pivotal roles in immune response regulation. Therapeutic antibodies targeting these molecules have shown potential to restore the immune system's capacity to recognize and attack tumor cells effectively. [151, 152]. Therapeutic antibodies that specifically target the PD-1/PD-L1 have demonstrated significant clinical responses across various tumor types. Patients with melanoma, renal cell carcinoma, non-small cell lung cancer [149], and bladder cancer [153] experienced tumor regression upon treatment with anti-PD-L1. In Phase I clinical trials, *nivolumab*, an anti-PD-1 agent, exhibited comparable clinical responses [121]. In a recent substantial phase I clinical trial, the therapeutic antibody MK-3475 targeting PD-1 exhibited remarkable response rates of approximately 37 to 38% among patients diagnosed with advanced melanoma [154].

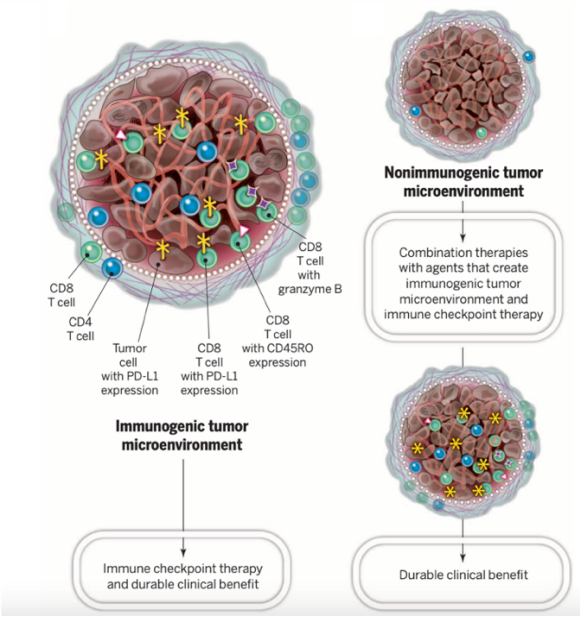

Figure 2.10. Immunogenic and non-immunogenic tumor environments [147].

PD-1 has been identified as a critical immune checkpoint that restricts the responses of activated T cells [155]. PD-1, expressed on various cell types, interacts with two ligands: PD-L1 and PD-L2. While PD-1 does not disrupt costimulation, it actively hinders signaling triggered by the T cell antigen receptor [156]. After exposure to the cytokine interferon-γ (IFN-γ), produced by activated T cells, PD-L1, one of its ligands, can be expressed on multiple cell types, such as T cells, epithelial cells, endothelial cells, and tumor cells (Figure 2.11) [157]. Recent observations suggest that the PD-1/PD-L1 pathway functions not primarily during early T cell activation but rather as a mechanism to shield cells from T cell-mediated attacks [147].

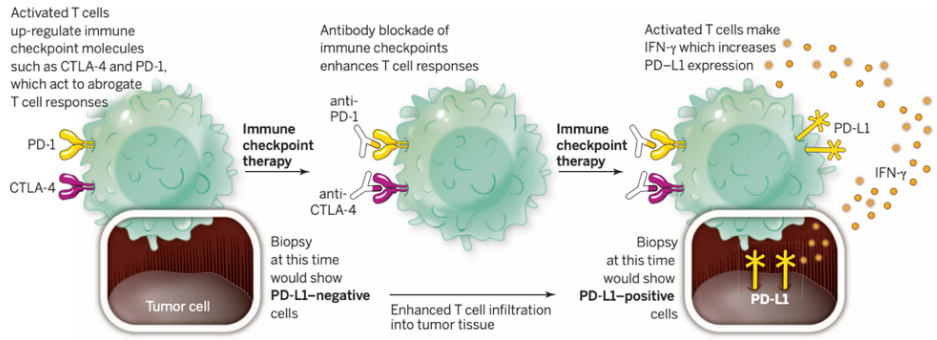

Figure 2.11. Immunomodulation via immune checkpoint inhibition to potentiate T-cell-mediated responses [147].

When tumor cells encounter stress, they have the potential to release molecules known as danger-associated molecular patterns (DAMPs). These released DAMPs can interact with Toll-like receptor (TLR) and MyD88 pathways in antigen-presenting cells (APCs), leading to the initiation of interferon type I (IFN-I) signaling. Additionally, tumor-derived DNA can activate the cytosolic DNA sensing pathway involving the cGAS/STING pathway, further stimulating the IFN-I pathways. [158, 159]. The transmembrane protein STING (Stimulator of IFN Gene), localized in the endoplasmic reticulum (ER), plays a crucial role in promoting the production of type I interferon (IFN). Additionally, STING serves as a mediator in autoimmune diseases triggered by the presence of abnormal cytoplasmic DNA [160, 161].

The development of potent anti-tumor adaptive immune responses necessitates the presentation of tumor antigens by antigen-presenting cells, which heavily depend

on appropriate innate sensing. This innate sensing is frequently facilitated by danger signals, including high mobility group box 1 protein, extracellular ATP (adenosine triphosphate), and tumor DNAs released from distressed tumor cells [162]. Recent research emphasizes the significant role of cytosolic DNA sensing in the context of radiation and DNA-damaging therapies [159, 163]. The occurrence of cytoplasmic DNA, exemplified by micronuclei (small organelles containing DNA) is characterized by the loss of nuclear envelope membranes, can initiate immune responses. Micronuclei arise from chromosomal damage due to genotoxic stress and chromosome missegregation during cell division [164]. Upon detecting cytosolic DNA by cGAS (cyclic GMP-AMP synthase) sensor, GTP (guanosine triphosphate) and ATP convert into 2',5'-cyclic GMP-AMP (cGAMP), a second messenger. Consequently, cGAMP associates and triggers the adaptor protein STING, initiating the STING signaling cascade [165-167].

Previous research has shown that tumor-intrinsic STING signaling plays a crucial role in initiating innate-sensing mechanisms essential for effective cancer therapies [163]. Another investigation demonstrated the ability of 6-thio-dG to induce innate sensing by activating the host's cytosolic DNA sensing pathway involving STING/IFN-I [126].

The implementation of immune checkpoint blockade (ICB) has resulted in long-lasting benefits for specific patients and substantially enhanced disease prognosis. Despite the considerable achievements of immunotherapies, their efficacy is hindered in a significant number of patients owing to the presence of an immunosuppressive tumor microenvironment, variations in tumor immunogenicity, and the emergence of both primary and adaptive resistance mechanisms [146, 147]. Due to the presence of PD-1 ligand, PD-L1 (and sometimes PD-L2), on both tumor cells and immune cells within the tumor microenvironment, considerable efforts have been made to use PD-L1 expression as a criterion for patient selection when considering treatments involving therapeutic antibodies designed to target the PD-1/PD-L1 pathway [147]. Despite efforts to target PD-1 or PD-L1 as a therapeutic approach, their inhibition exhibits restricted efficacy in the colorectal cancer treatment

[128]. Deficiencies in DNA mismatch repair (MMR) genes due to mutations can impair the accurate repair function during DNA replication, resulting in MSI. Both DNA mismatch repair deficiency (dMMR) and MSI-High (MSI-H) conditions can lead to the accumulation of DNA mutations within tumor cells, consequently generating an abundance of tumor neoantigens. The tumor immunogenicity facilitates robust T cell and tumor immune responses [168-170]. In contrast, colorectal tumor cells that are proficient in mismatch repair (pMMR) exhibit low immunogenicity and only modestly infiltrate immune cells, presenting challenges in eliciting a sufficient immune response [171, 172]. Consequently, some patients do not respond to ICB therapy. To enhance the efficacy of the immunotherapy, new approaches combining checkpoint inhibitors with chemotherapy, angiogenesis inhibitors and/or radiotherapy are under investigation.

As part of the present study, we sought to explore the combined impact of second-generation telomere targeted compound-L6 along with anti-PD-L1 treatment, aiming to assess their synergistic effects on tumor size reduction and overall survival.

3. MATERIALS AND METHODS

3.1. Chemicals, Assay Kits and Instruments

DMEM (Serena), RPMI (Serena), penicillin-streptomycin solution (Serena), FBS (Serena), trypsin-EDTA (Serena), and L-glutamine (Serena) were used for the cell culture. Formamide (Thermo), formaldehyde (Thermo), goat anti-mouse IgG H&L (Alexa Fluor 568, Abcam), phospho-histone H2A.X (Ser139, Cell Signalling), blocking reagent (Roche), bovine serum albumin (BSA, Serena), tween 20 (Bioshop), VECTASHIELD antifade mounting medium with DAPI (Vector), ethanol (Merck), TelG-FAM (Pnabio) and magnesium chloride hexahydrate (Fischer Sci.) were used for the TIF assay. DNasel, Mouse IL-10 secretion assay detection kit-APC, Mouse IFN-g secretion assay detection kit-PE, Anti-mouse CD45-PerCP (Cat:103130, Clone:30-F11, Biolegend), Anti-human/mouse CD11b-APC/Cy7 (Cat:1106130, Clone:M1/70, Sony), Anti-mouse F4/80-FITC (Cat:123108, Clone:BM8, Biolegend), Anti-mouse Gr1-PE (Cat:108408, Clone:RB6-8C5, Biolegend), Anti-mouse CD3-BV421 (Cat:100326, Clone:145-2C11, Biolegend), Anti-mouse CD4-FITC

(Cat:100510, Clone:RM4-5, Biolegend), Anti-mouse CD8a-PE (Cat:100708, Clone:53-6.7, Biolegend), Anti-mouse CD62L-APC (Cat:104412, Clone:MEL-14, Biolegend), Anti-mouse FoxP3-PE (Cat:126404, Clone:MF-14, Biolegend), True-Nuklear Transcription Factor Buffer Set (Cat:424401, Biolegend), Cell Wash (Cat:349524, BD), FACSFlow (Cat:342003, BD) were used for immunophenotyping. The JuliBR Smart bright-cell movie analyzer was used to quantify cell numbers and monitoring the cells. Leica sp8 laser scanning confocal microscope was used in the TIF assay to capture and quantify the telomere damage. The measurement of DNA damage products was conducted using the LC-MS/MS (Shimadzu, Kyoto, Japan- 4000 QTRAP Applied Biosystems, CA, USA) instrument. The impact on DNA repair proteins was evaluated through high-resolution liquid chromatography-mass spectrometry (HR-LC-MS) (Thermo Scientific™ Dionex™ UltiMate™ 3000 HPLC and Thermo Scientific™ Exactive Plus™ Orbitrap™ Mass Spectrometer) analysis. Anti-PD-L1/CD274 (InvivoMAb^{TM}, BE0101) antibody was used for syngeneic *in vivo* studies.

3.2. METHOD

3.2.1. Cell Culture and Reagents

A549, CT26, HT29, U87, HeLa and HFDa cells were purchased from ATCC. HT29, HeLa and HDFa cell lines were cultured in Dulbecco's modified Eagle's medium. HT29 and HeLa cells were supplemented with 10% heat-inactivated fetal bovine serum (FBS) and HDFa cells supplemented with 15% FBS, 100 U/ml penicillin, and 100 U/ml streptomycin under 5% CO_2 at 37^{o}C. A549 and CT26 cell lines were cultured in RPMI 1640 medium supplemented with 10% heat-inactivated fetal bovine serum, 100 U/ml penicillin, and 100 U/ml streptomycin under 5% CO_2 at 37^{o}C.

Anti-PD- L1 (Atezolizumab) was purchased from BioCell (#BE0101). 6-thio-dG and other candidate molecules were provided by MAIA Biotechnology (Chicago, USA). All drugs were kept frozen at -20^{o}C until use. For *in vitro* studies, 6-thio-dG and other molecules were dissolved in 100% DMSO to prepare 10mM and 30mM stock solutions simultaneously. For *in vivo* studies, 3 mg/kg 6-thio-dG and L6 was prepared in 5% DMSO (in phosphate-buffered saline, PBS) for intraperitoneal

injection. Anti-PD-L1 was prepared as 10 mg/kg with 1X PBS. After the preparation of drugs, they were kept in 4^{o}C.

3.2.2. Cell Viability Assay

For determination of EC_{50} with cell proliferation assays, murine and human cancer cell lines and HDFa cells were screened with 6-thio-dG and candidate compounds with a 3-fold dilution series in 9 different concentrations in 96-well plates. Cells were plated 24 hours prior to the addition of drug, incubated for 96 hours. MTT reagent was added to the per well as 1mg/ml and incubated for 2 hours. Cell number per well ranged from 1,000 to 10,000 cells per well inversely proportional to doubling times The determination of EC_{50} values was performed using sigmoidal dose-response curves generated with GraphPad Prism software. All samples were analyzed in triplicate and standard deviations are from at least 3 independent experiments.

3.2.3. Radiation Therapy

HT29 cells were seeded in 6-well plates (Nest) and treated with candidate compound L6 and 6-thio-dG at concentrations of 0.3 μM and 1 μM for 96 hours. Subsequently, radiation therapy was administered using the Varian DHX linear accelerator (Varian, MA, USA) with 6 MV X-rays at doses of 2 Gy, 4 Gy, and 8 Gy. The cells were cultured for an additional 24 hours and counted using methylene blue staining. Graphs were generated using GraphPad Prism.

3.2.4. Telomere Dysfunction Induced Foci (TIF) Assay

For TIF assay, round glasses were treated with poly L-lysine solution 0.01% (Sigma) (w/v in H_2O) and put into 24-well plates and then cells were seeded into plates. Next day, cells were treated with 1 mM 6-thio-dG, L6, MAIA-2022-013 and Ribo-thio for 96 h. Glasses were then rinsed twice with 1X PBS and washed with Pre-extraction buffer (20mM Tris HCI pH 8, 50mM NaCl, 3mM $MgCl_2$, 0.5% triton, 300mM sucrose) and fixed in 4% formaldehyde (Thermo Fisher) in PBS for 15 min. Then, cells were washed three times with 1X PBS and permeabilized in 0.5% PBST for 15 min. Following permeabilization, cells were washed and blocked with 5% BSA in 1X PBS for 1 h. g-H2AX (Millipore) was diluted as 1:500 in blocking solution and

incubated on cells for 2 h. Following washes with 0.1% PBST and PBS, cells were incubated with Alexaflour 568 conjugated goat anti-mouse antibody (Invitrogen) (1:1000) for at least 1 h, then washed three times with 0.1% PBST. Cells were fixed in 4% formaldehyde in PBS for 20 min at RT. The slides were sequentially dehydrated with 70%, 90%, 100% ethanol followed by denaturation with hybridization buffer containing FAM-conjugated telomere sequence-specific peptide nucleic acid (PNA) probe 70 % formamide, 30% 2 X SSC, 10% (w/v) $MgCl_2.6H_2O$ (Fisher Sci), 0.25% (w/v) blocking reagent for nucleic acid hybridization and detection (Roche) for 4 min at 85^{o}C on a heat block, followed by overnight incubation at RT. Glasses were washed sequentially with washing solution (1M Tris HCl pH 7.5/7.4, 50% formamide, 10% BSA in distilled water) twice for 15 min. Sequentially washed with 1X PBS, then mounted with Vectashield mounting medium with DAPI (Vector Laboratories). TIF images were captured with Leica sp8 confocal microscope using the 63X magnification and quantified using Image J with DiAna plugging.

3.2.5. Measurement of 8−OH-dG by LC–MS/MS

3.2.5.1. DNA Isolation

Lysis buffer (1 mL) of was added to 1 mL of cell sample and the mixture was vortexed. Then the samples were incubated at a temperature of 37°C for 24 h. Following the incubation, 500 µL of a 6M NaCl solution was added to the samples, vortexed for 15 min and subsequently incubated for 10 minutes at 56°C. After the incubation, the samples were divided into 3 separate Eppendorf tubes and centrifugated for 30 min at 5000 g. Carefully avoiding any contact with the pellet, the supernatants were transferred to new Eppendorf tubes and subjected to another round of centrifugation at 5000 g for 30 min. The resulting supernatants were transferred to the new Eppendorf tubes, and previously cooled ethanol, was added to the samples at twice their volume. The tubes were gently inverted, leading to the visualization of DNA at this stage. The samples were centrifugated at 5000 g for 15 min and the supernatants were subsequently discarded. The DNA pellets were washed by adding 200 µL of 70% ethanol. Then the samples were left to air-dry for 15-20 min at room temperature. Once dried, the samples were allowed to dissolve in 100 µL of nuclease-free distilled water at +4^{o}C for approximately 24 h. Subsequently, the amount of DNA

was quantified using Nanodrop. Then 3 Eppendorf tubes were combined, and the measurement was repeated to obtain a final DNA concentration.

3.2.5.2. LC-MS/MS Analysis

Precisely measured quantities of 8-OH-dG-$^{15}N_5$ internal standards were added into 50 µg DNA sample. Following the addition of the internal standards, the samples were dried in a SpeedVac. Subsequently, a 50 µL volume of buffer solution (composed of 100 µL 10mM Tris pH 7.5, 1.25 µL of 1M NaAc containing 45mM ZnCl) was added to the samples. The samples were incubated for 15 min at room temperature. To initiate enzymatic digestion, 1 unit of Nuclease P1, 0.0024 units of Phosphodiesterase 1, and 16 units of Alkaline phosphatase were added to the samples, followed by incubation at a temperature of 37°C for 24 h. After the incubation, the samples were centrifugated at 14.000 g for 5 min. and passed through ultrafiltration membranes with a molecular mass limit of 3kDa using centrifugation at 14.000g for 60 min. The resulting supernatants were subsequently transferred to vials and prepared for the injection.

Analyzes of damaged DNA nucleosides were performed in a triple quadrupole ion trap tandem mass spectrometer with a turbo V ion spray source in multiple reaction monitoring (MRM) mode. Analyst Software Version 1.5 was used for data analysis. Samples were separated by reversed phase C18 column (Zorbax SB Aq 2.1x150mm, 3.5µm) and guard column (Agilent Eclipse XDB C8 2.1x12.5mm, 5 µm) at a flow rate of 0.3 mL/min. Gradient analysis was performed using dH_2O (A) containing 0.1% formic acid and acetonitrile (B) containing 0.1% formic acid as mobile phase. Results are given at the level of 8-OH-dG/10^6 DNA nucleoside.

3.2.6. Measurement of APE1 and PARP1 by LC-HR/MS

Protein extraction from HT29 cells was performed using the Invent Minute Total Protein Extraction Kit in accordance with the manufacturer's guidelines. A fully ^{15}N-labeled analogue of hAPE1 and Lys-$^{13}C_6$, $^{15}N_2$– or Arg-$^{13}C_6$, $^{15}N_4$–labeled tryptic

peptides of hPARP1 were used for the quantitative measurements. The extracted protein samples (150 µg) were hydrolyzed with trypsin and quantified using HR LC-MS.

3.2.7. Humanized Mouse Tumor Models (Xenograft Model)

A subcutaneous xenograft mouse model of the human HT29 was used to evaluate the effects of L6 treatment in vivo. Six- to eight-weeks-old Nude CD1 mice were purchased from Kobay A.Ş. All mice were maintained in specific pathogen-free animal facility and all experiments were conducted in compliance with the regulations of the Kobay A.Ş. Ethical Committee. A total $2x10^6$ human HT29 cells were injected into the flank area. Following injection, tumor size was measured weekly, and treatment started when the tumor size reached approximately 80-100 mm^3. The mice were administered L6 doses (3mg/kg and 6mg/kg), twice a week for a duration of three weeks, with a two-day interval between administrations. The treatment was terminated upon observation of weight loss.

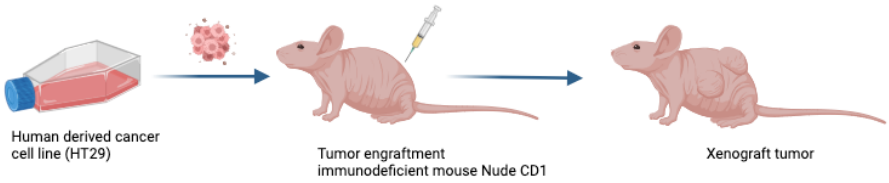

Figure 3.1. Xenograft mouse model

3.2.8. Syngeneic Mouse Models

Six- to eight-weeks-old male BALB/c mice were purchased from Kobay A.Ş. All mice were maintained in specific pathogen-free animal facility and all experiments were conducted in compliance with the regulations of the Kobay A.Ş. Ethical Committee. Mice were anaesthetized and then a total $2x10^6$ murine CT26 cells were prepared in PBS and and injected into the flank area as 100 µl for each mouse. Subsequent to the injection, tumor size was measured weekly. When tumors reached approximately 80-100 mm^3, mice with tumors were randomly assigned to treatment groups. In the L6 treatment group, the mice were administered doses of L6 3mg/kg,

twice a week for a duration of two weeks, with a two-day interval between administrations. In the sequential therapy group, the mice were administrated doses of 3 mg/kg L6, twice weekly over a two-week period, coupled with a weekly administration of 10 mg/kg anti-PD-L1for the same duration. In the anti-PD-L1 group the mice were administrated a weekly dosage of 10 mg/kg anti-PD-L1 for a duration of two weeks. The treatment was terminated upon observation of weight loss.

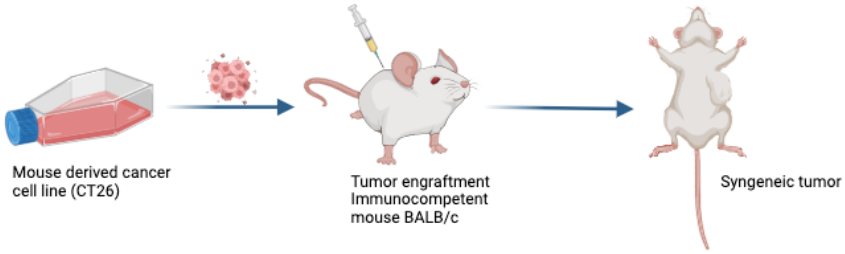

Figure 3.2. Syngeneic mouse model

Figure 3.3. CT26 cell injections for syngeneic mouse model

3.2.9. Immunophenotyping

Following the completion of the treatments, the animals were euthanized, and the tumor tissues were extracted and submerged in RPMI-1640 medium supplemented with 10% FBS. To assess the presence of immune cells within the tumor microenvironment, a mechanical fragmentation procedure was initially performed by using a scalpel. To obtain cell suspensions following mechanical fragmentation, a

sterile strainer with a pore size of 40 micrometers (μm) was used, and subsequently rinsed with RPMI-1640 medium supplemented with 10% FBS and centrifugated 5 min at 2000 rpm. The resulting cell suspensions were labeled with various combinations of specific surface markers for myeloid and T cells, including CD45-PerCP, CD11b-APC/Cy7, F4/80-FITC, Gr1-PE, CD3-BV421, CD4-FITC, CD8a-PE, CD62L-APC, FoxP3-PE, and the suspensions were then incubated for 40 minutes at +4°C. After incubation, the cell suspensions were centrifuged with washing solution at 2000 rpm for 5 min. The intracellular staining was performed following the True-Nuclear Transcription Factor Buffer set protocol. Cells labeled with various antibody combinations were examined with the BD-FACSCantoII flow cytometer, followed by analysis using the FACS Flow Jo v8.0.3 software (BD, USA).

3.2.10. Quantification and Statistical Analysis

All the data analyses were performed with GraphPad Prism and SPSS statistical software and presented as mean ± SEM. p value determined by two-way ANOVA for tumor growth. Multiple comparisons were conducted using mixed model with pairwise comparison. For flow-cytometry analysis, distribution of the groups was tested with the Student t test as the samples did not distribute normally; groups were compared with the nonparametric Mann-Whitney U test. In the radiation experiment, the p value was determined by unpaired t test. $p \leq 0.05$ was considered statistically significant.

4. RESULTS

4.1. Assessing the Impact of 6-thio-dG and Potential Compounds on Cellular Viability

To examine the impact of 6-thio-dG and our candidate compounds on various cell lines and to identify the cell line with higher sensitivity at lower concentrations, we cultured a variety of cell lines, including A549, HeLa, HT29, HDFa, U87 and CT26 in 96-well plates. After 96 hour treatment period involving nine different compound doses administered with 1:3 serial dilutions, cell viability was assessed using the MTT assay. In this investigation, we incorporated a compound known as MAIA-2022-013 as a negative control. MAIA-2022-013 contains 5-FU groups within its chemical structure, leading to selective induction of DNA damage without inducing the telomere dysfunction. Our research revealed that both the tested compounds and 6-thio-dG exhibited a dose-dependent reduction in cell viability. The EC_{50} (half maximal effective concentration) values of all cells are summarized in Table 4.1. Furthermore, below are presented some noteworthy findings of EC_{50} values. We observed that 6-thio-dG (observed EC_{50} values are between 0.12 - 3.036 μM, depending on the specific cell type), and compound called L6 (EC_{50} values are between 0.076 – 1.885 μM) exhibited significant sensitivity towards the different cancer cells. EC_{50} for both L6 and 6-thio-dG was over 100 μM in telomerase negative normal human dermal fibroblast cells. Following a comprehensive evaluation of the results, we have selected the HT29 cell line as our target, owing to its distinctive characteristics towards both L6 and 6-thio-dG (Figure 4.1). Additionally, due to the observed substantial sensitivity of nearly all cell types to the L6 compound (Figure 4.2), we have chosen it as our promising candidate for further investigation.

Table 4.1. The EC_{50} values of all compounds tested on HT29, HeLa, A549, HDFa, CT26 and U87 cells.

	EC_{50} Values (µM)					
	Cell Lines					
Compounds	HT29	HeLa	A549	HDFa	CT26	U87
6-thio-dG	0.20	0.1214	3.036	≥ 100	0.407	0.9485
L6	0.076	0.1537	1.063	≥ 100	0.3418	1.885
Ribo-thio	0.1434	0.1933	9.885	-	0.3622	1.70
L8	0.20	0.1750	10.76	-	0.3592	1.011
MAIA-2022-013	0.6528	0.3251	1.414	-	0.118	3.059

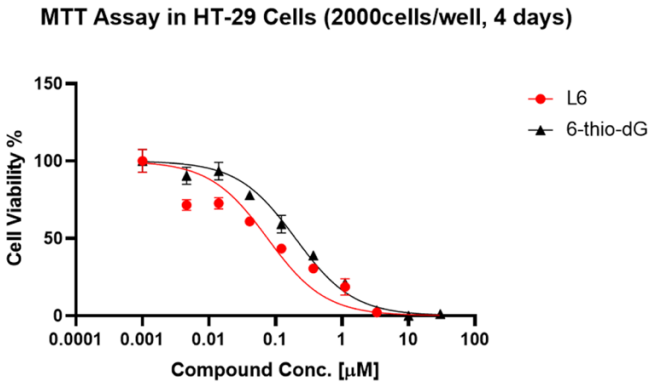

	L6	6-thio-dG
Bottom	= 0.000	= 0.000
Top	101	98.16
LogIC50	-1.12	-0.6992
HillSlope	-0.5685	-0.8847
IC50	0.076	0.2

Figure 4.1. EC_{50} value of L6 and 6-thio-dG on HT29 cells

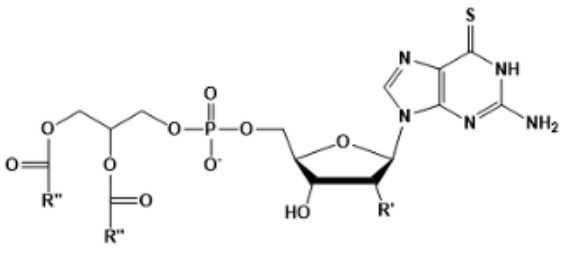

Figure 4.2. L6 molecular structure

4.2. Investigating the Impact of Radiation on HT29 Cell Line

In this study, the HT29 cell line was used to investigate the impact of L6 and 6-thio-dG on cellular radiation sensitivity. When tumor cells are exposed to radiation, it leads to the formation of DSBs. Based on this information, we hypothesize that the combination of our candidate compounds with radiation therapy will result in increased cell death compared to control groups. We conducted an experiment involving treatment with L6 and 6-thio-dG at doses of 0.3 µM, for a duration of 96 hours. Following 96 hours of treatment, cells were exposed to radiation doses of 2 Gy, and 4 Gy. After an additional 24-hour incubation period, the cells were harvested and quantified. In summary, our observations reveal a progressive, dose-dependent increase in radiation sensitivity in cells treated with L6, even at a radiation exposure as low as 2 Gy (Figure 4.3).

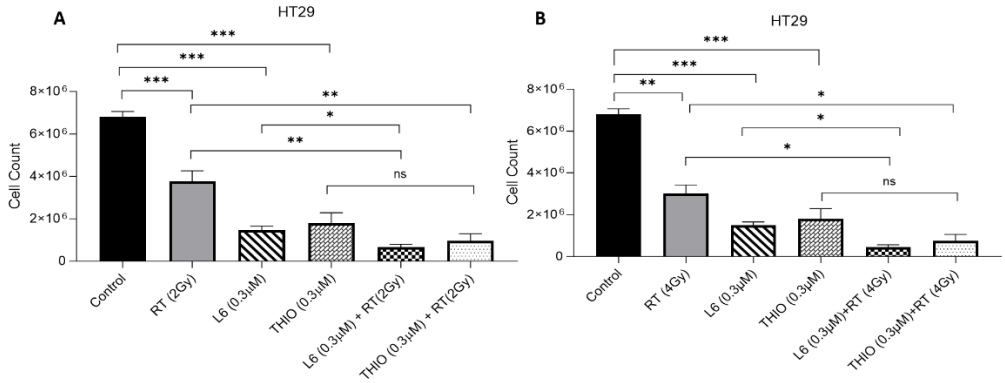

Figure 4.3. HT29 cells were pre-treated with 0.3µM L6 or 0.3µM 6-thio-dG and then irradiated with 2Gy (A), and 4Gy (B).

4.3. Treatment with 6-thio-dG and L6 induces telomere dysfunction at the cellular level

The TIF assay relies on the concurrent detection of DNA damage at telomeres through the utilization of antibodies targeting specific markers. Specifically, it involves the detection of broken double-stranded DNA by employing an antibody against gamma-H2AX and the identification of telomeres using an antibody against the telomeric shelterin protein TRF2.

As we selected the human HT29 cell line as our primary target, we sought to explore the impact of our compounds on the mice CT26 cell line, which we utilized to establish a syngeneic model for subsequent experiments. To investigate the impact of 6-thio-dG, MAIA-2022-013, Ribo-thio, and L6 treatments on telomere de-protection, HT29 and CT26 cells were cultured in 24-well plates on 12mm round glass coverslips pre-treated with a 0.01% poly L-lysine solution. After 24h of incubation, we added 1μM concentrations of 6-thio-dG, MAIA-2022-013, Ribo-thio, and L6. TIF images were captured using a confocal microscope (Leica, SP8), using an oil-immersion objective (63X, NA:1.4). For each region of interest, 50x50 μm2 areas were scanned at 512x512 pixel resolution and Z-stacks with 0.3 μm steps were recorded capturing the entire axial range of the cells to be analyzed. This raw data was further processed using ImageJ/FIJI (Version: 1.54b) and background subtraction (using a rolling ball radius and of 3 pixels, sliding paraboloid for green channel and 5 pixels for red channel) and a gaussian filter with sigma=1 pixel was applied. Quantitative analysis on these preprocessed images was then performed using DiAna plugin [173] for testing object-based 3D colocalization between green and red channels. Briefly, a 3D spot segmentation was performed with maxima detection radius in xy-axis=5, in z-axis=5 and noise parameter set to 5. Threshold for maxima selection was set by the user, and was readjusted by manually checking the segmentation results with the raw fluorescent image data, confirming that no artificial seeds were generated and at least 90% of the visible fluorescent foci are recognized as seed maxima. Parameters for gaussian fit and threshold calculation were radius maximum of 10, with a S.D. value of 1.5. Minimum and maximum object volume for detection was 3 and 10000 pixel-cube, respectively, for both channels. Once segmentation was complete for both channels, co-localization was determined by detection of overlapping objects and co-localizing object volumes were calculated for each pair of objects (Figure 4.4). The statistical significance of co-localization was calculated by comparing the experimental results with a random distribution, using the respective function of the DiAna plugin. The cumulative distribution of the mean distances between objects for experimental images and randomly shuffled images were compared and the colocalizations were considered as statistically significant if the experimental mean distance distribution curve was

localized outside the 95% confidence interval of the randomized distance. Only statistically significant co-localization analyses are reported in the experimental results.

By employing a combination of gamma-H2AX and telomere probe (TelG-FAM) co-localization through immuno-staining, we successfully discerned and differentiated between DNA damage occurring at non-telomeric genomic regions and damage specifically localized to telomeres (Figure 4.6 and Figure 4.8). After 96 hours, the administration of L6 treatment results an increase as a TIF volume in telomeric DNA damage compared to 6-thio-dG on HT29 (Figure 4.5) and CT26 (Figure 4.7) cells. Given that telomeric DNA accounts for only approximately 1/6,000th of the total genomic DNA, the presence of any TIFs above the background level would be considered notably significant [122].

Alongside the heightened telomere damage caused by L6, there was no significant increase in genomic DNA damage compared to 6-thio-dG, yet L6 generates more TIFs in HT29 (Figure 4.6), CT26 (Figure 4.8) and HeLa (Figure 4.9). cells. Given that MAIA-2022-013 is an analog of 5-FU, our hypothesis posits its exclusive induction of genomic DNA damage rather than the TIFs. As seen in the Figure 4.5, MAIA-2022-013 effectively induces global DNA damage but when we compare TIF results with the control group, no statistically significant differences were observed.

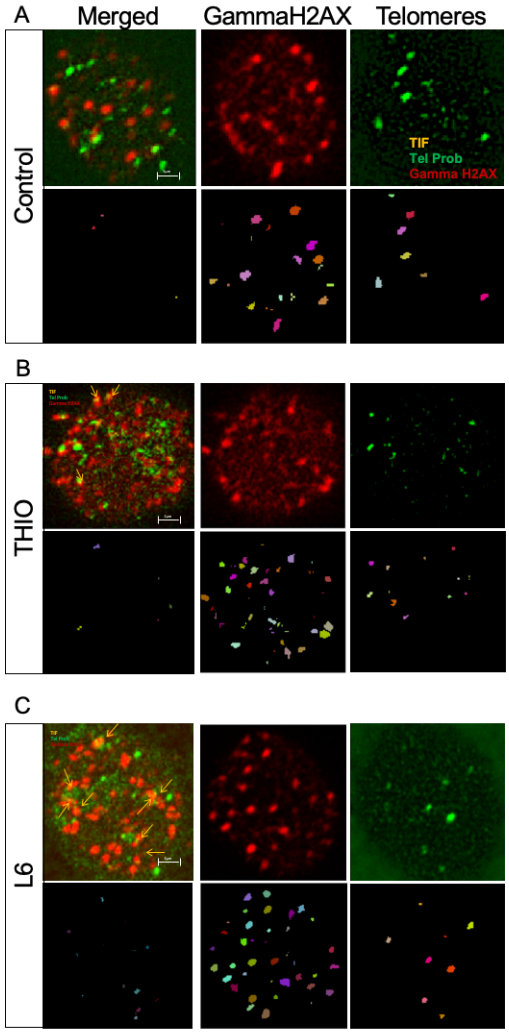

Figure 4.4. TIF and DiAna plugin colocalization images for HT29 cells treated with (B) 6-thio-dG (1μM) and (C) L6 (1μM). (A) Representative DiAna labelisation filters for each cell and obtained telomere, DNA damage and TIF volumes table for analyzed cells. (B) Green: Telomeric probe, red: gammaH2AX and yellow: TIFs (top) and merged, gammaH2AX and telomere figures (bottom) were randomly colorized by DiAna pluging.

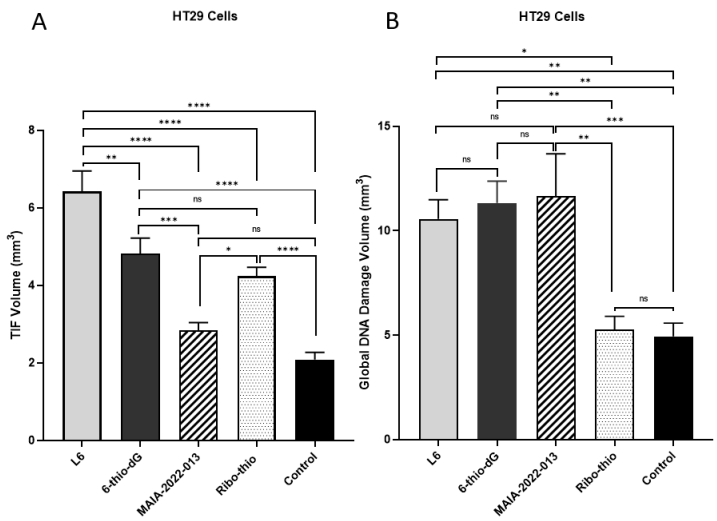

Figure 4.5. HT29 cells treated with L6 (1µM), 6-thio-dG (1µM), MAIA-2022-013 (1µM), and Ribo-thio (1µM) for 96 hours. (A) TIF volumes were scored by DiAna plugging and *p* value was determined by two-way ANOVA followed by post-hoc test (Tukey's) (n=50, **p*<0.05, ***p*=0.0077, ****p*=0.0004, *****p*<0.0001, ns, not significant) (Control; untreated). (B) global DNA damage volumes were scored by DiAna plugging (n=50, **p*=0.0140, ***p*=0.0079 L6 vs control, ***p*=0.029 6-thio-dG vs Ribo-thio, ***p*=0.0015 6-thio-dG vs control, ***p*=0.0015 MAIA-2022-103 vs Ribo-thio, ****p*=0.0008. Data are shown as means ± SEM.

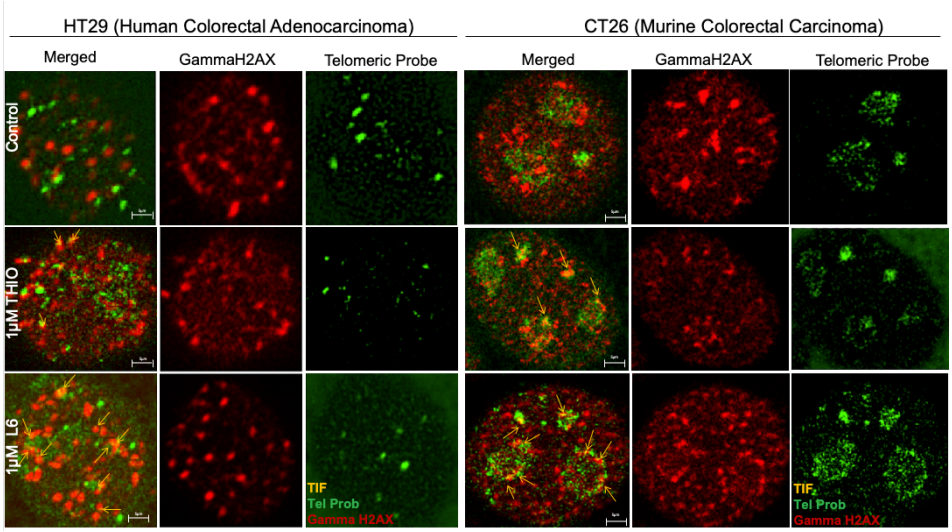

Figure 4.6. Representative 2D images of TIF and DNA damage foci for L6 and 6-thio-dG on HT29 cells with 1µM treatment for 4 days. Green: Telomeric probe, red: gammaH2AX and Yellow: TIFs

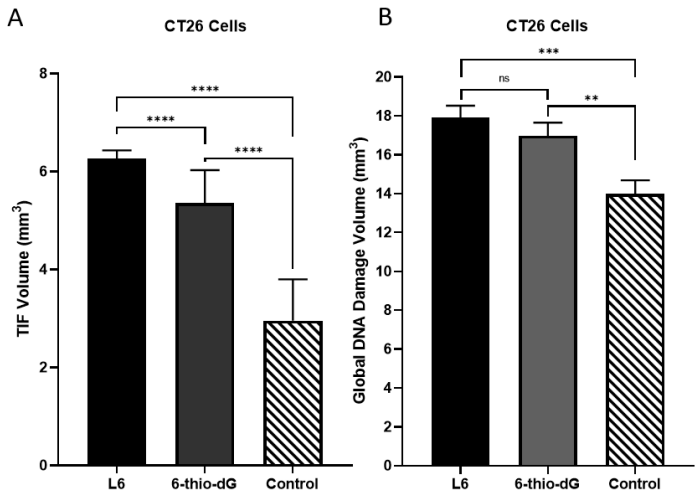

Figure 4.7. (A) CT26 cells treated with L6 (1µM) and 6-thio-dG (1µM) for 96 hours. TIF volumes were scored by DiAna plugging (n=50 for CT26 cells). ****p<0.0001, in the one-way ANOVA followed by post-hoc test (Tukey's) (Control; untreated). (B) CT26 cells treated with L6 (1µM) and 6-thio-dG (1µM) for 96 hours. Global DNA damage volumes were scored by DiAna plugging (n=50 for CT26 cells). ***p=0.0001, **p=0.0050 in the one-way ANOVA followed by post-hoc test (Tukey's) (Control; untreated).

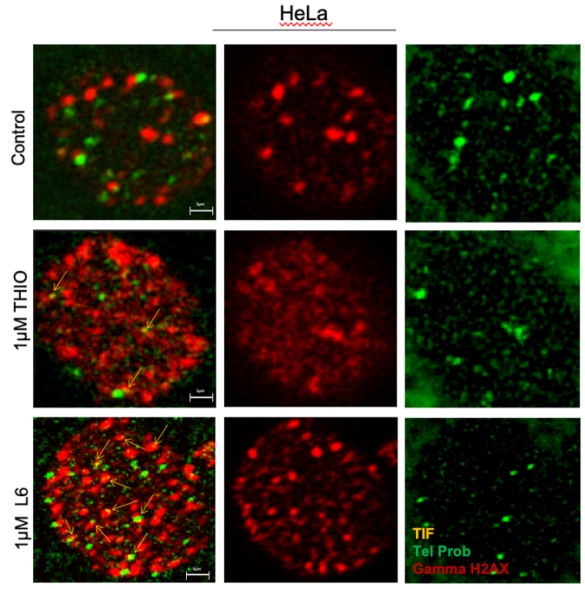

Figure 4.8. TIF images for HeLa cells treated with (B) 1 µM 6-thio-dG and (C) 1 µM L6.

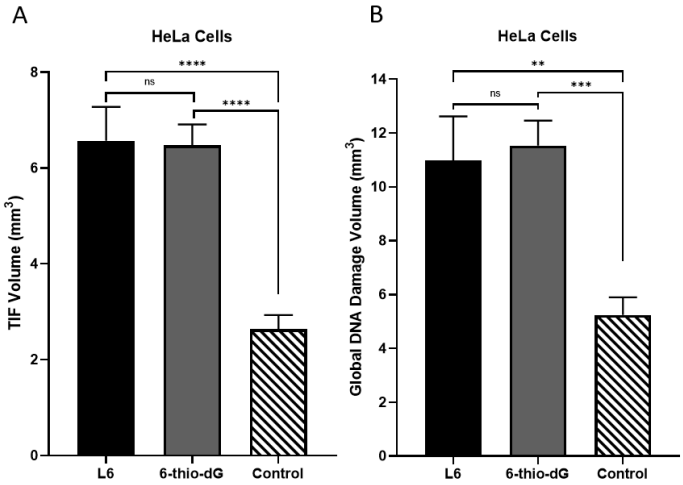

Figure 4.9. (A) HeLa cells treated with L6 (1µM) and 6-thio-dG (1µM) for 96 hours. TIF volumes were scored by DiAna plugging (n=50 for HeLa cells). ****p<0.0001, in the one-way ANOVA followed by post-hoc test (Tukey's) (Control; untreated). (B) HeLa cells treated with L6 (1µM) and 6-thio-dG (1µM) for 96 hours. Global DNA damage volumes were scored by DiAna plugging (n=50 for HeLa cells). ***p=0.0001, **p=0.0050 in the one-way ANOVA followed by post-hoc test (Tukey's) (Control; untreated).

In alignment with our findings in the HT29 cell line, we observed consistent results in CT26 cell line when exposed to 1 µM concentration of 6-thio-dG and L6 for 96 hours of treatment (Figure 4.7). While L6 induced a notable increase in telomere damage, there was no statistically significant rise in genomic DNA damage when compared to the effects of 6-thio-dG. Nevertheless, it is important to note that L6 did lead to a higher generation of TIFs compared to 6-thio-dG (Figure 4.7).

4.4. Evaluation of oxidative DNA damage and DNA repair proteins

Various methodologies have been proposed for the analysis of DNA damage in biological samples, such as the comet assay, ^{32}P post labeling, and immune-based assays [174, 175]; however, LC-MS strategies typically exhibit superior selectivity, sensitivity, accuracy, and reproducibility. In recent years, substantial progress has occurred within the realm of chemical DNA damage analysis. These advancements encompass heightened sensitivity in detection methods, the formulation of more

effective DNA pretreatment techniques, the utilization of high-resolution mass analyzers like the Orbitrap and time-of-flight instruments, DNA adductomics, and the investigation of DNA damage induced by emerging contaminants [176-179].

The formation of oxidatively modified nucleobases, such as 8-OHG or it's nucleoside form 8-OH-dG has been correlated with the processes of aging and the development of carcinogenesis. Therefore, in this study, we incubated HT29 cells with 6-thio-dG, L6 and Ribo-thio for 72-96 hours to analyze DNA damage by LC-MS/MS. 8-OH-dG, is generated through the influence of hydroxyl radicals, singlet oxygen, or photodynamic reactions. We analyzed the DNA damage, including both genomic and telomeric DNA damage, by measuring the levels of 8-OH-dG as a marker.

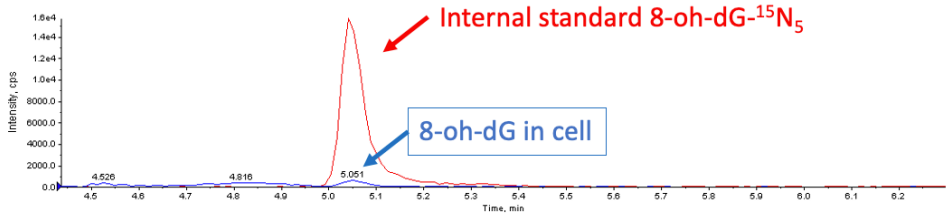

Figure 4.10. HT29 control cells

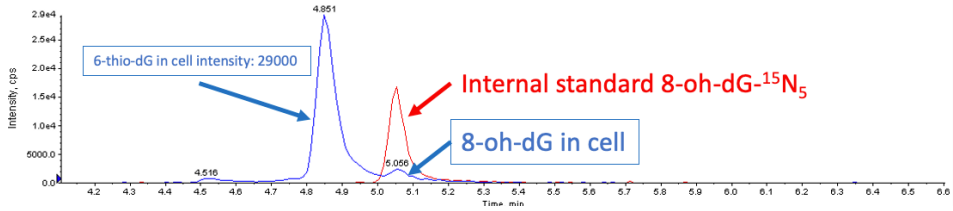

Figure 4.11. HT29 cells treated with 0.3µM 6-thio-dG

According to our LC-MS/MS data analysis, we conducted a comparative assessment of internal standards (Figure 4.10) against cells treated with 6-thio-dG, revealing the successful incorporation of 6-thio-dG into DNA (Figure 4.11). As L6 is derived from 6-thio-dG and undergoes a mechanism of action that converts it into 6-thio-dG, this dataset also provides evidence of the successful incorporation of L6 into DNA. Based on these findings, we have shown that our compound L6 induces substantial DNA damage by generating more 8-OH-dG, potentially resulting in the formation of TIFs and, ultimately, triggering apoptosis (Figure 4.12).

Malfunctions in the expression of DNA repair proteins can result in the development of therapy resistance and have a notable impact on the overall survival rates of cancer patients. Our objective was to quantify the levels of APE1 and PARP1 as a means of assessing the impact of the L6 molecule. Based on our findings, 6-thio-dG, L6, and Ribo-thio exhibited a statistically significant increase in DNA damage when compared to the control group, especially at 96 hours. Additionally, a notable reduction in PARP1 and APE1 expression was observed at 96 hours when cells were incubated with 1µM L6, as compared to the 72h (Figure 4.13 and Figure 4.14).

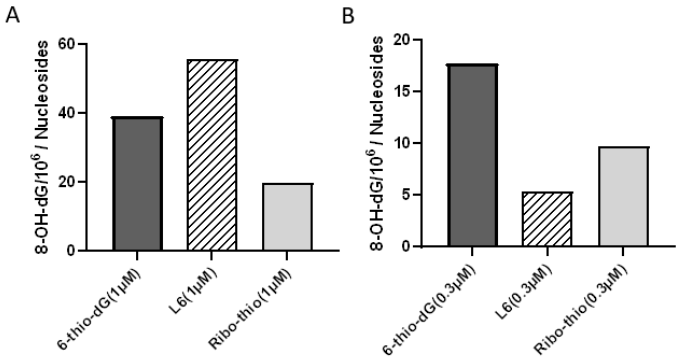

Figure 4.12. Measurements of 8-OH-dG levels in HT29 cells for (A) 72h and (B) 96h

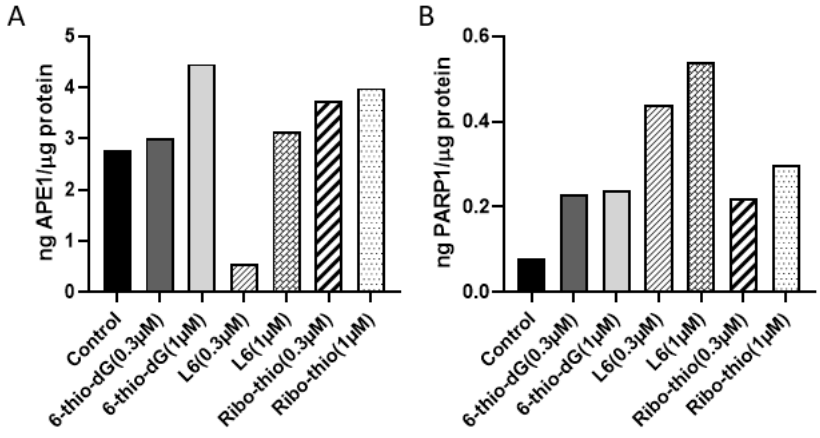

Figure 4.13. LC-HR/MS measurements for (A) APE1 and (B) PARP1 protein levels following 72h treatment with 6-thio-dG, L6 and Ribo-thio

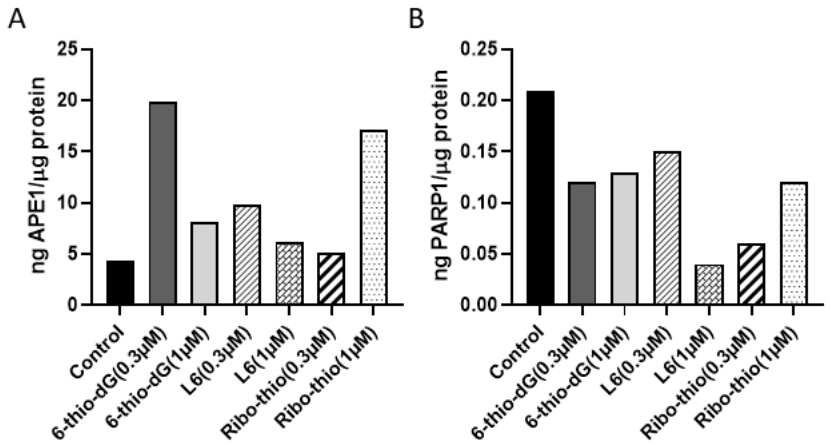

Figure 4.14. LC-HR/MS measurements for (A) APE1 and (B) PARP1 protein levels for 96h treatment of compounds

In cases where DNA repair mechanisms are not insufficient to fixing the present cellular damage, this leads in genomic instability, thereby promoting the cell to either programmed cell death or the development of tumorigenesis. Based on our findings, a 96-hour treatment with L6 leads to a reduction in PARP1 levels. PARP1 is integral to the intricate regulation of DNA repair and telomere maintenance. When conducting a comparative analysis between 6-thio-dG, and L6, particularly at a concentration of 1µM, it was observed that following a 96-hour treatment period, L6 induced a greater reduction in PARP1 levels compared to 6-thio-dG (Figure 4.14). Consequently, diminishing PARP1 levels through L6 treatment could potentially induce apoptosis in cancer cells, as their impaired DNA repair mechanisms may make them susceptible to accumulated DNA damage.

Based on our analysis of APE1 data, it appears that following a 72-hour treatment, APE1 levels show an increase across all tested compounds (Figure 4.13). However, at concentrations of 0.3 and 1µM, compound L6 still demonstrates a more pronounced decrease in APE1 levels compared to the other compounds. It is possible that extending the treatment duration to more than 96 hours may be required to achieve a substantial reduction in APE1 levels. Additionally, we observed a similar trend with PARP1 levels, which also exhibit a decrease after 96 hours of treatment (Figure 4.13 and Figure 4.14). Consequently, considering the diminished levels of both APE1 and

PARP1, it may be necessary to extend the treatment duration with L6 beyond 96 hours to achieve the desired reductions in both proteins.

4.5. *In vivo* assessment of L6 compound's general toxicity

To assess the optimal drug concentration for *in vivo* efficacy studies, we conducted initial experiments on Nude CD1 male mice. We exposed them to 3mg/kg and 6mg/kg of L6 to evaluate its overall toxicity. According to the previous report, doses of 6-thio-dG up to 5mg/kg were not toxic to mice [122]. Therefore, we decided to test two doses: 3mg/kg and 6mg/kg. We subcutaneously inoculated $2x10^6$ HT29 cells into the right dorsal flanks of the mice, in 100 mL of PBS. Upon reaching a tumor size of approximately 100 mm^3, the tumor-bearing mice were grouped into treatment groups randomly. L6 at a dosage of 3 mg/kg was administered intraperitoneally on days 0, 2, 4, 6, 8, and 10, with a dosage of 6 mg/kg given on days 0, 2, 4, and 6 in the tumor (Table 4.5). Tumor dimensions and body weights were measured at 2-day intervals. Tumor volumes were quantified using the dimensions of length (a), width (b), and height (h), and the calculation used for tumor volume was (a×b×h) / 2.

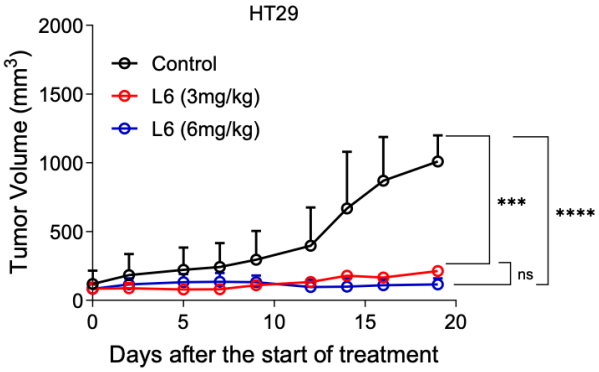

Figure 4.15. Xenograft model with HT29 cells for determining the optimal dose of L6. Tumor volumes were scored by GraphPad Prism (n=16 for nude CD1 mice, $2x10^6$ HT29 cells were injected). ***p=0.0007, ****p<0.0001, ns, not significant differences in the two-way ANOVA (Control; untreated).

Table 4.5. Xenograft Model Treatment Schedule

Days after the start of treatment											
	Day0	Day1	Day2	Day3	Day4	Day5	Day6	Day7	Day8	Day9	Day10
Control											
L6 (3mg/kg)	L6		L6		L6		L6		L6		L6
L6 (6mg/kg)	L6		L6		L6		L6				

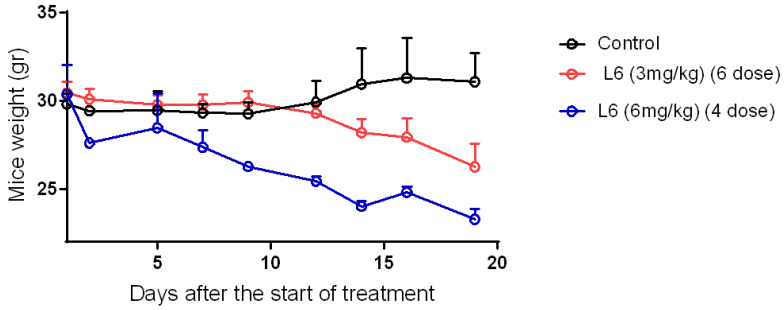

Figure 4.16. The weights of mice in the xenograft model

The treatment regimen was concluded upon reaching tumor volumes of up to 1000mm^3. Analysis of the tumor volumes revealed no statistically significant differences between the groups administered with doses of 3mg/kg and 6mg/kg (Figure 4.15). However, both the 3mg/kg and 6mg/kg groups exhibited weight loss after the fourth dose of treatment (Figure 4.16). Particularly, mice in the 6mg/kg group were unable to tolerate the fourth dose, necessitating the termination of treatment in that group. Conversely, mice in the 3mg/kg group tolerated the fourth dose, allowing us to continue treatment for up to 6 days (Table 4.5), although they continued to experience weight loss. Based on these observations, we determined that the optimal drug concentration was 3mg/kg, and the optimal treatment frequency was four doses.

4.6. Immunophenotyping by Flow Cytometry

$CD8^+$ cytotoxic T lymphocytes (CTLs) represent a pivotal immune cell population for targeting cancer. However, during cancer progression, CTLs experience

functional impairment and exhaustion as a consequence of immune-related tolerance and immunosuppression within the tumor microenvironment (TME). These factors collectively contribute to adaptive immune-resistance. Notably, cancer-associated fibroblasts (CAFs), type 2 macrophages (M2), and regulatory T cells (Tregs) create immunological barriers that hinder the efficacy of $CD8^+$T cell-mediated antitumor immune responses. Efficient and long-lasting antitumor immune responses rely on the priming and activation of $CD8^+$ T cells into effector CTLs during the tumor immunity cycle. This process involves collaborative interactions between innate immune cells, including DCs and natural killer (NK) cells, with $CD4^+$T cells in the context of adoptive immunity to direct $CD8^+$ T cell priming effectively. The intricate interplay between CTLs and Tregs can lead to a reduction in Treg activity, thereby augmenting CTL numbers and restoring their functional capacity. This enhanced CTL response serves to promote heightened immunosensitivity in cancer cells [137].

In their previous study, Mender et al. demonstrated that administration of 6-thio-dG led to the activation of $CD8^+$ T cells. However, the treatment was also found to concurrently induce an increase in PD-1 expression, both in the overall frequency of $CD8^+$ T cells on a per-cell basis [124]. Based on this study, PD-1 functions as a co-inhibitory molecule that restricts the activation of T cells and increased PD-1 expression impede the cytotoxic function of $CD8^+$ T cells after 6-thio-dG treatment.

Consequently, we hypothesize that combining our candidate compound L6 with anti-PD-L1 may enhance the overall anti-tumor immune response, particularly in advanced tumor settings where a more immune suppressive microenvironment exists, containing multiple resistance mechanisms that limit the efficacy of single-treatment approaches. After permitting the tumors to grow to a volume of 80-100 mm^3, we administered L6, sequential therapy and anti-PD-L1 treatments.

Upon conducting a thorough examination of the tumor microenvironment within the tumor tissue, our analysis revealed that the administration of anti-PD-L1 treatment had minimal impact on T cell activation. However, in the combination

treatment group, L6 predominates in the activation of $CD8^+$ cells, concomitant with a reduction in Treg cell populations (Figure 4.17).

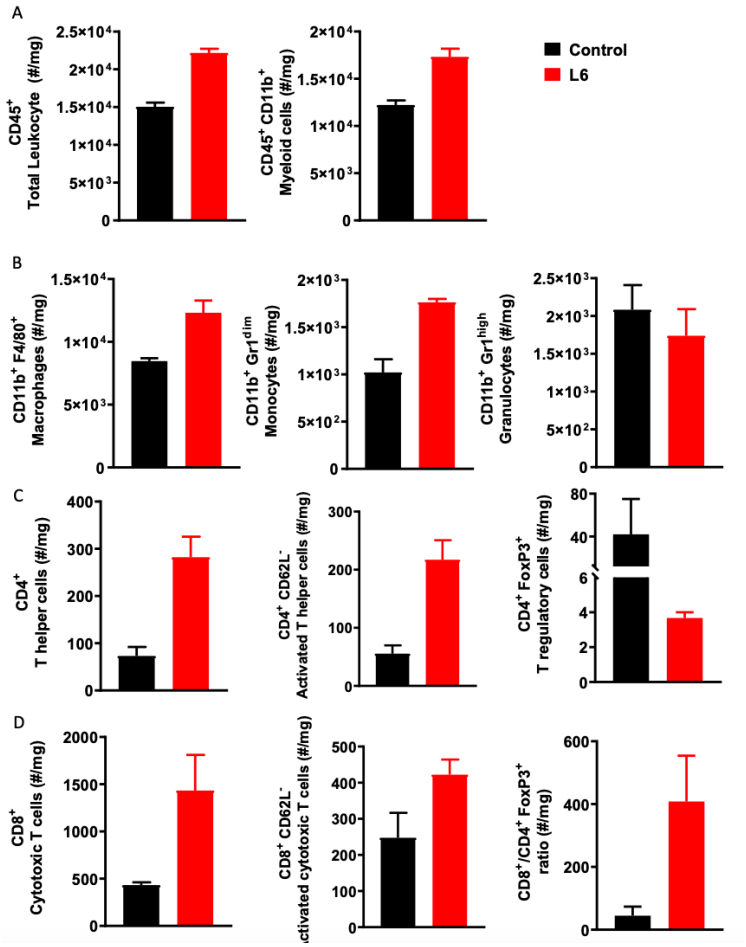

Figure 4.17. Immunophenotyping of CT26 bearing mice after L6 treatment (A) Total leukocyte and myeloid (B) Myeloid subpopulations (C) Lymphocyte subpopulations (D) Cytotoxic T cells/ T regulatory cells ratio in mg tissue. Data are shown as means ± SEM. p value was determined by Student-t test by using Graphpad Prism. Among the infiltrated immune cells, dominant population was myeloid subpopulations (A, B). Despite there was no statistically significance between groups for each panel ($p>0.05$), the trendline for T helper and cytotoxic T cells were indicated that L6 has potential to induce activated T cell infiltration (C). Oppositely, in treatment group, T regulatory cell numbers were decreased (C). Following L6 treatment cytotoxic T cells: T regulatory cells ratio increased (D).

4.7. *In Vivo* Assessment of L6 Treatment on Tumor Immunity and Immunotherapy Response

In their study, Mender et al. found that 6-thio-dG treatment resulted in the activation of $CD8^+$ T cells, leading to an increase in the frequency of total $CD8^+$ T cells expressing PD-1, both in terms of the number of cells and the expression levels per cell [126]. Also in the same study, Mender et al. has shown that heightened PD-1 expression inhibits the function of cytotoxic $CD8^+$T cells following 6-thio-dG treatment [126]. Since PD-1 is a crucial co-inhibitory molecule responsible for regulating T cell activation, we hypothesize that combining L6 with PD-1/PD-L1 blockade could enhance the overall anti-tumor immune response, like the observed effect with 6-thio-dG. This approach holds particular promise in the context of advanced tumors, where the microenvironment tends to be highly immune suppressive, incorporating multiple resistance mechanisms that limit the efficacy of single-treatment interventions. Given that our candidate compound, L6, was derived from 6-thio-dG and exhibits a similar mechanism of action, our objective was to explore the impact of L6 on tumor immunity and its potential in enhancing immunotherapy response.

In our study, we used male BALB/c mice for the syngeneic model. To evaluate the impact of L6 on tumor immunity, we administered a dosage of 3mg/kg to the mice. First, we subcutaneously injected $2x10^6$ CT26 cells into the right dorsal flanks of the mice, using a volume of 100 mL PBS mixed with 10% Matrigel. Upon reaching a tumor size of approximately 80-100 mm^3, the tumor-bearing mice were grouped into treatment groups randomly. L6 at a dosage of 3 mg/kg was administered intraperitoneally on days 0, 2, 7 and 9. For PD-L1 sequential therapy, L6 at a dosage of 3 mg/kg was administered intraperitoneally on days 0, 2, 7 and 9 and anti PD-L1 with a dosage of 10 mg/kg was given intraperitoneally on days 4 in the tumor. For only PD-L1 blockade therapy, 10mg/kg anti-PD-L1 was given only on day 4 and 11. Tumor dimensions and body weights were measured at 2-day intervals (Figure 18 and Figure 20). Tumor volumes were quantified using the dimensions of length (a), width (b), and height (h), and the calculation used for tumor volume was (a×b×h) / 2.

There was statistically significant difference between groups following third dose (day 10, *p=0.011 control vs L6 and *p=0.006 control vs L6 + anti-PD-L1) and fourth dose of L6 (day 12, *p= 0.006 control vs L6 and *p= 0.003 control vs L6 + anti-PD-L1). However, at the end of the treatment (day 19) no statistical difference was observed among the all-experimental groups since the animals that tumor size reached up to approximately 2500 mm^3 were sacrificed in the group and number of animals were not equally distributed between groups. Despite the absence of statistical significance between groups at the end of treatment, the evaluation of the trendline between groups indicated that L6 has potential for tumor growth reduction (Figure 4.18 and Figure 4.19).

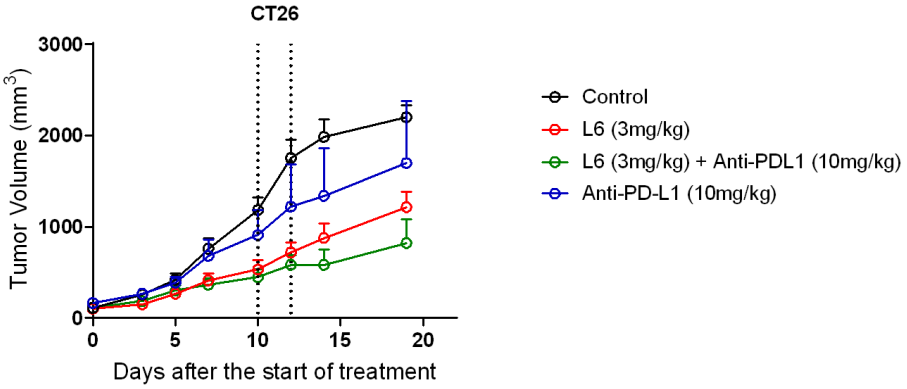

Figure 4.18. Therapeutic efficacy of L6 when sequentially combined with anti-PD-L1 (n=36, Data are shown as means ± SEM. p value was determined by mixed model with pairwise comparisons by using SPSS).

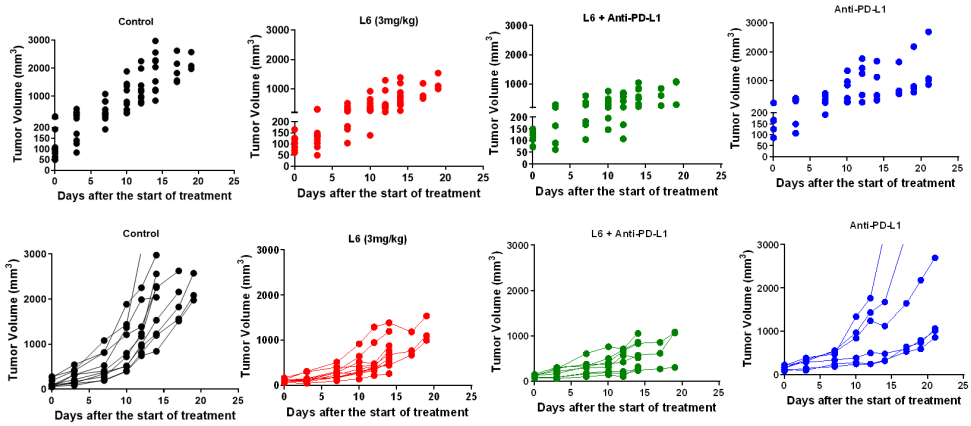

Figure 4.19. Individual tumor growth following graphs for each treatment groups.

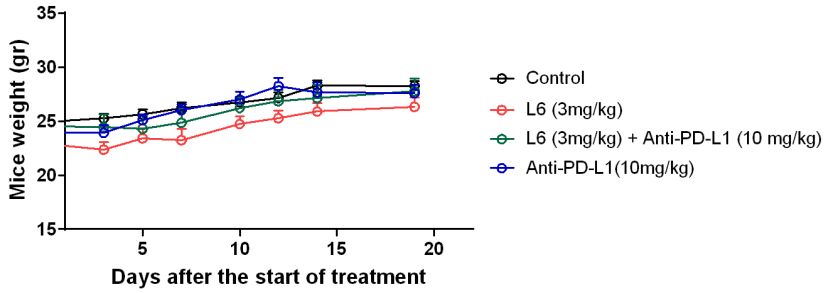

Figure 4.20. Mice weight following L6, anti-PD-L1 and sequential therapy. The mice weight (gram: gr) were measured every 2 days.

5. DISCUSSION

CRC ranks as the third most prevalent cause of cancer-associated mortality globally. The 5-year relative survival rate, encompassing the overall prognosis, stands at 63%. Within clinical contexts, the selection of primary therapeutic modalities for colorectal cancer is contingent upon both the cancer's stage and the individual circumstances of the patient. Immunotherapy represents an innovative and promising paradigm within the realm of cancer therapeutics. Its efficacy in addressing gastrointestinal malignancies, particularly in the context of advanced disease, is notable. Despite the existence of diverse therapeutic modalities for the management of advanced colorectal cancer, the prognosis for individuals with this condition remains markedly unfavorable.

Elevated telomerase expression within tumor cells is recognized as an adverse prognostic determinant for carcinogenesis. Purine analogs, such as 6-thioguanine and 6-mercaptopurine, represent chemotherapeutic modalities with the capacity for in vivo transformation into nucleotide analogs. Nucleoside substrates with therapeutic employment encompass mono-, di-, and tri-phosphate prodrug iterations alongside antimetabolite agents. One of the primary challenges associated with these compounds resides in their comparatively elevated cytotoxicity towards non-malignant somatic cells [122]. Furthermore, their therapeutic efficacy against a significant proportion of solid tumors is comparatively limited [180]. Therefore, the limited utilization of 6-thioguanine within contemporary cancer therapeutic regimens predominantly stems from its diminished pharmacological potency and the constraining manifestation of dose-dependent adverse reactions [181]. In previous study, Mender et al. reported that 6-thio-dG possesses the capacity to interact with telomerase, then integrate into telomeres, and induce a notably superior incorporation of telomeric structure compare to 6-thioguanine [122]. We additionally demonstrated that the increased effectiveness of L6 derived from 6-thio-dG is attributable to its lipidized configuration, affording superior cellular assimilation compared to non-lipidized 6-thio-dG.

In this research, we used a series of THIO molecules conjugated with phosphatidyl-lipids, discovering that L6 has better effectiveness and solubility

compared to non-conjugated form. Prodrugs linked to phosphatidyl lipids commonly have the therapeutic agent, a phosphate group, and glycerol. Similarly, the L6 molecule consist of THIO as the therapeutic agent, along with a phosphate group and glycerol in its composition. Currently, the most promising mechanism of action indicator is Telomere-targeted therapy-induced TIF. In the present study, our results indicate a proficient recognition of L6 by telomerase and its subsequent integration into telomeres. L6 exhibits selective incorporation into de-novo-synthesized telomeric regions, generates rapid reduction in tumor dimensions primarily through the incorporation of telomeric structures and the initiation of DNA lesions. In contrast, direct telomerase inhibitors function through the suppression of telomerase activity and rely on the gradual attrition of telomeric length. This particular incorporation of L6 create a notable elevation in TIFs in HT29 cells. In this study, for the first time, we applied a novel ImageJ-based technique named DiAna, which enables spatial analysis in three dimensions and computes the spatial separation between co-localized object volumes for every object pair. According to our TIF and DNA damage results, the integration of L6 into telomeres, as well as its integration into genomic DNA, suggests a bifunctional mechanism of operation for the compound. This mechanism potentially encompasses the dual targeting of both telomeric and genomic DNA, alongside its potential role as a nucleoside antimetabolite. Additionally, our study demonstrates a substantial co-localization between DNA damage initiated by L6 and telomeric regions, thereby suggesting the emergence of TIF. Considering that telomeres constitute approximately 1/6,000th fraction of the genomic DNA, any observed instances of TIF manifest remarkable significance.

The clinical efficacy of the majority of monotherapeutic anticancer interventions remains limited, primarily attributable to the emergence of acquired drug resistance, culminating in the resurgence of neoplastic recurrences and metastatic progression. Imetelstat (GRN163L), a potent inhibitor of telomerase has major limitation in clinical trials, as resides in the inherent variability of telomere lengths within the neoplastic cells of the afflicted individuals. Consequently, the variance in telomere lengths within tumors along with a considerable temporal "lag phase" constitutes the principal constraining factors for therapeutic interventions reliant upon

telomerase inhibition. A series of clinical investigations involving human subjects, wherein imetelstat was concomitantly administered with various chemotherapeutic agents targeting solid malignancies, have been early terminated due to adverse effects [182, 183]. Favorable outcomes were reported following the completion of the phase III IMerge trial (ClinicalTrials.gov identifier NCT02598661), wherein the initial telomerase inhibitor imetelstat was assessed in patients exhibiting lower-risk myelodysplastic syndromes (MDS) characterized by relapse, refractoriness or ineligibility for erythropoiesis-stimulating agents.

Hence, it is imperative to assess additional novel methodologies directed towards augmenting comprehensive therapeutic efficacy while concomitantly minimizing adverse effects. In this present study, our attention has been directed towards the heterocyclic guanine base, specifically the altered nucleoside analogue denoted as L6. Unlike alternative therapeutic approaches reliant upon telomerase inhibition, L6 distinguishes itself by functioning not as a direct telomerase inhibitor, but rather as a precursor to the telomerase substrate 6-thio-dGTP. In addition, the majority of preceding investigations have commonly employed elevated dosage or rigorous dosing regimens, resulting in heightened lethality towards neoplastic cells. However, these approaches inadvertently elicit suppression of immune reactions, either attributable to the deleterious impact on immunocytes or the induction of non-immunogenic death in malignant cellular populations [184]. Moreover, the employment of intensified dosing strategies frequently leads the genesis of neoplastic resistance mechanisms.

Prior researches demonstrates that telomere malfunction represents a definitive attribute of senescence, which, in select scenarios, may precipitate apoptotic cellular death [106, 185]. It has been previously demonstrated that the induction of senescence or apoptosis due to telomere dysfunction has the capacity to restrict tumor proliferation within animal model systems [186, 187]. Moreover, in conjunction with the in vitro investigations, we conducted in vivo studies with BALB/c, as well as Nude CD1, to facilitate a comparative evaluation between 6-thio-dG and L6. We additionally aim to conduct a comprehensive evaluation of lower doses and shorter treatment regimens

with L6, thereby elucidating the influence of L6 on host immune responses in tumor-bearing mice. Mender et al. previously reported that the administration of 6-thio-dG elicits potent immune responses against tumors in murine syngeneic colon and lung models, as well as in humanized mouse cancer models [126]. This phenomenon operates via the initiation of the intracellular DNA-sensing pathway involving the STING/IFN-I cascade within DCs. Ultimately, this process augments the antigen-presenting capacity of DCs, leading to the subsequent activation of tumor-specific T cells. Concordant with this noteworthy discovery, we hypnotized that a combined therapy involving L6 and anti-PD-L1 therapies would likely replicate or even more favorable outcomes compared to those achieved with 6-thio-dG, as suggested by our experimental outcomes. Evidently, our investigation demonstrated that the successive administration of L6 alongside anti-PD-L1 precipitates a synergistic outcome in progressive neoplasms and in cases of PD-L1 blockade resistance. This phenomenon is primarily associated with DNA recognition mechanisms, leading to subsequent modulation of immune responses mediated by T cells, resulting in the augmentation of $CD8^+$ cell populations. Moreover, L6 exhibited diminished cytotoxicity, evident through the absence of weight reduction, while manifesting heightened effectiveness surpassing that of 6-thio-dG. While originating from 6-thio-dG, L6 exhibits dissimilarities in terms of biodistribution, lipid-based solubility (where L6 demonstrates increased hydrophilicity in comparison to 6-thio-dG), binding with plasma proteins, in vivo. These multifaceted variations could collectively underlie the discernible variations in toxicity outcomes.

While the impact on telomerase-positive stem cells remains a prospective apprehension regarding the progression of L6 into human clinical trials, it is noteworthy to mention that previous findings by Mender et al. have documented that exhaustive in vivo toxicity evaluations encompassing efficacious dosages have not unveiled any noteworthy hematology, renal, or gastrointestinal system impediments attributable to 6-thio-dG [122]. In harmony with this line of evidence, given the origin of L6 from 6-thio-dG, any potential influences of L6 on transient amplifying telomerase-positive cells are conceivable; however, it is crucial to recognize that

quiescent stem cells, characterized by telomerase silence, are improbable to be influenced by the effects of L6.

In summary, given their mechanistic functions of L6 and 6-thio-dG similar, it also induces aberrations in telomere structure and function, thereby promoting an elevated release of cytosolic DNA. These fragments of telomeric DNA are internalized by DCs, prompting activation of the DC-intrinsic STING/IFN-I pathway. This activation culminates in an augmented capacity for cross-priming of DCs, subsequently leading to the activation of tumor-specific T cells. Furthermore, our investigation, which highlights the remarkable effectiveness of sequential administration of L6 and anti-PD-L1 within both advanced tumors and PD-L1 blockade-resistant tumors, provides an initial scientific foundation for the development of novel clinical strategies for cancer treatment. These strategies revolve around the precise manipulation of telomeres within telomerase-positive cancer. In the context of minimal residual disease, a scenario frequently associated with anticipated cancer relapse, the application of modified nucleoside derivatives like L6 holds the potential to prevent or postpone disease resurgence. Furthermore, within the realm of disease maintenance, when used in conjunction with other chemotherapeutic agents, L6 exhibits the potential for heightened effectiveness, concurrently lowering global toxicity levels.

6.CONCLUSION AND SUGGESTIONS

Telomerase stands as a pivotal enzymatic factor accountable for the proliferative immortality exhibited by the majority of neoplastic cells. In this study, we introduced a novel telomere-targeted nucleoside molecule that conjugated with specific lipid molecule. This compound induces the formation of TIFs within diverse lines of tumor cells, with EC_{50} values ranging from 0.076 to 1.885 μM, all without the requirement of any cellular uptake enhancers. *In vivo* studies demonstrated that L6 manifested strong anticancer efficacy, prominently tied to its sequence-specific activities.

Significant advancements have been achieved in enhancing comprehension of the programmed death-1/programmed death ligand-1 (PD-1/PD-L1) pathway. Monoclonal antibodies (mAbs) are presently employed for the inhibition of the PD-1 pathway in the therapeutic intervention of human cancers (anti-PD therapy), with a particular emphasis on advanced solid tumors. Our investigation also demonstrates the notable effectiveness of sequential administration of L6 followed by anti-PD-L1 in cases of advanced tumors and tumors resistant to PD-L1 blockade.

These findings provide an initial scientific justification for the development of novel clinical methodologies for cancer treatment. These methodologies are centered on the precise targeting of telomeres within telomerase-positive neoplastic cells. In the context of minimal residual disease, wherein the anticipation of cancer relapse frequently arises, modified nucleoside molecules, such as L6, hold the potential for preventing or delaying the recurrence of the disease. Furthermore, in the maintenance context, when utilized in conjunction with other chemotherapeutic agents, L6 might exhibit heightened effectiveness, concomitant with reduced overall cytotoxicity.

We believe that these findings will serve as a foundation for the clinical interventions, thereby will guide our efforts to develop more efficacious and less toxic therapeutics to treat cancer in the near future.

7. REFERENCES

1. Guterres, A.N. and J. Villanueva, *Targeting telomerase for cancer therapy.* Oncogene, 2020. **39**(36): p. 5811-5824.

2. Shay, J.W. and W.E. Wright, *Telomeres and telomerase: three decades of progress.* Nat Rev Genet, 2019. **20**(5): p. 299-309.

3. Trybek, T., et al., *Telomeres and telomerase in oncogenesis.* Oncol Lett, 2020. **20**(2): p. 1015-1027.

4. Martinez, P. and M.A. Blasco, *Telomeric and extra-telomeric roles for telomerase and the telomere-binding proteins.* Nat Rev Cancer, 2011. **11**(3): p. 161-76.

5. Blackburn, E.H., *Telomere states and cell fates.* Nature, 2000. **408**(6808): p. 53-6.

6. Collins, K., *The biogenesis and regulation of telomerase holoenzymes.* Nat Rev Mol Cell Biol, 2006. **7**(7): p. 484-94.

7. Matsuda, Y., et al., *Association of longer telomere length in cancer cells and cancer-associated fibroblasts with worse prognosis.* J Natl Cancer Inst, 2023. **115**(2): p. 208-218.

8. Holesova, Z., et al., *Telomere Length Changes in Cancer: Insights on Carcinogenesis and Potential for Non-Invasive Diagnostic Strategies.* Genes (Basel), 2023. **14**(3).

9. Shay, J.W. and W.E. Wright, *Hayflick, his limit, and cellular ageing.* Nat Rev Mol Cell Biol, 2000. **1**(1): p. 72-6.

10. Campisi, J., *Cancer and ageing: rival demons?* Nat Rev Cancer, 2003. **3**(5): p. 339-49.

11. Diotti, R. and D. Loayza, *Shelterin complex and associated factors at human telomeres.* Nucleus, 2011. **2**(2): p. 119-35.

12. Palm, W. and T. de Lange, *How shelterin protects mammalian telomeres.* Annu Rev Genet, 2008. **42**: p. 301-34.

13. Martinez, P. and M.A. Blasco, *Heart-Breaking Telomeres.* Circ Res, 2018. **123**(7): p. 787-802.

14. Kibe, T., et al., *Telomere protection by TPP1 is mediated by POT1a and POT1b.* Mol Cell Biol, 2010. **30**(4): p. 1059-66.

15. Jones, M., et al., *The shelterin complex and hematopoiesis.* J Clin Invest, 2016. **126**(5): p. 1621-9.

16. Loayza, D. and T. De Lange, *POT1 as a terminal transducer of TRF1 telomere length control.* Nature, 2003. **423**(6943): p. 1013-8.

17. Srinivas, N., S. Rachakonda, and R. Kumar, *Telomeres and Telomere Length: A General Overview.* Cancers (Basel), 2020. **12**(3).

18. Guo, X., et al., *Dysfunctional telomeres activate an ATM-ATR-dependent DNA damage response to suppress tumorigenesis.* EMBO J, 2007. **26**(22): p. 4709-19.

19. Dratwa, M., et al., *TERT-Regulation and Roles in Cancer Formation.* Front Immunol, 2020. **11**: p. 589929.

20. Aramburu, T., S. Plucinsky, and E. Skordalakes, *POT1-TPP1 telomere length regulation and disease.* Comput Struct Biotechnol J, 2020. **18**: p. 1939-1946.

21. Oganesian, L. and J. Karlseder, *Telomeric armor: the layers of end protection.* J Cell Sci, 2009. **122**(Pt 22): p. 4013-25.

22. Celli, G.B. and T. de Lange, *DNA processing is not required for ATM-mediated telomere damage response after TRF2 deletion.* Nat Cell Biol, 2005. **7**(7): p. 712-8.

23. Hockemeyer, D., et al., *Recent expansion of the telomeric complex in rodents: Two distinct POT1 proteins protect mouse telomeres.* Cell, 2006. **126**(1): p. 63-77.

24. Wu, L., et al., *Pot1 deficiency initiates DNA damage checkpoint activation and aberrant homologous recombination at telomeres.* Cell, 2006. **126**(1): p. 49-62.

25. Sfeir, A., et al., *Mammalian telomeres resemble fragile sites and require TRF1 for efficient replication.* Cell, 2009. **138**(1): p. 90-103.

26. Artandi, S.E. and R.A. DePinho, *Telomeres and telomerase in cancer.* Carcinogenesis, 2010. **31**(1): p. 9-18.

27. Muoio, D., N. Laspata, and E. Fouquerel, *Functions of ADP-ribose transferases in the maintenance of telomere integrity.* Cell Mol Life Sci, 2022. **79**(4): p. 215.

28. de Lange, T., *Shelterin: the protein complex that shapes and safeguards human telomeres.* Genes Dev, 2005. **19**(18): p. 2100-10.

29. Lengauer, C., K.W. Kinzler, and B. Vogelstein, *Genetic instabilities in human cancers.* Nature, 1998. **396**(6712): p. 643-9.

30. Meeker, A.K., et al., *Telomere length abnormalities occur early in the initiation of epithelial carcinogenesis.* Clin Cancer Res, 2004. **10**(10): p. 3317-26.

31. Shay, J.W. and W.E. Wright, *Senescence and immortalization: role of telomeres and telomerase.* Carcinogenesis, 2005. **26**(5): p. 867-74.

32. Blackburn, E.H., *Switching and signaling at the telomere.* Cell, 2001. **106**(6): p. 661-73.

33. Sedivy, J.M., *Telomeres limit cancer growth by inducing senescence: long-sought in vivo evidence obtained.* Cancer Cell, 2007. **11**(5): p. 389-91.

34. Pandita, T.K., *Telomerase and the cell cycle*, in *Advances in Cell Aging and Gerontology*. 2001, Elsevier. p. 61-88.

35. Wright, W.E. and J.W. Shay, *The two-stage mechanism controlling cellular senescence and immortalization.* Exp Gerontol, 1992. **27**(4): p. 383-9.

36. Yang, J., et al., *Human endothelial cell life extension by telomerase expression.* J Biol Chem, 1999. **274**(37): p. 26141-8.

37. Noureen, N., et al., *Integrated analysis of telomerase enzymatic activity unravels an association with cancer stemness and proliferation.* Nat Commun, 2021. **12**(1): p. 139.

38. Fernandes, S.G., et al., *Role of Telomeres and Telomeric Proteins in Human Malignancies and Their Therapeutic Potential.* Cancers (Basel), 2020. **12**(7).

39. Shay, J.W., *Role of Telomeres and Telomerase in Aging and Cancer.* Cancer Discov, 2016. **6**(6): p. 584-93.

40. Heidenreich, B., et al., *TERT promoter mutations in cancer development.* Curr Opin Genet Dev, 2014. **24**: p. 30-7.

41. Chang, C., et al., *A laminin 511 matrix is regulated by TAZ and functions as the ligand for the alpha6Bbeta1 integrin to sustain breast cancer stem cells.* Genes Dev, 2015. **29**(1): p. 1-6.

42. Huang, F.W., et al., *Highly recurrent TERT promoter mutations in human melanoma.* Science, 2013. **339**(6122): p. 957-9.

43. Killela, P.J., et al., *TERT promoter mutations occur frequently in gliomas and a subset of tumors derived from cells with low rates of self-renewal.* Proc Natl Acad Sci U S A, 2013. **110**(15): p. 6021-6.

44. Blackburn, E.H., *The end of the (DNA) line.* Nat Struct Biol, 2000. **7**(10): p. 847-50.

45. Lin, S.Y. and S.J. Elledge, *Multiple tumor suppressor pathways negatively regulate telomerase.* Cell, 2003. **113**(7): p. 881-9.

46. Akincilar, S.C., B. Unal, and V. Tergaonkar, *Reactivation of telomerase in cancer.* Cell Mol Life Sci, 2016. **73**(8): p. 1659-70.

47. Betts, D.H. and W.A. King, *Telomerase activity and telomere detection during early bovine development.* Dev Genet, 1999. **25**(4): p. 397-403.

48. Xu, J. and X. Yang, *Telomerase activity in bovine embryos during early development.* Biol Reprod, 2000. **63**(4): p. 1124-8.

49. Kyo, S., et al., *Expression of telomerase activity in human chorion.* Biochem Biophys Res Commun, 1997. **241**(2): p. 498-503.

50. Gielen, M., et al., *Placental telomere length decreases with gestational age and is influenced by parity: a study of third trimester live-born twins.* Placenta, 2014. **35**(10): p. 791-6.

51. Stewart, S.A., et al., *Telomerase contributes to tumorigenesis by a telomere length-independent mechanism.* Proc Natl Acad Sci U S A, 2002. **99**(20): p. 12606-11.

52. Hoffmeyer, K., et al., *Wnt/beta-catenin signaling regulates telomerase in stem cells and cancer cells.* Science, 2012. **336**(6088): p. 1549-54.

53. Wu, K.J., et al., *Direct activation of TERT transcription by c-MYC.* Nat Genet, 1999. **21**(2): p. 220-4.

54. Vertecchi, E., A. Rizzo, and E. Salvati, *Telomere Targeting Approaches in Cancer: Beyond Length Maintenance.* Int J Mol Sci, 2022. **23**(7).

55. Cong, Y. and J.W. Shay, *Actions of human telomerase beyond telomeres.* Cell Res, 2008. **18**(7): p. 725-32.

56. Artandi, S.E., et al., *Telomere dysfunction promotes non-reciprocal translocations and epithelial cancers in mice.* Nature, 2000. **406**(6796): p. 641-5.

57. van Heek, N.T., et al., *Telomere shortening is nearly universal in pancreatic intraepithelial neoplasia.* Am J Pathol, 2002. **161**(5): p. 1541-7.

58. Munoz, P., et al., *XPF nuclease-dependent telomere loss and increased DNA damage in mice overexpressing TRF2 result in premature aging and cancer.* Nat Genet, 2005. **37**(10): p. 1063-71.

59. Hanahan, D. and R.A. Weinberg, *Hallmarks of cancer: the next generation.* Cell, 2011. **144**(5): p. 646-74.

60. Ciccia, A. and S.J. Elledge, *The DNA damage response: making it safe to play with knives.* Mol Cell, 2010. **40**(2): p. 179-204.

61. Barnes, R.P., E. Fouquerel, and P.L. Opresko, *The impact of oxidative DNA damage and stress on telomere homeostasis.* Mech Ageing Dev, 2019. **177**: p. 37-45.

62. Nakamura, H. and K. Takada, *Reactive oxygen species in cancer: Current findings and future directions.* Cancer Sci, 2021. **112**(10): p. 3945-3952.

63. Sies, H. and D.P. Jones, *Reactive oxygen species (ROS) as pleiotropic physiological signalling agents.* Nat Rev Mol Cell Biol, 2020. **21**(7): p. 363-383.

64. Kryston, T.B., et al., *Role of oxidative stress and DNA damage in human carcinogenesis.* Mutat Res, 2011. **711**(1-2): p. 193-201.

65. von Zglinicki, T., *Oxidative stress shortens telomeres.* Trends Biochem Sci, 2002. **27**(7): p. 339-44.

66. Yin, J., N. Zhang, and H. Wang, *Liquid chromatography- mass spectrometry for analysis of DNA damages induced by environmental exposure.* TrAC Trends in Analytical Chemistry, 2019. **120**: p. 115645.

67. Tubbs, A. and A. Nussenzweig, *Endogenous DNA Damage as a Source of Genomic Instability in Cancer.* Cell, 2017. **168**(4): p. 644-656.

68. Suzuki, T. and H. Kamiya, *Mutations induced by 8-hydroxyguanine (8-oxo-7,8-dihydroguanine), a representative oxidized base, in mammalian cells.* Genes Environ, 2017. **39**: p. 2.

69. Kasai, H., *What causes human cancer? Approaches from the chemistry of DNA damage.* Genes Environ, 2016. **38**: p. 19.

70. Kino, K., et al., *Generation, repair and replication of guanine oxidation products.* Genes Environ, 2017. **39**: p. 21.

71. Oikawa, S., S. Tada-Oikawa, and S. Kawanishi, *Site-specific DNA damage at the GGG sequence by UVA involves acceleration of telomere shortening.* Biochemistry, 2001. **40**(15): p. 4763-8.

72. De Rosa, M., S.A. Johnson, and P.L. Opresko, *Roles for the 8-Oxoguanine DNA Repair System in Protecting Telomeres From Oxidative Stress.* Front Cell Dev Biol, 2021. **9**: p. 758402.

73. Opresko, P.L., et al., *Oxidative damage in telomeric DNA disrupts recognition by TRF1 and TRF2.* Nucleic Acids Res, 2005. **33**(4): p. 1230-9.

74. Wallace, S.S., *DNA glycosylases search for and remove oxidized DNA bases.* Environ Mol Mutagen, 2013. **54**(9): p. 691-704.

75. Schreiber, V., et al., *Poly(ADP-ribose): novel functions for an old molecule.* Nat Rev Mol Cell Biol, 2006. **7**(7): p. 517-28.

76. Smith, S., *Telomerase can't handle the stress.* Genes Dev, 2018. **32**(9-10): p. 597-599.

77. Fung, H. and B. Demple, *A vital role for Ape1/Ref1 protein in repairing spontaneous DNA damage in human cells.* Mol Cell, 2005. **17**(3): p. 463-70.

78. Whitaker, A.M. and B.D. Freudenthal, *APE1: A skilled nucleic acid surgeon.* DNA Repair (Amst), 2018. **71**: p. 93-100.

79. Dyrkheeva, N.S., N.A. Lebedeva, and O.I. Lavrik, *AP Endonuclease 1 as a Key Enzyme in Repair of Apurinic/Apyrimidinic Sites.* Biochemistry (Mosc), 2016. **81**(9): p. 951-67.

80. Whitaker, A.M., T.S. Flynn, and B.D. Freudenthal, *Molecular snapshots of APE1 proofreading mismatches and removing DNA damage.* Nat Commun, 2018. **9**(1): p. 399.

81. Beaver, J.M., et al., *AP endonuclease 1 prevents trinucleotide repeat expansion via a novel mechanism during base excision repair.* Nucleic Acids Res, 2015. **43**(12): p. 5948-60.

82. Mazouzi, A., et al., *Insight into mechanisms of 3'-5' exonuclease activity and removal of bulky 8,5'-cyclopurine adducts by apurinic/apyrimidinic endonucleases.* Proc Natl Acad Sci U S A, 2013. **110**(33): p. E3071-80.

83. Fan, Z., et al., *Cleaving the oxidative repair protein Ape1 enhances cell death mediated by granzyme A.* Nat Immunol, 2003. **4**(2): p. 145-53.

84. Madlener, S., et al., *Essential role for mammalian apurinic/apyrimidinic (AP) endonuclease Ape1/Ref-1 in telomere maintenance.* Proc Natl Acad Sci U S A, 2013. **110**(44): p. 17844-9.

85. Lee, O.H., et al., *Genome-wide YFP fluorescence complementation screen identifies new regulators for telomere signaling in human cells.* Mol Cell Proteomics, 2011. **10**(2): p. M110 001628.

86. Miller, A.S., et al., *Telomere proteins POT1, TRF1 and TRF2 augment long-patch base excision repair in vitro.* Cell Cycle, 2012. **11**(5): p. 998-1007.

87. Burra, S., et al., *Human AP-endonuclease (Ape1) activity on telomeric G4 structures is modulated by acetylatable lysine residues in the N-terminal sequence.* DNA Repair (Amst), 2019. **73**: p. 129-143.

88. Lindahl, T. and D.E. Barnes, *Repair of endogenous DNA damage.* Cold Spring Harb Symp Quant Biol, 2000. **65**: p. 127-33.

89. Allgayer, J., et al., *Widespread transcriptional gene inactivation initiated by a repair intermediate of 8-oxoguanine.* Nucleic Acids Res, 2016. **44**(15): p. 7267-80.

90. Laev, S.S., N.F. Salakhutdinov, and O.I. Lavrik, *Inhibitors of nuclease and redox activity of apurinic/apyrimidinic endonuclease 1/redox effector factor 1 (APE1/Ref-1).* Bioorg Med Chem, 2017. **25**(9): p. 2531-2544.

91. Liu, T.C., et al., *APE1 distinguishes DNA substrates in exonucleolytic cleavage by induced space-filling.* Nat Commun, 2021. **12**(1): p. 601.

92. Harvey, A., et al., *PARP1 is required for preserving telomeric integrity but is dispensable for A-NHEJ.* Oncotarget, 2018. **9**(78): p. 34821-34837.

93. Martin-Hernandez, K., et al., *Expanding functions of ADP-ribosylation in the maintenance of genome integrity.* Semin Cell Dev Biol, 2017. **63**: p. 92-101.

94. Bryant, H.E., et al., *Specific killing of BRCA2-deficient tumours with inhibitors of poly(ADP-ribose) polymerase.* Nature, 2005. **434**(7035): p. 913-7.

95. D'Amours, D., et al., *Poly(ADP-ribosyl)ation reactions in the regulation of nuclear functions.* Biochem J, 1999. **342 (Pt 2)**(Pt 2): p. 249-68.

96. Parsons, J.L. and G.L. Dianov, *Monitoring base excision repair proteins on damaged DNA using human cell extracts.* Biochem Soc Trans, 2004. **32**(Pt 6): p. 962-3.

97. Doksani, Y. and T. de Lange, *Telomere-Internal Double-Strand Breaks Are Repaired by Homologous Recombination and PARP1/Lig3-Dependent End-Joining.* Cell Rep, 2016. **17**(6): p. 1646-1656.

98. Gomez, M., et al., *PARP1 Is a TRF2-associated poly(ADP-ribose)polymerase and protects eroded telomeres.* Mol Biol Cell, 2006. **17**(4): p. 1686-96.

99. Salvati, E., et al., *PARP1 is activated at telomeres upon G4 stabilization: possible target for telomere-based therapy.* Oncogene, 2010. **29**(47): p. 6280-93.

100. Rizzo, A., et al., *Stabilization of quadruplex DNA perturbs telomere replication leading to the activation of an ATR-dependent ATM signaling pathway.* Nucleic Acids Res, 2009. **37**(16): p. 5353-64.

101. Verdun, R.E. and J. Karlseder, *Replication and protection of telomeres.* Nature, 2007. **447**(7147): p. 924-31.

102. Verdun, R.E., et al., *Functional human telomeres are recognized as DNA damage in G2 of the cell cycle.* Mol Cell, 2005. **20**(4): p. 551-61.

103. Shiloh, Y., *ATM and related protein kinases: safeguarding genome integrity.* Nat Rev Cancer, 2003. **3**(3): p. 155-68.

104. Zou, L. and S.J. Elledge, *Sensing DNA damage through ATRIP recognition of RPA-ssDNA complexes.* Science, 2003. **300**(5625): p. 1542-8.

105. Bartek, J. and J. Lukas, *Chk1 and Chk2 kinases in checkpoint control and cancer.* Cancer Cell, 2003. **3**(5): p. 421-9.

106. Takai, H., A. Smogorzewska, and T. de Lange, *DNA damage foci at dysfunctional telomeres.* Curr Biol, 2003. **13**(17): p. 1549-56.

107. Karlseder, J., et al., *p53- and ATM-dependent apoptosis induced by telomeres lacking TRF2.* Science, 1999. **283**(5406): p. 1321-5.

108. Tong, A.S., et al., *ATM and ATR Signaling Regulate the Recruitment of Human Telomerase to Telomeres.* Cell Rep, 2015. **13**(8): p. 1633-46.

109. Lee, S.S., et al., *ATM Kinase Is Required for Telomere Elongation in Mouse and Human Cells.* Cell Rep, 2015. **13**(8): p. 1623-32.

110. Dikmen, Z.G., et al., *Targeting critical steps of cancer metastasis and recurrence using telomerase template antagonists.* Biochim Biophys Acta, 2009. **1792**(4): p. 240-7.

111. Shay, J.W. and W.E. Wright, *Telomerase therapeutics for cancer: challenges and new directions.* Nat Rev Drug Discov, 2006. **5**(7): p. 577-84.

112. Corey, D.R., *Telomerase inhibition, oligonucleotides, and clinical trials.* Oncogene, 2002. **21**(4): p. 631-7.

113. Asai, A., et al., *A novel telomerase template antagonist (GRN163) as a potential anticancer agent.* Cancer Res, 2003. **63**(14): p. 3931-9.

114. Burchett, K.M., Y. Yan, and M.M. Ouellette, *Telomerase inhibitor Imetelstat (GRN163L) limits the lifespan of human pancreatic cancer cells.* PLoS One, 2014. **9**(1): p. e85155.

115. Herbert, B.S., et al., *Oligonucleotide N3'-->P5' phosphoramidates as efficient telomerase inhibitors.* Oncogene, 2002. **21**(4): p. 638-42.

116. Chiappori, A.A., et al., *A randomized phase II study of the telomerase inhibitor imetelstat as maintenance therapy for advanced non-small-cell lung cancer.* Ann Oncol, 2015. **26**(2): p. 354-62.

117. Baerlocher, G.M., et al., *Telomerase Inhibitor Imetelstat in Patients with Essential Thrombocythemia.* N Engl J Med, 2015. **373**(10): p. 920-8.

118. Tefferi, A., et al., *A Pilot Study of the Telomerase Inhibitor Imetelstat for Myelofibrosis.* N Engl J Med, 2015. **373**(10): p. 908-19.

119. Salloum, R., et al., *A molecular biology and phase II study of imetelstat (GRN163L) in children with recurrent or refractory central nervous system malignancies: a pediatric brain tumor consortium study.* J Neurooncol, 2016. **129**(3): p. 443-451.

120. Gellert, G.C., et al., *Effects of a novel telomerase inhibitor, GRN163L, in human breast cancer.* Breast Cancer Res Treat, 2006. **96**(1): p. 73-81.

121. Dikmen, Z.G., et al., *In vivo inhibition of lung cancer by GRN163L: a novel human telomerase inhibitor.* Cancer Res, 2005. **65**(17): p. 7866-73.

122. Mender, I., et al., *Induction of telomere dysfunction mediated by the telomerase substrate precursor 6-thio-2'-deoxyguanosine.* Cancer Discov, 2015. **5**(1): p. 82-95.

123. Bruedigam, C., et al., *Imetelstat-mediated alterations in fatty acid metabolism to induce ferroptosis as a therapeutic strategy for acute myeloid leukemia.* Nat Cancer, 2023.

124. Platzbecker, U., et al., *Imetelstat in patients with lower-risk myelodysplastic syndromes who have relapsed or are refractory to erythropoiesis-stimulating agents (IMerge): a multinational, randomised, double-blind, placebo-controlled, phase 3 trial.* Lancet, 2023.

125. Mender, I., S. Gryaznov, and J.W. Shay, *A novel telomerase substrate precursor rapidly induces telomere dysfunction in telomerase positive cancer cells but not telomerase silent normal cells.* Oncoscience, 2015. **2**(8): p. 693-5.

126. Mender, I., et al., *Telomere Stress Potentiates STING-Dependent Anti-tumor Immunity.* Cancer Cell, 2020. **38**(3): p. 400-411 e6.

127. Sengupta, S., et al., *Induced Telomere Damage to Treat Telomerase Expressing Therapy-Resistant Pediatric Brain Tumors.* Mol Cancer Ther, 2018. **17**(7): p. 1504-1514.

128. Reyes-Uribe, P., et al., *Exploiting TERT dependency as a therapeutic strategy for NRAS-mutant melanoma.* Oncogene, 2018. **37**(30): p. 4058-4072.

129. Siegel, R.L., K.D. Miller, and A. Jemal, *Cancer statistics, 2019.* CA Cancer J Clin, 2019. **69**(1): p. 7-34.

130. Triantafillidis, J.K., G. Nasioulas, and P.A. Kosmidis, *Colorectal cancer and inflammatory bowel disease: epidemiology, risk factors, mechanisms of carcinogenesis and prevention strategies.* Anticancer Res, 2009. **29**(7): p. 2727-37.

131. Testa, U., E. Pelosi, and G. Castelli, *Colorectal cancer: genetic abnormalities, tumor progression, tumor heterogeneity, clonal evolution and tumor-initiating cells.* Med Sci (Basel), 2018. **6**(2).

132. Malki, A., et al., *Molecular Mechanisms of Colon Cancer Progression and Metastasis: Recent Insights and Advancements.* Int J Mol Sci, 2020. **22**(1).

133. Hossain, M.S., et al., *Colorectal Cancer: A Review of Carcinogenesis, Global Epidemiology, Current Challenges, Risk Factors, Preventive and Treatment Strategies.* Cancers (Basel), 2022. **14**(7).

134. Safiejko, K., et al., *Robotic-Assisted vs. Standard Laparoscopic Surgery for Rectal Cancer Resection: A Systematic Review and Meta-Analysis of 19,731 Patients.* Cancers (Basel), 2021. **14**(1).

135. Xie, Y.H., Y.X. Chen, and J.Y. Fang, *Comprehensive review of targeted therapy for colorectal cancer.* Signal Transduct Target Ther, 2020. **5**(1): p. 22.

136. Hu, T., et al., *Mechanisms of drug resistance in colon cancer and its therapeutic strategies.* World J Gastroenterol, 2016. **22**(30): p. 6876-89.

137. Kuipers, E.J., et al., *Colorectal cancer.* Nat Rev Dis Primers, 2015. **1**: p. 15065.

138. Siegel, R.L., et al., *Cancer statistics, 2023.* CA Cancer J Clin, 2023. **73**(1): p. 17-48.

139. Johdi, N.A. and N.F. Sukor, *Colorectal Cancer Immunotherapy: Options and Strategies.* Front Immunol, 2020. **11**: p. 1624.

140. Jacome, A.A. and C. Eng, *Role of immune checkpoint inhibitors in the treatment of colorectal cancer: focus on nivolumab.* Expert Opin Biol Ther, 2019. **19**(12): p. 1247-1263.

141. Li, J. and X. Xu, *Immune Checkpoint Inhibitor-Based Combination Therapy for Colorectal Cancer: An Overview.* Int J Gen Med, 2023. **16**: p. 1527-1540.

142. Marcus, L., et al., *FDA Approval Summary: Pembrolizumab for the Treatment of Microsatellite Instability-High Solid Tumors.* Clin Cancer Res, 2019. **25**(13): p. 3753-3758.

143. Stein, A., et al., *Immuno-oncology in GI tumours: Clinical evidence and emerging trials of PD-1/PD-L1 antagonists.* Crit Rev Oncol Hematol, 2018. **130**: p. 13-26.

144. Mizukoshi, E. and S. Kaneko, *Telomerase-Targeted Cancer Immunotherapy.* Int J Mol Sci, 2019. **20**(8).

145. Farhood, B., M. Najafi, and K. Mortezaee, *CD8(+) cytotoxic T lymphocytes in cancer immunotherapy: A review.* J Cell Physiol, 2019. **234**(6): p. 8509-8521.

146. Durgeau, A., et al., *Recent Advances in Targeting CD8 T-Cell Immunity for More Effective Cancer Immunotherapy.* Front Immunol, 2018. **9**: p. 14.

147. Sharma, P. and J.P. Allison, *The future of immune checkpoint therapy.* Science, 2015. **348**(6230): p. 56-61.

148. Topalian, S.L., et al., *Safety, activity, and immune correlates of anti-PD-1 antibody in cancer.* N Engl J Med, 2012. **366**(26): p. 2443-54.

149. Brahmer, J.R., et al., *Safety and activity of anti-PD-L1 antibody in patients with advanced cancer.* N Engl J Med, 2012. **366**(26): p. 2455-65.

150. Ribas, A. and J.D. Wolchok, *Cancer immunotherapy using checkpoint blockade.* Science, 2018. **359**(6382): p. 1350-1355.

151. Socinski, M.A., et al., *Atezolizumab for First-Line Treatment of Metastatic Nonsquamous NSCLC.* N Engl J Med, 2018. **378**(24): p. 2288-2301.

152. Ribas, A., et al., *Association of Pembrolizumab With Tumor Response and Survival Among Patients With Advanced Melanoma.* JAMA, 2016. **315**(15): p. 1600-9.

153. Powles, T., et al., *MPDL3280A (anti-PD-L1) treatment leads to clinical activity in metastatic bladder cancer.* Nature, 2014. **515**(7528): p. 558-62.

154. Hamid, O., et al., *Safety and tumor responses with lambrolizumab (anti-PD-1) in melanoma.* N Engl J Med, 2013. **369**(2): p. 134-44.

155. Freeman, G.J., et al., *Engagement of the PD-1 immunoinhibitory receptor by a novel B7 family member leads to negative regulation of lymphocyte activation.* J Exp Med, 2000. **192**(7): p. 1027-34.

156. Greenwald, R.J., G.J. Freeman, and A.H. Sharpe, *The B7 family revisited.* Annu Rev Immunol, 2005. **23**: p. 515-48.

157. Dong, H., et al., *Tumor-associated B7-H1 promotes T-cell apoptosis: a potential mechanism of immune evasion.* Nat Med, 2002. **8**(8): p. 793-800.

158. Li, X., et al., *NQO1 targeting prodrug triggers innate sensing to overcome checkpoint blockade resistance.* Nat Commun, 2019. **10**(1): p. 3251.

159. Deng, L., et al., *STING-Dependent Cytosolic DNA Sensing Promotes Radiation-Induced Type I Interferon-Dependent Antitumor Immunity in Immunogenic Tumors.* Immunity, 2014. **41**(5): p. 843-52.

160. Ishikawa, H. and G.N. Barber, *STING is an endoplasmic reticulum adaptor that facilitates innate immune signalling.* Nature, 2008. **455**(7213): p. 674-8.

161. Gehrke, N., et al., *Oxidative damage of DNA confers resistance to cytosolic nuclease TREX1 degradation and potentiates STING-dependent immune sensing.* Immunity, 2013. **39**(3): p. 482-95.

162. Pitt, J.M., G. Kroemer, and L. Zitvogel, *Immunogenic and Non-immunogenic Cell Death in the Tumor Microenvironment.* Adv Exp Med Biol, 2017. **1036**: p. 65-79.

163. Sen, T., et al., *Targeting DNA Damage Response Promotes Antitumor Immunity through STING-Mediated T-cell Activation in Small Cell Lung Cancer.* Cancer Discov, 2019. **9**(5): p. 646-661.

164. Fenech, M., et al., *Molecular mechanisms of micronucleus, nucleoplasmic bridge and nuclear bud formation in mammalian and human cells.* Mutagenesis, 2011. **26**(1): p. 125-32.

165. Wu, J., et al., *Cyclic GMP-AMP is an endogenous second messenger in innate immune signaling by cytosolic DNA.* Science, 2013. **339**(6121): p. 826-30.

166. Wu, J. and Z.J. Chen, *Innate immune sensing and signaling of cytosolic nucleic acids.* Annu Rev Immunol, 2014. **32**: p. 461-88.

167. Zhang, X., et al., *Cyclic GMP-AMP containing mixed phosphodiester linkages is an endogenous high-affinity ligand for STING.* Mol Cell, 2013. **51**(2): p. 226-35.

168. Stadler, Z.K., et al., *Reliable Detection of Mismatch Repair Deficiency in Colorectal Cancers Using Mutational Load in Next-Generation Sequencing Panels.* J Clin Oncol, 2016. **34**(18): p. 2141-7.

169. Cancer Genome Atlas, N., *Comprehensive molecular characterization of human colon and rectal cancer.* Nature, 2012. **487**(7407): p. 330-7.

170. Maby, P., et al., *Correlation between Density of CD8+ T-cell Infiltrate in Microsatellite Unstable Colorectal Cancers and Frameshift Mutations: A Rationale for Personalized Immunotherapy.* Cancer Res, 2015. **75**(17): p. 3446-55.

171. Marisa, L., et al., *The Balance Between Cytotoxic T-cell Lymphocytes and Immune Checkpoint Expression in the Prognosis of Colon Tumors.* J Natl Cancer Inst, 2018. **110**(1).

172. Llosa, N.J., et al., *The vigorous immune microenvironment of microsatellite instable colon cancer is balanced by multiple counter-inhibitory checkpoints.* Cancer Discov, 2015. **5**(1): p. 43-51.

173. Gilles, J.F., et al., *DiAna, an ImageJ tool for object-based 3D co-localization and distance analysis.* Methods, 2017. **115**: p. 55-64.

174. Cayir, A., et al., *Comet assay for assessment of DNA damage in greenhouse workers exposed to pesticides.* Biomarkers, 2019. **24**(6): p. 592-599.

175. Li, J., et al., *Emerging Disinfection Byproducts, Halobenzoquinones: Effects of Isomeric Structure and Halogen Substitution on Cytotoxicity, Formation of Reactive Oxygen Species, and Genotoxicity.* Environ Sci Technol, 2016. **50**(13): p. 6744-52.

176. Yu, Y., et al., *Chemical Analysis of DNA Damage.* Anal Chem, 2018. **90**(1): p. 556-576.

177. Tretyakova, N., P.W. Villalta, and S. Kotapati, *Mass spectrometry of structurally modified DNA.* Chem Rev, 2013. **113**(4): p. 2395-436.

178. Ma, B., et al., *Identification of more than 100 structurally unique DNA-phosphate adducts formed during rat lung carcinogenesis by the tobacco-specific nitrosamine 4-(methylnitrosamino)-1-(3-pyridyl)-1-butanone.* Carcinogenesis, 2018. **39**(2): p. 232-241.

179. Gaskell, M., et al., *Detection of phosphodiester adducts formed by the reaction of benzo[a]pyrene diol epoxide with 2'-deoxynucleotides using collision-induced dissociation electrospray ionization tandem mass spectrometry.* Nucleic Acids Res, 2007. **35**(15): p. 5014-27.

180. Tang, B., J.R. Testa, and W.D. Kruger, *Increasing the therapeutic index of 5-fluorouracil and 6-thioguanine by targeting loss of MTAP in tumor cells.* Cancer Biol Ther, 2012. **13**(11): p. 1082-90.

181. Brem, R. and P. Karran, *Oxidation-mediated DNA cross-linking contributes to the toxicity of 6-thioguanine in human cells.* Cancer Res, 2012. **72**(18): p. 4787-95.

182. Williams, S.C., *No end in sight for telomerase-targeted cancer drugs.* Nat Med, 2013. **19**(1): p. 6.

183. Thompson, P.A., et al., *A phase I trial of imetelstat in children with refractory or recurrent solid tumors: a Children's Oncology Group Phase I Consortium Study (ADVL1112).* Clin Cancer Res, 2013. **19**(23): p. 6578-84.

184. Galluzzi, L., et al., *Immunogenic cell death in cancer and infectious disease.* Nat Rev Immunol, 2017. **17**(2): p. 97-111.

185. Campisi, J., *Cellular senescence as a tumor-suppressor mechanism.* Trends Cell Biol, 2001. **11**(11): p. S27-31.

186. Cosme-Blanco, W., et al., *Telomere dysfunction suppresses spontaneous tumorigenesis in vivo by initiating p53-dependent cellular senescence.* EMBO Rep, 2007. **8**(5): p. 497-503.

187. Feldser, D.M. and C.W. Greider, *Short telomeres limit tumor progression in vivo by inducing senescence.* Cancer Cell, 2007. **11**(5): p. 461-9.

8.SUPPLEMENTS

SUPPLEMENT 1 Turnitin digital receipt

turnitin

Dijital Makbuz

Bu makbuz ödevinizin Turnitin'e ulaştığını bildirmektedir. Gönderiminize dair bilgiler şöyledir:

Gönderinizin ilk sayfası aşağıda gönderilmektedir.

Gönderen:	Merve Yılmaz
Ödev başlığı:	INVESTIGATION OF THE IN VITRO AND IN VIVO EFFECTS OF T...
Gönderi Başlığı:	INVESTIGATION OF THE IN VITRO AND IN VIVO EFFECTS OF T...
Dosya adı:	Doktora_Tez_copy.docx
Dosya boyutu:	4.95M
Sayfa sayısı:	84
Kelime sayısı:	19,126
Karakter sayısı:	116,336
Gönderim Tarihi:	18-Ara-2023 11:52ÖS (UTC+0300)
Gönderim Numarası:	2262157704

SUPPLEMENT 2 Turnitin originality report

THESIS TITLE: Investigation of the *in vitro* and *in vivo* effects of telomere-targeted new drug candidate compounds on different cancer cell lines

STUDENT NAME AND SURNAME: Merve YILMAZ

TOTAL NUMBER OF PAGE: 84

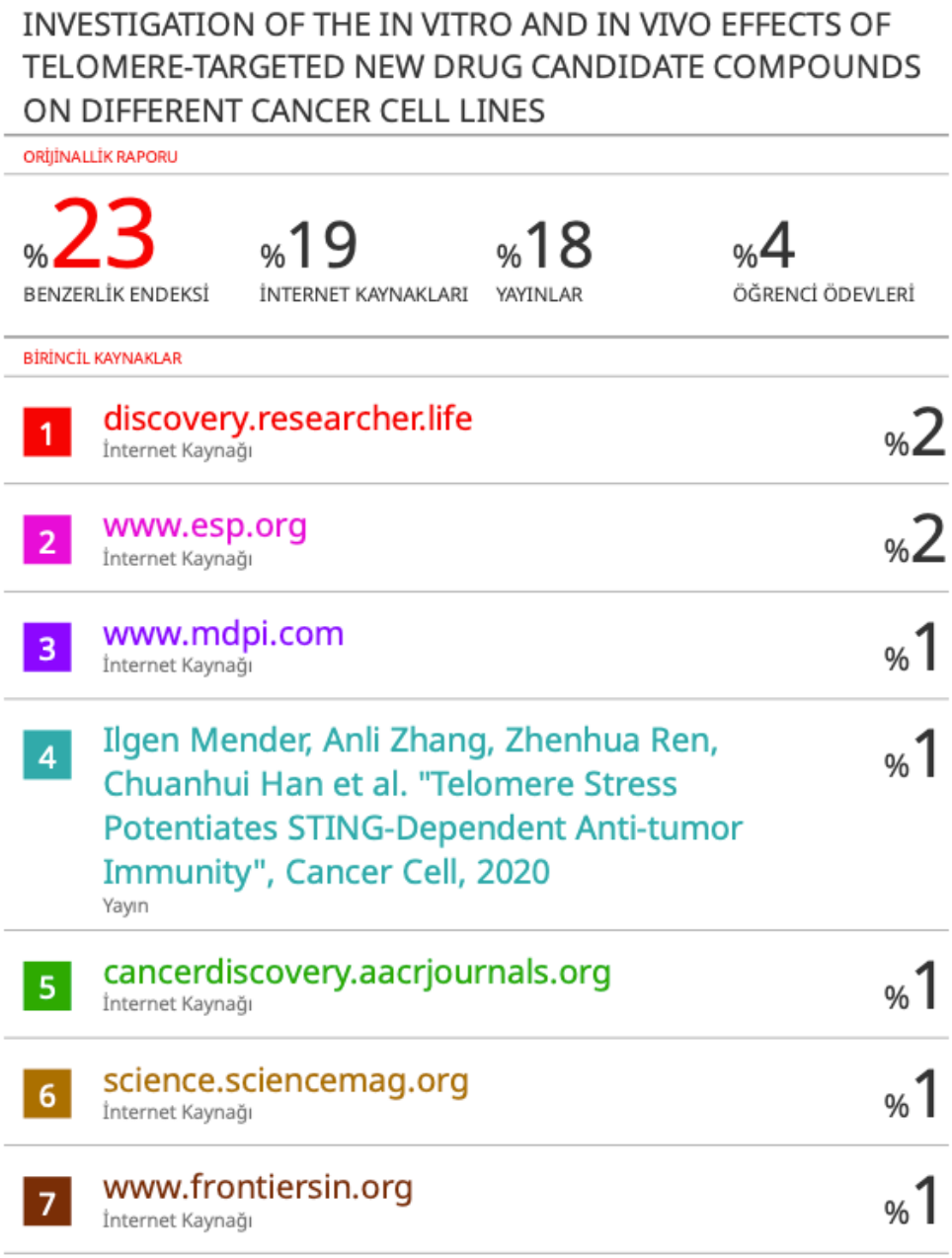

INVESTIGATION OF THE IN VITRO AND IN VIVO EFFECTS OF TELOMERE-TARGETED NEW DRUG CANDIDATE COMPOUNDS ON DIFFERENT CANCER CELL LINES

ORİJİNALLİK RAPORU

%23	%19	%18	%4
BENZERLİK ENDEKSİ	İNTERNET KAYNAKLARI	YAYINLAR	ÖĞRENCİ ÖDEVLERİ

BİRİNCİL KAYNAKLAR

1	discovery.researcher.life İnternet Kaynağı	%2
2	www.esp.org İnternet Kaynağı	%2
3	www.mdpi.com İnternet Kaynağı	%1
4	Ilgen Mender, Anli Zhang, Zhenhua Ren, Chuanhui Han et al. "Telomere Stress Potentiates STING-Dependent Anti-tumor Immunity", Cancer Cell, 2020 Yayın	%1
5	cancerdiscovery.aacrjournals.org İnternet Kaynağı	%1
6	science.sciencemag.org İnternet Kaynağı	%1
7	www.frontiersin.org İnternet Kaynağı	%1

SUPPLEMENT 3 Ethics Committee Document

KOBAY DHL A.Ş. YEREL ETİK KURULU BAŞVURU ONAYI		
BAŞVURU BİLGİLERİ	Protokol Numarası	603
	Protokol Adı	Telomer hedefli yeni ilaç adayı bileşiklerin in vivo etkilerinin incelenmesi
	Başvuru Tarihi	01.02.2022
	Sorumlu Araştırmacı Adı-Unvanı	Prof. Dr. Z. Günnur DİKMEN
	Sorumlu Araştırmacı Çalıştığı Kurum	Hacettepe Üniversitesi Tıp Fakültesi
	Yardımcı Araştırmacılar	Arş. Gör. Merve YILMAZ
KARAR BİLGİLERİ	Onay Numarası	603
	Onay Tarihi	04.02.2022
	Onaylanan Hayvan Türü ve Sayısı	20 adet erkek, Nude CD1, Fare
	Onay Bilgileri	Proje amaç, gerekçe, yaklaşım ve yöntem yönünden incelenmiş, çalışmanın gerçekleşmesinde etik sakınca bulunmadığına karar verilmiştir.
KOBAY DHL. A.Ş. YEREL ETİK KURUL ÜYELERİ	Etik Kurul Başkanı A.Begüm BUĞDAYCI AÇIKKOL	e- imzalı
	Etik Kurul Başkan Yardımcısı Prof. Dr. Güneş ESENDAĞLI	e- imzalı
	Etik Kurul Üyesi Prof. Dr. Belma GÜMÜŞEL	e- imzalı
	Etik Kurul Üyesi Doç. Dr. M. Kürşat DERİCİ	e- imzalı
	Sorumlu Veteriner Hekim Orkun TARKUN	e- imzalı
	Etik Kurul Üyesi Biyolog Fatma Nur İNÇEH	e- imzalı
	Etik Kurul Üyesi Veteriner Hekim Murat Okan HATİPOĞLU	-
	Etik Kurul Üyesi Biyolog Canan ÇAKIR ÇOBAN	e- imzalı
	Etik Kurul Üyesi Zeynep AYDIN TARAKÇI	e- imzalı
	Etik Kurul Üyesi Adil KIŞ	e- imzalı
	Etik Kurul Üyesi Uzman Diğdem YÖYEN ERMİŞ	e- imzalı
	Etik Kurul Üyesi Ali VAROL	e- imzalı

Etikimza Süreç No : wnw9unok3p00b513254c Bu belge, güvenli elektronik imza ile imzalanmıştır

Kobay Deney Hayvanları Laboratuarı Sanayi ve Ticaret A.Ş.
Merkez Ofis : Uzay Çağı Caddesi, 1308. Sokak No:6 (Odtü Teknokent) Yenimahalle - Ankara
Şube Ofis : İ.O.S.B 21.Cadde 520.Sokak No:2/2 Yenimahalle – Ankara
Telefon : 0 (312) 394 70 94 | Faks : 0(312) 995 06 94
www.kobay.com.tr– bilgi@kobay.com.tr

10.02.2023

Sn. Prof. Dr. Z. Günnur DİKMEN

Kurumumuz etik kurulunca 603 protokol numarası ile onaylanan “Telomer hedefli yeni ilaç adayı bileşiklerin in vivo etkilerinin incelenmesi” başlıklı çalışmanız için 23.01.2023 tarihli başvurunuz değerlendirilmiş olup çalışmanızda ilave olarak konvansiyonel 29 adet erkek Balb/C farelerin eklenmesinin uygun olduğu değerlendirilmiştir.

Gereğini arz ederim.

A.Begüm BUĞDAYCI
Yönetim Kurulu Başkanı
Veteriner Hekim

KOBAY DENEY HAYVANLARI
LABORATUARI SANAYİ VE TİCARET A.Ş.
İvedik Organize Sanayi 21 Cadde
520. Sokak No: 27 Yenimahalle/ANKARA
Ostim V.D. 584 053 4744

Kobay Deney Hayvanları Laboratuarı Sanayi ve Ticaret A.Ş.
Merkez Ofis : Uzay Çağı Caddesi, 1308. Sokak No:6 (Odtü Teknokent) Yenimahalle - Ankara
Şube Ofis : İ.O.S.B 21.Cadde 520.Sokak No:2/2 Yenimahalle – Ankara
(0312) 394 70 94 – (0542) 394 70 94 www.kobay.com.tr– bilgi@kobay.com.tr